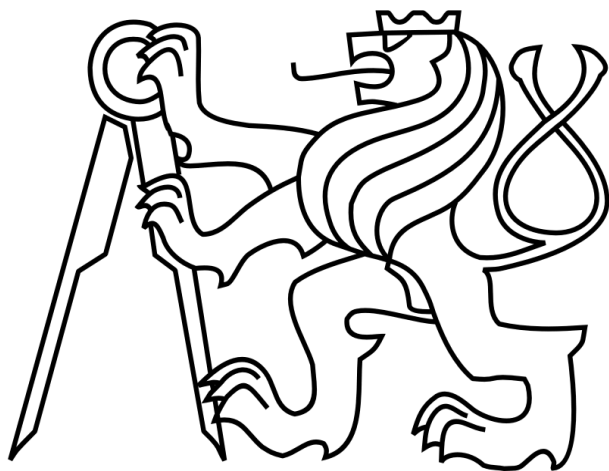


CZECH TECHNICAL UNIVERSITY IN PRAGUE, FACULTY OF ELECTRICAL ENGINEERING  
DEPARTMENT OF MEASUREMENT

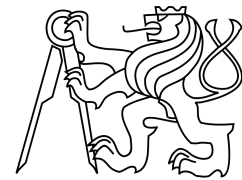


**IMPROVEMENT OF INERTIAL NAVIGATION SYSTEM ACCURACY  
USING ALTERNATIVE SENSORS**

Doctoral Thesis

January, 2015

Martin Šipoš



DOCTORAL THESIS:

*Improvement of Inertial Navigation System Accuracy Using Alternative Sensors*  
Prague, January 2015

AUTHOR:

*Martin Šipoš*

Department of Measurement  
Faculty of Electrical Engineering  
Czech Technical University in Prague

PH.D. PROGRAMME:

*Electrical Engineering and Information Technology*

BRANCH OF STUDY:

*Air Traffic Control*

SUPERVISOR:

*Doc. Ing. Jan Roháč, Ph.D.*  
Department of Measurement  
Faculty of Electrical Engineering  
Czech Technical University in Prague

## **Declaration**

I hereby declare I have written this doctoral thesis independently and quoted all the sources of information used in accordance with methodological instructions on ethical principles for writing an academic thesis. Moreover, I state that this thesis has neither been submitted nor accepted for any other degree.

*Prague, January 2015*

---

Martin Šipoš

## Acknowledgement

This doctoral thesis is dedicated to my wife Lucie, son Filip and my parents who have helped and supported me in a lot of situations when it was the most needed. I would like to thank them greatly in this place.

My great thanks belong to Jan Roháč and Karel Draxler, associate professors at the Department of Measurement (FEE, CTU in Prague), for their patience, wisdom and helpful advices, as well as to my colleagues in Laboratory of Aircraft Systems for helping me in the friendliest manner during my studies.

This work was partially supported by Czech Science Foundation project 102/09/H082: "Sensors and Intelligent Sensors Systems"; partially by the Grant Agency of the CTU in Prague under Grants CTU0909913: "*Integration of Low-cost Inertial Navigation Unit with Secondary Navigation Systems (GPS, Magnetometer)*", SGS10/288/OHK3/3T/13: "*Modular Navigation System for Attitude and Position Estimation*", and SGS13/144/OHK3/2T/13: "*Modern Methods in Development of Inertial Navigation Systems*".

## Abstract

Navigation systems providing the attitude, position and velocity of an object play a key role in a wide range of applications. Their accuracy depends on the choice of sensors. The most precise sensors are ring laser gyroscopes, fiber optic gyroscopes and servo and Quartz accelerometers for angular rate/acceleration measurements. These navigation grade sensors would be convenient for all applications; however, their price can be too high. A cheaper alternative can be Micro-Electro-Mechanical-Systems (MEMS). The technological progress in the precision of MEMS has enabled their use in cost-effective applications, such as in unmanned aerial vehicles (UAVs) or small aircrafts. Despite the MEMS-based inertial sensors carrying a lot of advantages, their performance has many weaknesses such as low resolution, noisy output, worse bias stability, etc. For these reasons, as a standalone system they are not able to provide a navigation solution and thus they need to be fused with other aiding sources via adaptive data processing approaches. GNSS, a magnetometer, a pressure-based altimeter, an electrolytic tilt sensor (ETS), and so on can be employed as possible aiding sources.

A main aim of the doctoral thesis is an improvement of overall accuracy of the developed low-cost inertial navigation system (INS) by means such as usage of alternative sensors, estimation of sensor errors and usage of adaptive attitude estimation approaches. The INS utilizes data from the MEMS-based inertial sensors (accelerometers and gyroscopes), magnetometer and an ETS. The intention is paid just to attitude, thus the objectives are focused on a design and development of algorithms for attitude evaluation excluding GPS. The final low-cost INS realization is primarily developed for usage on UAVs or small aircrafts.

The first part is focused on inertial sensors and magnetometer calibration. It covers design of the sensor error models (SEMs) which contain scale factors, non-orthogonality angles, offsets and measuring framework misalignments. The parameters of the SEMs are identified by proposed calibration procedures and algorithms and, in the end, the sensor errors compensations are applied and evaluated.

The second part provides the overview of different ETSs, their principle of operation, parameters and performed analyses which are focused on correction of triaxial accelerometer data. Based on several performed analyses, the most convenient ETS is chosen for use in the INS realization.

The last part deals with adaptive data processing approaches for attitude estimation. The algorithm for attitude estimation preprocesses data from accelerometer, magnetometer and ETS data via Gauss-Newton method and the resultant quaternion is fused with gyroscope data via extended Kalman filter which provides as estimates three angular rates, four components of quaternion and three gyroscope biases. The proposed algorithms are evaluated using real flight data and the final accuracy of attitude estimation as well as accuracy analyses are presented.

## Abstrakt

Navigační systémy poskytující polohové úhly, pozici a rychlosť navigovaného objektu jsou v současné době využívány v širokém spektru uživatelských aplikací. Přesnost těchto systémů závisí především na přesnosti použitých senzorů. Mezi nejpřesnější patří laserové gyroskopy, gyroskopy s optickým vláknem, servo a quartz akcelerometry měřící úhlové rychlosti/zrychlení. Tyto velmi přesné senzory by bylo vhodné využít pro všechny požadované aplikace, kdyby jejich cena nebyla příliš vysoká. Levnější alternativou mohou být senzory vyrobené MEMS technologií, které vzhledem ke zvyšující se přesnosti mohou být využity např. na bezpilotních prostředcích, malých letadlech, atd. Ačkoliv mají MEMS inerciální senzory mnoho výhod, mají rovněž i své slabé stránky jako nízké rozlišení, vysoký šum výstupních dat, nízká stabilita, atd. Z těchto důvodů nejsou schopny MEMS senzory poskytovat navigační úlohu nezávisle a tudíž potřebují být integrovány s doplňkovými zdroji informací jako např. GNSS, magnetometr, barometrický výškoměr, elektrolytická libela, atd.

Hlavním cílem této disertační práce je zvýšení přesnosti inerciálního navigačního systému (INS), který využívá levné senzory, a to pomocí alternativních senzorů, kalibrací použitých senzorů a využitím adaptivních algoritmů pro odhad polohových úhlů. INS využívá data z tříosého akcelerometru, gyroskopu, magnetometru a elektrolytické libely, která jsou pomocí vhodných algoritmů použita pro odhad polohových úhlů bez nutnosti využití GPS.

První část disertační práce je zaměřena na kalibraci tříosých akcelerometrů, gyroskopů a magnetometrů, což zahrnuje návrh deterministických chybových modelů (obsahují převodní konstanty, úhly neortogonalit, ofsety a koeficienty matice zarovnání), návrh a realizaci algoritmů a kalibračních postupů.

Ve druhé části je uveden přehled elektrolytických libel včetně jejich nejvýznamnějších parametrů, princip jejich činnosti a experimentální ověření jejich parametrů. Na základě provedených analýz byl vybrán nevhodnější senzor pro využití v inerciálním navigačním systému.

Poslední část disertační práce je zaměřena na adaptivní metody určení polohových úhlů. Výsledný algoritmus je založen na kombinaci Gauss-Newtonovy metody a algoritmu rozšířeného Kalmanova filtru. Gauss-Newtonova metoda je využita pro odhad kvaternionu na základě dat z akcelerometru, magnetometru a elektrolytické libely. Tento kvaternion je následně integrován s daty ze tříosého gyroskopu pomocí algoritmu rozšířeného Kalmanova filtru. Výstupními odhady je trojice úhlových rychlostí a jejich biasy a čtveřice komponent kvaternionu reprezentujícího orientaci navigovaného objektu. Navržené algoritmy a přesnost určení polohových úhlů byly ověřeny na základě reálných dat získaných na bezpilotním prostředku.

## Contents

List of Abbreviations.....	9
1. Introduction .....	10
2. Aims of the Doctoral Thesis.....	11
3. Current State of the Art .....	12
3.1. Inertial Sensors and Magnetometer Calibration .....	12
3.2. Usage of Electrolytic Tilt Sensor for Attitude Determination.....	13
3.3. Algorithms and Methods for Attitude Estimation .....	15
4. Published Results.....	17
4.1. Analyses of Triaxial Accelerometer Calibration Algorithms.....	19
4.2. Calibration of Triaxial Gyroscopes .....	28
4.3. Improvement of Electronic Compass Accuracy Based on Magnetometer and Accelerometer Calibration.....	33
4.4. Comparison of Electrolytic Tilt Sensors for Accelerometer Data Correction.....	38
4.5. Analyses of Electrolytic Tilt Sensor Data for Triaxial Accelerometer's Initial Alignment .....	49
4.6. Practical Approaches to Attitude Estimation in Aerial Applications .....	54
5. Unpublished Results Related to the Thesis .....	66
5.1. Results Related to Triaxial Gyroscope Calibration.....	66
5.1.1. Verification of Gyroscope Calibration .....	67
5.1.2. Angular Rate Domain Approach of Gyroscope Calibration .....	67
5.2. Analyses of Electrolytic Tilt Sensors for Accelerometer Data Correction .....	68
5.2.1. Transfer Characteristics of Electrolytic Tilt Sensors .....	69
5.2.2. Deviations of Tilt Angles Evaluated by Electrolytic Tilt Sensors .....	70
5.2.3. Analyses of Settling Time.....	71
5.2.4. Influence of Vibrations on Attitude Determined by Electrolytic Tilt Sensors.....	72
5.2.5. Triaxial Accelerometer Initial Bias Estimation based on Electrolytic Tilt Sensor Data.....	73
6. Conclusion .....	74
6.1. Summary and Contribution .....	74
6.2. Future Work .....	75
References .....	76
Appendix A: Author's Publications and Grants.....	81
A.1. Publications Related to the Thesis .....	81
A.1.1. Publications in Journals with Impact Factor .....	81
A.1.2. Publications in Peer-reviewed Journals .....	81
A.1.3. Conference Proceedings (WoS).....	81
A.1.4. Conference Proceedings .....	81
A.1.5. Invited Presentations .....	82

---

A.2.	Publications Not Related to the Thesis.....	83
A.2.1.	Publications in Journals with Impact Factor .....	83
A.2.2.	Publications in Peer-reviewed Journals .....	83
A.2.3.	Conference Proceedings (WoS).....	83
A.2.4.	Conference Proceedings.....	83
A.2.5.	Utility Models .....	84
A.2.6.	Functional Prototypes.....	84
A.3.	Grants and Projects Related to the Thesis .....	84
A.4.	Response to Author's Publications.....	85

**List of Abbreviations**

ACC	Accelerometer
AHRS	Attitude and Heading Reference System
CF	Complementary Filter
CTU	Czech Technical University
EGF	Earth Gravity Field
EKF	Extended Kalman Filter
EMF	Earth Magnetic Field
ETS	Electrolytic Tilt Sensor
FEE	Faculty of Electrical Engineering
FOG	Fiber Optic Gyroscope
FQA	Factored Quaternion Algorithm
GNM	Gauss-Newton Method
GNSS	Global Navigation Satellite System
IMU	Inertial Measurement Unit
INS	Inertial Navigation System
KF	Kalman Filter
RLG	Ring Laser Gyroscope
UKF	Unscented Kalman Filter

## 1. Introduction

Navigation systems which provide information on attitude, position and velocity of object are nowadays used in a wide range of civil and military applications, such as in unmanned aerial vehicles (UAVs), aircrafts, indoor and outdoor personal navigation, human motion tracking, attitude control systems, in mobile phones, terrestrial vehicles, biomedical systems and so on [1] - [5]. The accuracy of the navigation solution depends strongly on the inertial sensors employed: accelerometers and gyroscopes (the term gyroscope is also used for angular rate sensor in the thesis) and on the algorithms utilized for data processing.

The most precise sensors are ring laser gyroscopes (RLGs), fiber optic gyroscopes (FOGs) and servo and Quartz accelerometers (ACCs) which belong to the navigation grade category. Nowadays, these sensors are mainly used on transport airplanes, helicopters, etc. Their main disadvantage is that they are too expensive, thereby limiting their usage. In applications where it is not possible to use these sensors, because their price is comparable to price of navigated object, the alternative Micro-Electro-Mechanical-Systems (MEMS) can be used. The technological progress in precision of MEMS has enabled their usage in cost-effective applications, such as in UAVs or small aircrafts [5], [6]. They provide low power consumption, light weight, small size and low price. On the other hand they have some weaknesses, such as low resolution, a high level of noise, worse bias stability, etc., limiting their usage in navigation systems. Due to the aforementioned weaknesses, MEMS-based inertial sensors are not able to provide a standalone navigation solution, so they need to be combined with other sources such as GNSS, a magnetometer, a pressure-based altimeter, an ultrasonic sensor for distance measurement, a visual odometer, electrolytic tilt sensor (ETS), etc. The fusion of inertial sensors and aiding sources is currently done via adaptive data processing algorithms which increase the overall accuracy, reliability and robustness of navigation solution.

This doctoral thesis deals with improvement of overall accuracy of the developed inertial navigation system (INS) by means such as usage of alternative sensors, estimation of sensor errors and usage of adaptive attitude estimation approaches. The INS consists of low-cost inertial measurement unit (IMU) which is aided by a triaxial magnetometer and a biaxial electrolytic tilt sensor. The data fusion is performed via the Gauss-Newton method (GNM) and extended Kalman filter (EKF) in quaternion domain.

The doctoral thesis is organized as follows. In chapter 2, the objectives of the doctoral thesis are defined, and the current state of the art is described in chapter 3. Results, in the form of the six most significant journal and conference papers of the author, are related to the thesis and presented in chapter 4. They describe the calibration procedures of accelerometers, gyroscopes and magnetometers, an overview of electrolytic tilt sensors utilization in navigation systems, the correction of accelerometer data by ETS's data and attitude estimation approach which uses the Gauss-Newton method and extended Kalman filter. The additional unpublished results are presented in chapter 5; and the author's contribution, fulfillment of thesis objectives and future work are concluded in chapter 6. The author's publications are listed in Appendix A.

## 2. Aims of the Doctoral Thesis

A main aim of the thesis is improvement of overall attitude estimation accuracy of inertial navigation system (INS) developed primarily for use on UAVs or small aircrafts. Considering the application of INS, it consists of a MEMS-based, low-cost IMU which is not possible to use as a standalone solution, requiring that it is assisted to function properly. As convenient aiding sensors, the triaxial magnetometer and biaxial electrolytic tilt sensor are chosen for fusion with inertial sensors. The intention is paid just to attitude, therefore the objectives are focused on a design and development of adaptive data processing approaches for attitude evaluation in situations when GPS signal is not available.

The partial objectives of the thesis which lead to improvement of INS overall accuracy are as follows:

➤ **Calibration of inertial sensors and magnetometer used in inertial navigation system**

The main aim of this part is definition of deterministic sensor error models (SEMs) and estimation of their parameters. To estimate them, the calibration procedures and algorithms are proposed, realized and the influence of applied compensations is analyzed for both types of inertial sensors and magnetometer.

➤ **Usage of electrolytic tilt sensor in navigation systems**

This part of the thesis is focused on usage of ETS in navigation systems to improve the final accuracy of attitude estimation. The ETS is finally used for correction of triaxial accelerometer initial bias error under static conditions and for corrections of acceleration under low-dynamic conditions.

➤ **Evaluation of adaptive data processing approaches for attitude estimation**

This part deals with the implementation of adaptive data processing approaches for attitude estimation. To aid data from triaxial accelerometer, triaxial magnetometer and biaxial electrolytic tilt sensor, the Gauss-Newton method (GNM) is implemented and the resultant product of GNM is then fused with gyroscope data via extended Kalman filter.

The design and realization of INS using the aforementioned sensors include hardware as well as software realization. The developed algorithms are firstly evaluated using simulations and finally the attitude estimation accuracy is evaluated and confirmed using real flight data measured on UAV.

### 3. Current State of the Art

Inertial navigation systems provide information on orientation, position and velocity of navigated object. The core of INS is based on an Inertial Measurement Unit (IMU) containing accelerometers and gyroscopes. Thus, the accuracy of the navigation solution depends on the precision of the sensors, their performance and the algorithms utilized for data processing. The most precise sensors, and also most expensive, are RLGs, FOGs, servo and Quartz ACCs. Unfortunately, their usage is limited because often their price is comparable to or higher than that of object navigated. Due to this reason, the MEMS based IMUs are used nowadays as an alternative. They have many advantages allowing them to be used in a wide range of applications. On the other hand, their usage is limited due to used technology imperfections such as misalignments, temperature dependency, etc., and weaknesses such as low resolution and so on. These imperfections need to be compensated for, corrected, and adaptively processed for proper function of an INS.

Since low-cost MEMS inertial sensors are employed, there are some limitations in comparison with precise sensors such as RLGs, servo ACCs, etc. To achieve the accuracy for the desired application, the MEMS accelerometers and gyroscopes cannot be used as a standalone solution for attitude and position estimation. They need to be combined with other sources such as GNSS, a magnetometer, a pressure-based altimeter, an electrolytic tilt sensor (ETSS), etc.

Accordingly, this doctoral thesis aims at dealing with improving the overall accuracy of the proposed INS and with the state of the art overview through three main areas of research:

- calibration of triaxial accelerometers, gyroscopes, and magnetometers,
- usage of electrolytic tilt sensors in navigation systems,
- algorithms and methods for attitude estimation.

#### 3.1. Inertial Sensors and Magnetometer Calibration

Over the past decades, the MEMS inertial sensors and magnetometers have been widely used due to their small size, light weight, low power consumption and low price [7]. On the other hand, they have imperfections caused by manufacturing technology which need to be compensated for their proper function [8]. Although the manufacturers perform the sensor calibration, it is not good enough, and therefore, individual sensors must be calibrated [3], [9]. The calibration process means to identify the parameters of the deterministic sensor errors such as scale factors, non-orthogonality angles, offsets, and measuring framework misalignments [1], [3], [10], [11]. These errors are further applied to be called sensor error model (SEM). For identifying SEMs' parameters, a wide range of calibration approaches are well known, but their usage is often limited by a precise and thus very expensive positioning platform [11] - [16]. The current research aims to design and realize calibration approaches that save process time, overall workload, and costs [3].

In case of accelerometer calibration, the Earth Gravity Field (EGF) is commonly and with advantage used as a reference [12], [17]. Further, several calibration procedures and algorithms with different workloads and using different SEMs are known. One example of a simple calibration process is based on measuring six static positions used only for scale factor and offset determination [12], [17];

but, the calibration accuracy strongly depends on the alignment accuracy [9]. The precise alignment for calibration purposes can be done, for example, by a 3D optical tracking system [10], robotic arm [12] or a 3D positioning platform [18]. Using these platforms, the SEMs with more parameters than the scale factors and offsets can be estimated by several estimation techniques such as a nonlinear least square algorithm [12], fminunc Matlab function, Newton method [19], a linearized and modified ellipsoid fitting algorithm [20], Quasi-Newton factorization algorithm [21] and so on.

When magnetometers are calibrated, it is possible to use similar SEMs and algorithms for parameter determination as to those in the case with accelerometers. Similarly to EGF, the Earth Magnetic Field (EMF) is in most calibration approaches utilized as a reference but the close attention should be paid to data measurement procedure which supposes the homogenous and non-disturbed EMF [11], [18]. Due to this reason, it is hard to perform calibration under laboratory conditions using EMF [22]. To calibrate magnetometers, for example in laboratory environment, it is possible to use another approach without using EMF, such as system which uses 3D Helmholtz coils [23]. The principle of this is a system in which the sensor is stationary and the magnetic field generated by the 3D Helmholtz coils is rotated around the sensor.

In the case of gyroscope calibration, it is possible to use the Earth's rotation as a reference value [24]. It can be employed in cases of RLGs, FOGs, and precise MEMS gyroscopes, when the sensors are able to resolve the Earth's angular rate. In the case of low-cost MEMS gyroscopes calibration, the Earth rotation is mostly under their resolution and thus the calibration cannot be performed in this way. This leads to using devices such as single-axis turntable [14], [15], [19] a bike wheel as a turntable [25], or a dual-axis rotational gimbal motion system [26]. For estimation of SEMs' parameters, the different algorithms can be applied. The algorithm for automatic real-time offset calibration is proposed in [15], the other possible algorithm is based on non-linear least squares method [14], Newton's method [19] or Gauss-Newton iterative algorithm [26].

In this doctoral thesis, the SEMs are defined for inertial sensors and the magnetometer; and the calibration procedures are proposed for all sensors. In terms of accelerometers and magnetometers, the iterative algorithm such as Levenberg-Marquardt is proposed, implemented, and evaluated. For gyroscope calibration, the procedure which requires only a simple manually-driven platform is implemented according to [1]. For estimation of parameters, the Cholesky decomposition and LU factorization are used. All applied compensations are successfully evaluated by several analyses. The calibration approaches are presented in chapter 4 in selected papers [3], [27], [28].

### 3.2. Usage of Electrolytic Tilt Sensor for Attitude Determination

Using tilt sensors is one of possible ways to determine the pitch and roll angles (orientation or inclination angles). Based on principle of tilt measurements the several types of tilt sensors such as MEMS accelerometer (MEMS ACC) based tilt sensor, electrolytic tilt sensor, optical tilt sensor, or magnetoresistive tilt sensor exist [29]. As the most sufficient sensors for aerial applications, the MEMS ACC-based tilt sensors and electrolytic tilt sensors can be used.

The principle of these sensors is the determination of an object's tilt angles with respect to gravity. In the case of MEMS ACC-based tilt sensors, the core of the sensor consists of a proof of mass which is

connected by flexible beams to the fixed sensor part. The proof of mass as well as the fixed part contains electrodes – sensing fingers forming differential capacitors. If the sensor is tilted, the mass changes its position respecting the applied acceleration, thus the position of flexible electrodes is also changed causing the change of capacitance which leads to tilt angle observability [30].

In the case of an electrolytic tilt sensor, the body of the sensor is formed by three electrodes for single axis sensor and five electrodes for dual-axis sensor and fluid electrolyte. When the sensor is tilted, the fluid inside the sensor covers more or less the outer electrodes. This causes the conductive path to present a ratio between the electrodes. Electrically, the ETS provides an output voltage which is proportional to the tilt angles and thus it can be compared to a potentiometer with the wiper forming the common electrode [31], [32].

Focusing on ETSs, they are designed to measure angles along two axes [32], [33] in a wide range applications that include, but not limited to, aircraft avionics, machine tool leveling, geophysical monitoring, construction lasers, constructions equipment, systems for platform and camera stabilization, as magnetometer correction in compasses [34], geophysical tilt meters, industrial application, etc. [31] - [37]. The performance of an ETS is based on several properties, including the low noise of the sensor, excellent repeatability, stability, environmental durability, and accuracy when operating at low frequencies [38], [39]. According to [35], [36], [39] they can be used under conditions of extreme temperature, humidity, dynamics conditions, and shock with very good linearity and high resolution. On the other hand, the main disadvantage of ETSs is that they can be significantly influenced by cross-coupling errors and long-term electrolyte stability [40]. Thus, for the best performance, the sensors should be calibrated before they are used [41].

Compared to electrolytic tilt sensors, MEMS-based sensors generally are smaller in size and lower in cost, making them attractive components for use in manufacturing. On the other hand, most MEMS-based sensors require stable voltage power supplies which increase their manufacturing costs. Properly designed ETSs have an advantage of ratiometric measurements not affected by the variations of power supply. While the performance of MEMSs has improved, they still cannot compete with ETSs in high-repeatability applications. The high-end ETSs typically provide a sub-arc-second repeatability; even low-cost products can provide the five-arc-second repeatability [39]. The other advantage is that ETSs do not have any moving parts to wear out; they can have long lifetimes and can handle vibration and shock [32].

Nowadays, ETSs are employed in applications where static or quasi-static conditions are ensured or under slow movements [42], [43] such as in low-cost head gesture recognition system [44], in fusion with gyroscopes for attitude estimation [45] or in the six-wheel robotic platform [42].

Innovations in ETSs development increase their performance and durability. For example, novel thick film-based glass ETSs are able to measure with sub-arc second repeatability at significantly lower cost, ceramic sensors are able operate in high temperatures, and so on. With recent and emerging innovations, ETSs continue to be a proven, reliable, and cost-effective technology [39], [46].

In this doctoral thesis, the biaxial ETS is employed to increase the overall accuracy of attitude estimation. The five ETSs with different parameters are analyzed and the most suitable sensor is chosen. It is used for determining the triaxial accelerometer initial bias error under static conditions and, during

the flight, accelerometer data corrections are used under low dynamics. The suitability of ETS usage is confirmed according performance analyses in chapter 4 and in papers [47], [48], [49].

### 3.3. Algorithms and Methods for Attitude Estimation

As stated earlier, for obtaining the navigation solution the IMU contains accelerometers and gyroscopes that measure acceleration/angular rate in 3-dimmensional coordinate system. When precise sensors such as RLG and servo accelerometers are employed, it can be possible to use INS as a standalone system. However, for MEMS-based sensors, other sources of information must be added.

If only the attitude (roll, pitch, yaw angles) is required, the accelerometer, gyroscope and magnetometer are used for data processing and they form a so-called Attitude and Reference Heading System (AHRS). If the algorithm of attitude determination is extended to incorporate position and velocity estimation, an Inertial Navigation System (INS) is created. The following state of the art overview is focused on the INS part of attitude estimation using low-cost sensors.

The most commonly used attitude representation approaches employed in navigation systems are Euler angles (roll, pitch, and yaw) [49], [50], [51], and quaternions [52], [53]. The overview describing the attitude representation approaches and their transformations are presented in [54].

The simplest attitude determination approach is based on gyroscope-only data by numerical integration of angular rates [50]. Since the gyroscope data is burdened with imperfections, the attitude estimation is limited to a short time; thus, for longer periods, the use of additional aiding sources takes place. To aid attitude determination, sensors or systems such as accelerometers and magnetometers, GPS, or cameras are commonly used to limit unbounded error caused by the integration of noises included in measured angular rates [55] - [58].

To fuse inertial sensors and aiding sources data for obtaining the attitude, several estimation techniques can be applied. An efficient and cost effective way of attitude estimation is done via a complementary filter [56], [59], [60]. It combines the long-term stability of roll, pitch and yaw angle estimates based on accelerometer and magnetometer data with short-term stability of integrated angular rates.

The other commonly used estimation technique for aided attitude estimation and for suppression of measurement noise is a Kalman Filter (KF) [61], [62]. Though originally designed for linear systems, it has been modified for nonlinear solutions and is known as an Extended Kalman Filter (EKF). There are two possible implementations of EKF: total state (direct) and error state (indirect) which are described in [50], [63]. The tutorial summarizing the implementation and description of linearized and extended KFs with navigation solution examples is published in [64]. An alternative to EKF can be, for example, an Unscented Kalman Filter (UKF). The difference between these approaches lies in that the EKF linearizes the model through the Jacobians or Hessians, while the UKF computes the estimates of the state vector through a nonlinear model directly, and thus, the estimation is more accurate than in the case of EKF [53], [65].

Another kind of estimation technique method relies on estimation techniques coming from the artificial intelligence research community. For example, the attitude estimation approach which relies on a digital neural network is presented in [66], the INS/GPS data fusion via the Monte Carlo method is

evaluated in [67]. Although many different approaches for attitude estimation exist, the EKF is still the standard and commonly-used estimation technique [50].

A different approach for attitude estimation utilizes a combination of EKF and other optimization algorithms which preprocesses the data from accelerometers and magnetometers. There are several possible optimization algorithms such as the Gauss-Newton method (GNM) [68], [69], the gradient descent method [70], the Quest algorithm [71], and the Factored Quaternion Algorithm (FQA) [71]. The usage of these optimization algorithms reduces the state space model applied in EKF and thus simplifies the evaluation process and decrease the calculation load [71], [72]. Despite the better performance of FQA and Quest compared to GNM or similar approaches, for aircraft parameter estimation purposes, the GNM is still widely used [69], [73].

In this doctoral thesis the approach utilizing the combination of EKF with Gauss-Newton optimization algorithm in quaternion domain is employed. The GNM uses data from accelerometer, magnetometer, and also from an electrolytic tilt sensor. The resulting quaternion computed by GNM is then fused with gyroscope data via EKF. The performance analyses of EKF with GNM are presented in chapter 4 and in [49].

## 4. Published Results

This chapter deals with author's results related to his doctoral thesis. It is written in the form of the reviewed journal and conference papers. This format is approved by a directive issued by the Dean of Faculty of Electrical Engineering (FEE) of Czech Technical University in Prague (CTU) called "*Directive of the Dean for dissertation theses defense at CTU in Prague, FEE*"<sup>1</sup>. In the following, the author's six most important journal and conference papers relevant to the topic of the doctoral thesis are presented, with co-authorship at least 50%. The rest of author's papers are listed in the Appendix A.

Considering chapter 2, there are described tasks which deal with the design and development of INS and with improving of its accuracy. In the INS, the low-cost MEMS based inertial sensors (accelerometers and gyroscopes), magnetometer, and biaxial electrolytic tilt sensor are employed. The intention is paid to algorithms for attitude estimation only, thus the GPS receiver is not used in this work. The final application is focused on INS usage for example on UAVs and small aircrafts in GPS denied applications.

First of all, the calibration process needs to be performed to eliminate the sensors' deterministic errors. Although the most of sensors are calibrated by the manufacturer, the calibration is not good enough in most cases and the additional calibration can take a place. It means to find parameters of sensor error model as scale factors, non-orthogonality angles, offsets, etc. The overview on the triaxial accelerometer calibration, SEM parameters identification, sensor errors compensation and proposal of new calibration procedure is described in paper:

- Šipoš, M. - Pačes, P. - Roháč, J. - Nováček, P.: „Analyses of Triaxial Accelerometer Calibration Algorithms“, *IEEE Sensors Journal*, 2012, vol.12, no.5, p.1157-1165, ISSN 1530-437X, DOI: 10.1109/JSEN.2011.2167319, co-authorship: 65%, IF: 1.852.

The slightly extended SEM is defined for triaxial gyroscope calibration. In comparison with accelerometer's SEM, it contains also an alignment matrix. The SEM as well as the estimation of its parameters, calibration procedure and results after sensor error compensation are described in details in following paper. Additional unpublished results related to gyroscope calibration are mentioned in chapter 5.1.

- Šipoš, M. - Roháč, J.: „Calibration of Tri-axial Angular Rate Sensors“, *Proceedings of z 10<sup>th</sup> International Conference Measurement, Diagnostics, Dependability of Aircraft Systems, Brno, University of Defence, Faculty of Military Technology*, p. 148-152, 2010, ISBN 978-80-7231-741-7, co-authorship: 80%, IF: --.

In the case of the triaxial magnetometer, the slightly modified accelerometer calibration procedure is used for parameters estimation. The magnetometer calibration procedure, estimated SEMs' parameters of accelerometer and magnetometer and analyses of the influence of SEMs' compensation to yaw angle estimates are described in paper:

- Šipoš, M. - Roháč, J.- Nováček, P.: „Improvement of Electronic Compass Accuracy Based on Magnetometer and Accelerometer Calibration“, *Acta Physica Polonica A*, 2012, vol. 121, no. 4, p. 1111-1115, ISSN 0587-4246, co-authorship: 70%, IF: 0.604.

---

<sup>1</sup> <http://www.fel.cvut.cz/cz/vv/doktorandi/predpisy/SmobhDIS.pdf>

Although the triaxial accelerometer is calibrated, its performance can be improved by other aiding sensors. For these purposes, the electrolytic tilt sensor is used and evaluated in this thesis. The overview about principle and parameters of ETSs and analyses of different ETSs from viscosity point of view under static and dynamic conditions are published in the following paper. The unpublished results and analyses of five ETSs are summarized in chapter 5.2.

- Šipoš, M. - Roháč, J.: „Comparison of Electrolytic Tilt Modules for Attitude Correction“, *Proceedings of z 12<sup>th</sup> International Conference Measurement, Diagnostics, Dependability of Aircraft Systems, Brno, University of Defence, Faculty of Military Technology, 2012*, p. 3-13, ISBN 978-80-7231-894-0, co-authorship: 80%, invited paper, IF: --.

To confirm that the electrolytic tilt sensor is useful for improvement of triaxial accelerometer performance, several characteristics under static conditions are measured and analyzed. The results presented in the following paper show that the usage of ETS can reduce the accelerometer initial bias error and thus it can improve the final accuracy of attitude determination. The procedure of initial bias error estimation is described in chapter 0.

- Šipoš, M. - Roháč, J. - Nováček, P.: „Analyses of Electronic Inclinometer Data for Tri-axial Accelerometer's Initial Alignment“, *Przeglad Elektrotechniczny, 2012, vol. 88, no. 01a, p. 286-290, ISSN 0033-2097*, co-authorship: 60%, IF: 0.24 (2011).

Since the low-cost IMU is used as a part of INS, it is not possible to use it as a standalone system because the sensors' imperfections causing the unbounded error in attitude estimation by numerical integration of measured angular rates. To reduce these errors, the adaptive algorithms (KF is commonly used) which fuse data from IMU and aiding sources are used for attitude estimation. The last provided paper

- Šipoš, M. - Šimánek, J. - Roháč, J.: „Practical Approaches to Attitude Estimation in Aerial Applications“, *International Journal of Aerospace Engineering, ISSN 1587-5974, (submitted for publication 2014)*, co-authorship: 50%, IF: --.

deals with design and realization of Extended Kalman Filter with Gauss-Newton minimization method. This approach is used for attitude estimation based on data from accelerometer, gyroscope, magnetometer and electrolytic tilt sensor and it is evaluated on real flight data obtained from sensors mounted on UAV Bellanca Super Decathlon XXL. The complete GNM and EKF algorithm, analyses of applied compensations and corrections on final accuracy of attitude estimation in GPS denied environment are presented. The results are also compared to results of other approaches for attitude estimation.

## 4.1. Analyses of Triaxial Accelerometer Calibration Algorithms

# Analyses of Triaxial Accelerometer Calibration Algorithms

Martin Šipoš, Pavel Pačes, *Member, IEEE*, Jan Roháč, and Petr Nováček

**Abstract**—This paper proposes a calibration procedure in order to minimize the process time and cost. It relies on the suggestion of optimal positions, in which the calibration procedure takes place, and on position number optimization. Furthermore, this paper describes and compares three useful calibration algorithms applicable on triaxial accelerometer to determine its mathematical error model without a need to use an expensive and precise calibration means, which is commonly required. The sensor error model (SEM) of triaxial accelerometer consists of three scale-factor errors, three nonorthogonality angles, and three offsets. For purposes of calibration, two algorithms were tested—the Levenberg–Marquardt and the Thin-Shell algorithm. Both were then related to algorithm based on Matlab *fminunc* function to analyze their efficiency and results. The proposed calibration procedure and applied algorithms were experimentally verified on accelerometers available on market. We performed various analyses of proposed procedure and proved its capability to estimate the parameters of SEM without a need of precise calibration means, with minimum number of iteration, both saving time, workload, and costs.

**Index Terms**—Accelerometers, calibration, error analysis, inertial navigation.

## I. INTRODUCTION

OVER the last decades technological progress in the precision and reliability of Micro-Electro-Mechanical-Systems (MEMS) has enabled the usage of inertial sensors based on MEMS in a wide range of military and commercial applications, e.g., in Unmanned Aircraft Systems (UASs), indoor and personal navigation, human motion tracking, and attitude-control systems [1]–[5].

The Inertial Measurement Unit (IMU), which forms a basic part of Inertial Navigation System (INS), primarily contains only inertial sensors—accelerometers and angular rate sensors or gyroscopes to provide inertial data, and additionally magnetometers. The major errors of electronically-gimballed navigation systems with accelerometers and magnetometers

Manuscript received May 13, 2011; revised August 01, 2011; accepted August 24, 2011. Date of publication September 08, 2011; date of current version April 11, 2012. This work was supported in part by the Czech Science Foundation project 102/09/H082; in part by the Research Program No. MSM6840770015 “Research of Methods and Systems for Measurement of Physical Quantities and Measured Data Processing” of the CTU in Prague sponsored by the Ministry of Education, Youth, and Sports of the Czech Republic; and in part by the Grant Agency of the Czech Technical University in Prague under Grant SGS10/288/OHK3/3T/13. The associate editor coordinating the review of this paper and approving it for publication was Prof. Boris Stoeber.

The authors are with the Department of Measurement, Faculty of Electrical Engineering, Czech Technical University in Prague, Technická 2, 166 27 Prague, Czech Republic (e-mail: sipošmar@fel.cvut.cz; pacesp@fel.cvut.cz; xrohac@fel.cvut.cz; petr.novacek@fel.cvut.cz).

Digital Object Identifier 10.1109/JSEN.2011.2167319

are caused by sensor triplet deviations (mutual misalignment) [6], and therefore, a calibration has to take a place for their proper function. The calibration is necessary to be performed to estimate sensor errors like nonorthogonalities (misalignment) and scale factor errors for their compensation. Factory based sensor calibration is an expensive and time-consuming process, which is typically done for specific high-grade IMUs. For low-cost inertial sensors, such as MEMS based ones, manufacturers perform only basic calibration [7] which is very often insufficient, because even small uncompensated imperfections can cause position deviation growth and also inaccuracy in tilt angle evaluation [8], [9].

There are already known different sensor error models (SEMs) [10] and calibration methods based on different principles, but they have limitations such as the necessity of precise position system or a platform providing precise alignment. This requirement increases manufacturing costs, and therefore, there is a need for investigating alternatives.

One example of a commonly used calibration procedure described by Titterton and Weston in ([11] p. 238) and by Won in [8] uses six static positions, in which the sensors’ axes are consecutively aligned up and down along the vertical axis of the local level frame. The calibration is capable to determine only offsets and scale factor errors, not nonorthogonalities. The calibration accuracy strongly depends on the alignment precision [7]. To increase the precision of alignment an accurate reference system is usually used, as presented in [10], [11]. In the first case a 3-D optical tracking system and nonlinear least squares algorithm were applied, the other case used an *fminunc* Matlab function as a minimizing algorithm and a robotic arm. In both cases the calibration is capable to estimate sensor’ axes misalignments, offsets, and electrical gains/scale factors, which define nine-parameter-error model. The same model for a triaxial accelerometer can be estimated by an iterative calibration procedure described by Petrucha *et al.* in [12] using an automated nonmagnetic system, or the one described by Syed *et al.* in [7], in which offset and scale factor initial values are required for a modified multiposition method. Other method for an accelerometer calibration, presented by Skog and Hänel in [13], is based on the cost function formulation and its minimization with respect to unknown model parameters using Newton’s method. The cost function can reach several local optima, and therefore, the initial starting values have to be determined. Automatic adaptive method of a 3-D field sensor based on a linearized version of an ellipsoid fitting problem has been published in [14]. It relies on a procedure that fits an ellipsoid to data using linear regression. Based on estimated ellipsoid parameters the unknown model parameters can be evaluated. An alternative to this method using modified ellipsoidal-fitting procedure has

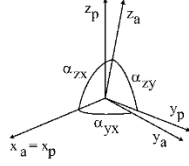


Fig. 1. Orthogonalization of sensor frame; a—nonorthogonal sensor frame; p—orthogonal sensor frame.

been described by Bonnet *et al.* in [15]. He proved that an ellipsoid fitting using either linear optimization (Merayo's algorithm) or nonlinear optimization (Quasi-Newton factorization algorithm) is robust with data sets from static positions obtained within free rotations along a vertical axis in case of accelerometers and free rotations along East-West axis in case of magnetometers.

In Section II, the SEM of triaxial accelerometer is described. We present three algorithms for its calibration in Section III; the Levenberg–Marquardt algorithm, the Thin-Shell algorithm, and an algorithm based on Matlab *fminunc* function. First two algorithms were related to third one, which was used as a reference, in order to have a means for the comparison of algorithms efficiency. In Section IV, we shortly present the most important parameters of calibrated sensors and used measurement setup. To compare a calibration effect on measured and evaluated data based on applied algorithms and SEMs we used a Rotational-Tilt Platform with precise positioning capability to provide precise tilt angles. The experiments, analyses, and result accuracy are provided in Section V.

## II. SENSOR ERROR MODEL

For triaxial accelerometer calibration we considered the sensor error model (SEM), which consisted of nine unknown parameters—three scale factor corrections, three angles of nonorthogonality, and three offsets. The SEM can be defined as (1). Offset forms a stochastic part of biases and can be modeled as a random constant. The time variant part of the bias is drift, which changes based on environmental and other sensor conditions. The calibration process is supposed to be performed during short-time period; therefore, drift can be considered as zero

$$\begin{aligned} a_p &= T_a^p \text{SF}_a (a_m - b_a) \\ &= \begin{pmatrix} 1 & 0 & 0 \\ \alpha_{yx} & 1 & 0 \\ \alpha_{zx} & \alpha_{zy} & 1 \end{pmatrix} \begin{pmatrix} \text{SF}_{ax} & 0 & 0 \\ 0 & \text{SF}_{ay} & 0 \\ 0 & 0 & \text{SF}_{az} \end{pmatrix} \\ &\quad \times \left( \begin{pmatrix} a_{mx} \\ a_{my} \\ a_{mz} \end{pmatrix} - \begin{pmatrix} b_{ax} \\ b_{ay} \\ b_{az} \end{pmatrix} \right) \end{aligned} \quad (1)$$

where  $a_p = [a_{px}, a_{py}, a_{pz}]^T$  is the compensated vector of a measured acceleration defined in the orthogonal system (platform frame);  $T_a^p$  denotes matrix providing transformation from nonorthogonal frame to orthogonal one with nondiagonal terms  $\alpha_{yx}, \alpha_{zx}, \alpha_{zy}$  that correspond to the axes misalignment (nonorthogonality angles) (Fig. 1);  $\text{SF}_a$  represents a scale factor matrix;  $b_a = [b_{ax}, b_{ay}, b_{az}]^T$  is the vector of sensor off-

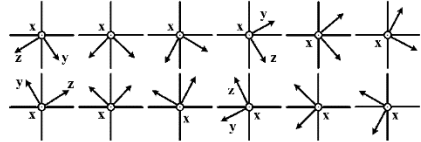


Fig. 2. Positions for calibration; rotation around x axis.

sets;  $a_m = [a_{mx}, a_{my}, a_{mz}]^T$  denotes the vector of measured accelerations. The SEM and its derivation are described in more detail in [13] and [16].

## III. CALIBRATION ALGORITHMS

This section briefly describes the algorithms for triaxial accelerometer calibration—Levenberg–Marquardt (LM) algorithm, Thin-Shell (TS) algorithm, and algorithm based on Matlab *fminunc* function. The fundamental principle of the proposed calibration procedure is based on the fact that the magnitude of measured acceleration should be equal to the gravity magnitude, which is ensured by static conditions (2). It corresponds to “scalar field calibration” used in [17]. The proposed procedure uses only general knowledge about the applied quantity, which is in contrast to the case when precise positioning system is available, and thus, the knowledge about precise tilt angle is also provided in all steps of iteration

$$g_x^2 + g_y^2 + g_z^2 = |g|^2 \quad (2)$$

where  $g_i$  denotes sensed acceleration in direction of  $i$  axis and  $|g|$  is the magnitude of gravity vector, ideally equal to  $1g$ .

To obtain the most accurate estimation without the need of having a precise positioning system, the sensor should be consecutively placed to positions in manner to cover the whole globe surface and the sensor should be influenced only by gravity. In practice, it is not possible to do so, because the number of measurements would be infinite. Therefore, in the proposed procedure, the number of positions is optimized and suggested their orientation, in which a high influence of all errors is expected. Only 36 positions are used, 3 times 12 positions along  $x, y, z$  axis. The positions along  $x$  axis are shown in Fig. 2. Precise knowledge of their orientations is not required, only 3 positions per quadrant are recommended.

### A. Principle of Levenberg–Marquardt Algorithm

The Levenberg–Marquardt (LM) algorithm is one of the most efficient and popular algorithms. It has better convergence than the other ones for nonlinear minimization. The LM algorithm is widely utilized in software applications, neural networks, and curve-fitting problems [18]–[21]. The LM algorithm combines two algorithms: the Gradient Descent (GD) and the Gauss–Newton (GN) algorithm [22]. The LM algorithm can be described by (3)

$$S(\beta) = \sum_{i=1}^m [y_i - f(x_i, \beta)]^2 = \sum_{i=1}^m q_i(\beta)^2 \quad (3)$$

where  $S(\beta)$  denotes the sum of residuals  $q_i(\beta)^2$ ;  $m$  is the number of measurements;  $x_i$  are measured data;  $y_i$  are the reference values, and  $\beta$  is a vector of parameters being estimated

and forming the SEM defined in (1). The LM algorithm is iterative algorithm reducing  $S(\beta)$  with respect to the parameters in vector  $\beta$ .

1) *Gradient Descent Algorithm*: The Gradient Descent (GD) algorithm is a minimization algorithm updating the estimated parameters in the direction opposite to the gradient of the cost function. The GD algorithm is highly convergent and can be used for problems with thousands of parameters forming the cost function. The  $h_{\text{GD}}$  modifies the GD algorithm step to reduce  $S(\beta)$  in the direction of steepest descent and is defined by (4) [22]

$$h_{\text{GD}} = \alpha J^T W (y_i - f(x_i, \beta)) \quad (4)$$

where  $\alpha$  is a parameter corresponding to the length of step in the steepest descent direction;  $J$  is the Jacobian related to the vector  $\beta$ ;  $W$  is the weighting diagonal matrix [22].

2) *Gauss–Newton Algorithm*: A main advantage of Gauss–Newton (GN) algorithm is its rapid convergence; however, it depends on the initial conditions. The GN algorithm does not require the calculation of second-order derivatives [21]. The equation for GN algorithm reducing  $S(\beta)$  is given by (5)

$$[J^T W J] h_{\text{GN}} = J^T W (y_i - f(x_i, \beta)) \quad (5)$$

where  $h_{\text{GN}}$  denotes the GN algorithm update of estimated parameter leading to a minimization of  $S(\beta)$ .

3) *Levenberg–Marquardt Algorithm*: As was mentioned, the Levenberg–Marquardt (LM) algorithm combines both the GD and GN algorithm. In the LM algorithm, the parameter  $h_{\text{LM}}$  is adaptively weighted with respect to  $h_{\text{GD}}$  and  $h_{\text{GN}}$  to reach optimal progress in  $S(\beta)$  minimization, and thus, the LM algorithm equation is given by (6)

$$[J^T W J + \lambda \text{ diag}(J^T W J)] h_{\text{LM}} = J^T W (y_i - f(x_i, \beta)) \quad (6)$$

where  $\lambda$  is a damping parameter and  $h_{\text{LM}}$  is the LM algorithm update. The parameter  $\lambda$  has several characteristics [23]:

- for all  $\lambda > 0$ , the coefficient matrix  $(J^T W J + \lambda \text{ diag}(J^T W J))$  is positive definite, and this fact ensures that  $h_{\text{LM}}$  is descent directional;
- for large values of  $\lambda$  the iteration step (parameter modification) is in the steepest descent direction, which is good when the current stage is far from required solution;
- for small values of  $\lambda$ , the  $h_{\text{LM}} \approx h_{\text{GN}}$  and it is good for final phases of iteration, when estimated parameters are close to required solution.

In other words, if the iteration step decreases the error, it implies that quadratic assumption  $f(x_i)$  is working and  $\lambda$  can be reduced (usually by a factor of 10) to decrease the influence of GD. On the other hand, if  $S(\beta)$  increases,  $\lambda$  is increased by the same factor increasing GD influence and the iteration step is repeated.

#### B. Thin-Shell Algorithm

The Thin-Shell (TS) algorithm is based on an estimation of Linear Minimum Mean Square Error, which is applied on SEM

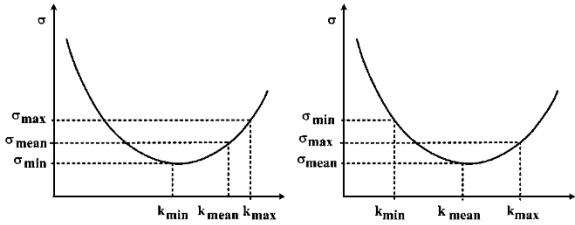


Fig. 3. Criterions for halving the interval, for which the estimated parameters are searched.

(1) of calibrated sensor. According to (1) nine parameters have to be estimated. The iteration is based on successive halving of intervals, in which the estimated parameter is searched for. The intervals are halved based on a standard deviation defined by (7) and if-conditions related to Fig. 3

$$\sigma = \sqrt{\frac{\sum_{i=1}^m (\hat{a}_{xi}^2 + \hat{a}_{yi}^2 + \hat{a}_{zi}^2 - |g|^2)^2}{m-1}} \quad (7)$$

where  $\sigma$  is the standard deviation;  $m$  is the number of positions;  $\hat{a}_{xi}$ ,  $\hat{a}_{yi}$ ,  $\hat{a}_{zi}$  are estimations of compensated measured gravity vector components and  $|g|$  is the magnitude of gravity vector corresponding to the reference value.

At the beginning of the algorithm, the minimal and maximal values of each parameter must be set (it defines the interval, in which the unknown parameter is searched for); the mean value is computed as an average of them. Each iteration cycle can be divided into three steps:

- 1) Min., max, and mean values of the parameter being searched for ( $k_{\min}$ ,  $k_{\text{mean}}$ , and  $k_{\max}$ ) are used for the estimation of compensated accelerations in all positions.
- 2) Three corresponding standard deviations ( $\sigma_{\min}$ ,  $\sigma_{\text{mean}}$ , and  $\sigma_{\max}$ ) are then obtained based on (7). Other parameters are set to their mean values.
- 3) Based on  $\sigma_{\min}$ ,  $\sigma_{\text{mean}}$ , and  $\sigma_{\max}$  the interval, in which estimated parameter should be, is halved according to Fig. 3 and following conditions:
  - if  $(\sigma_{\min} > \sigma_{\text{mean}})$  and  $(\sigma_{\max} > \sigma_{\text{mean}})$ , the interval is reduced to a half around the mean value  $k_{\text{mean}}$ .
  - if  $(\sigma_{\min} < \sigma_{\text{mean}})$  and  $(\sigma_{\text{mean}} < \sigma_{\max})$  the true value of the parameter should be in the interval  $(k_{\min}, k_{\text{mean}})$ ; for the following iteration cycle  $k_{\max} = k_{\text{mean}}$  and  $k_{\text{mean}}$  is computed as a mean value of  $k_{\min}$  and new  $k_{\max}$ .
  - if  $(\sigma_{\max} < \sigma_{\text{mean}})$  and  $(\sigma_{\text{mean}} < \sigma_{\min})$  the true value of the parameter should be in the interval  $(k_{\text{mean}}, k_{\max})$ ; for the following iteration cycle  $k_{\min} = k_{\text{mean}}$  and  $k_{\text{mean}}$  is computed as a mean value of new  $k_{\min}$  and  $k_{\max}$ .

The steps described above are repeated until the computed standard deviation is less than the required value or required number of iteration cycles is reached. Consequently the rest of the parameters are estimated in the same manner. The final value of standard deviation defines the calibration algorithm accuracy. This algorithm is described in more detail in [24].

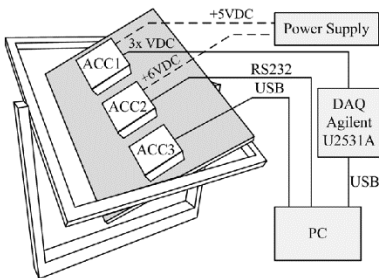


Fig. 4. Measurement setup for triaxial accelerometer calibration; ACC1—CXL02LF3; ACC2—AHRS M3; ACC3—ADIS16405.

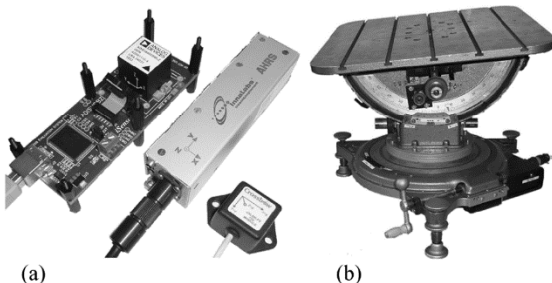


Fig. 5. (a) Calibrated systems (from left): ADIS16405, AHRS M3, CXL02LF3; (b) Rotational-tilt platform.

### C. Algorithm Based on Fminunc Matlab Function

To evaluate the efficiency of Levenberg–Marquardt (LM) and Thin-Shell (TS) algorithms with respect to minimum required number of iterations and reached accuracy Matlab functions *fminunc*, *lsqnonlin*, and *fminsearch* were tested. Based on their performances the function *fminunc* was chosen as a reference and a means for LM and TS algorithm evaluation. Function *fminunc* is based on quasi-Newton minimization with numerical gradients [25]. Its description is not the subject of this paper and can be found [26].

## IV. CALIBRATED SENSORS AND MEASUREMENT SETUP

In this section, we briefly present the systems used for the calibration and measurement setup (Fig. 4) which uses a simple platform enabling to measure accelerometer data in the static positions defined approximately as shown in Fig. 2. Furthermore, we used a Rotational-Tilt Platform (RoTiP), see Fig. 5(b), as a reference for analyses needed to verify the results of the proposed calibration procedure according to applied algorithms. The RoTiP parameters are shown in Table I. Although we evaluated five sensors in sum, such as AHRS M3's accelerometer (Innolabs [27]), ADIS16405's accelerometer (Analog Devices [28]), CXL02LF3 accelerometer (Crossbow [29]), 3DM-GX2's accelerometer (MicroStrain [30]), and STEVAL-MKI062V2's accelerometer (STMicroelectronics [31]), we present the results of analyses only from first three accelerometers of calibrated systems [see Fig. 5(a)]. The analyses of last two sensors were very similar.

TABLE I  
PARAMETERS OF ROTATIONAL-TILT PLATFORM

Parameter	Range	Speed of Motion	Resolution
Pitch	±45 deg	±42 deg/s	0.00033 deg
Roll	±25 deg	±60 deg/s	0.00065 deg
Heading	0 to 360 deg	±310 deg/s	0.00074 deg

## V. CALIBRATION ANALYSES

Three aforementioned algorithms were used to estimate SEMs of three triaxial accelerometers described in Section IV according to measured data in suggested positions. It helped to decrease the influence of manufacturing imperfection on the sensor precision. As said in [32] other problematic errors can show up with incorrect determination of sensor error parameters; therefore, for results, a comparison Root Mean Square Error (RMSE) defined by (8) was used

$$\text{RMSE}(p, g) = \sqrt{\frac{\sum_{i=1}^n (x_i - g)^2}{n}} \quad (8)$$

$$x_i = \sqrt{g_{xi}^2 + g_{yi}^2 + g_{zi}^2}$$

where  $p = (x_1, \dots, x_n)^T$  is  $n$ -dimensional vector;  $n$ —number of evaluated positions;  $g$  is an ideal magnitude of the gravity vector equal to  $1g$ ;  $g_{xi}, g_{yi}, g_{zi}$  are components of the estimated gravity vector.

For the calibration purposes and consecutive analyses we measured the raw data from sensors and evaluated data in 364 positions. The number was chosen with respect to the number of suggested positions in Section III multiplied by 10 and modified to have uniformly spaced data along all axes. The analyses included the observation of estimated parameters of SEM with respect to algorithms applied, the RMSE dependence on the number of taken positions and the number of iterations, and the observation of a long-period permutation of estimated SEMs. Furthermore, the calibration effect on the precision of evaluated tilt angles and the calibration effect from the sensors' drift point of view were performed.

### A. Sensor Error Models

We estimated Sensor Errors Models (SEM) of three accelerometers. Results are listed for LM and TS algorithms in Table II. Although we estimated the SEMs using three algorithms, only LM and TS algorithms' results are listed due to the fact that the results estimated by LM algorithm were identical to the ones from algorithm based on *fminunc* function. From Table II, it can be seen that SEMs estimated by LM and TS algorithms are comparable for all tested units, which also proves the values of RMSE. The effect of SEM applying on measured data is shown in Fig. 6, where magnitude of compensated acceleration vector has approximately 100 times smaller deviation from  $1g$  than the one before calibration.

### B. Dependence of RMSE on Evaluated Data Positions

To prove that only 36 static positions are sufficient for the calibration purposes, we measured 364 positions uniformly spaced, and analyzed the variation of RMSE for the different number of

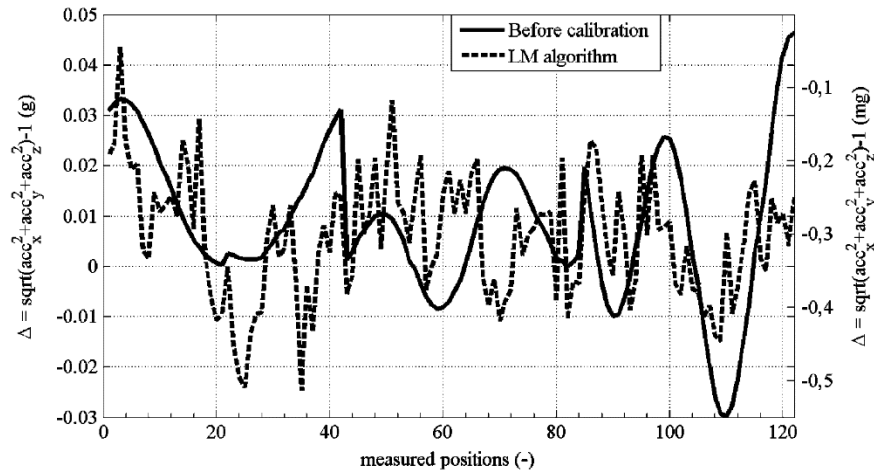


Fig. 6. Dependence of deviations of measured accelerations before (left vertical axis) and after (right vertical axis) calibration using LM algorithm applied on AHRS M3's accelerometer data in evaluated different positions.

TABLE II  
SENSOR ERROR MODELS OBTAINED USING LEVENBERG–MARQUARDT (LM)  
AND THIN-SHELL (TS) ALGORITHM FOR ACCELEROMETERS OF AHRS M3'S  
(AHRS) AND ADIS16405'S (ADIS) AND CXL02LF3 (CXL) ACCELEROMETER

Par	LM AHRS	LM ADIS	LM CXL	TS AHRS	TS ADIS	TS CXL
$\alpha_{\text{ax}}$ (deg)	-0.8758	-0.0230	1.0237	-0.8760	-0.0227	1.0235
$\alpha_{\text{ay}}$ (deg)	3.0286	0.0351	-0.5217	3.0229	0.0350	-0.4476
$\alpha_{\text{az}}$ (deg)	0.1765	-0.1639	-1.4939	0.1784	-0.1639	-1.4829
SF <sub>ax</sub> (-)	0.99865	0.99956	1.05591	0.99866	0.99957	1.05664
SF <sub>ay</sub> (-)	0.98946	1.00194	1.06517	0.98946	1.00194	1.06508
SF <sub>az</sub> (-)	0.98611	0.99828	1.06144	0.98608	0.99828	1.06128
b <sub>ax</sub> (g)	0.00173	-0.01354	-0.00255	0.00172	-0.01353	-0.00272
b <sub>ay</sub> (g)	-0.00602	-0.00671	-0.03445	-0.00598	-0.00678	-0.03675
b <sub>az</sub> (g)	0.01440	-0.00402	0.03690	0.01427	-0.00400	0.04003
RMSE <sup>1</sup>	0.01810	0.00948	0.06628	0.01810	0.00948	0.06628
RMSE <sup>2</sup>	0.00015	0.00252	0.01527	0.00017	0.00252	0.01545

Superscript 1 denotes RMSE before calibration and 2 after calibration.

positions (NoP) in intervals from 12 to 364. NoP can be seen in Table III, where N represents the relationship between Figs. 7–9 horizontal axes and the NoP used for calculation. In each static position, an average of 100 measured data samples was calculated to reduce noise. The dependence between RMSE defined in (8) and NoP is shown in Fig. 7 for AHRS M3, in Fig. 8 for ADIS16405, and in Fig. 9 for CXL02LF3. The RMSE was evaluated between an ideal magnitude of gravity vector and the magnitude of compensated measured gravity. The compensated measured gravity obtained from the measured data multiplication with SEM is further notified as a compensated result. The left vertical axes of Figs. 7–9 correspond to RMSE before calibration and right vertical axes correspond to RMSE after calibration. As a criterion for the evaluation of RMSE dependence on the number of evaluated positions we considered a maximum deviation of RMSE from RMSE in N = 1 position to be equal or less than 1 mg, which corresponds to sensor resolutions. From Figs. 7–9 it can be seen, that 21 positions and more satisfy desired limitation no matter which algorithm was used. This means that the variation of the compensated results in the case of usage

TABLE III  
RELATIONSHIP BETWEEN THE NUMBER OF EVALUATED POSITIONS (NoP) AND  
NOTATION OF FIGS. 7–9 HORIZONTAL AXES (N)

N	NoP	N	NoP	N	NoP	N	NoP	N	NoP
1	364	7	52	13	28	19	20	25	14
2	182	8	46	14	26	20	19	26	13
3	122	9	41	15	25	21	18	27	12
4	91	10	36	16	23	22	17		
5	73	11	34	17	22	23	16		
6	61	12	31	18	21	24	15		

21 positions or more (up to 364) differs under the required value; therefore, further differences are considered as negligible. Because having 7 positions in 360 deg and also in 4 quadrants does not have a uniform distribution with a constant number of positions per quadrant, it is suitable to increase the number to 12. This leads to having 36 positions covering all axes, which was the number we used in Section III-A. The result optimizes the number of positions needed for the calibration with respect to a workload and precision.

### C. Dependence of RMSE on Number of Iterations

Based on the data measured in 36 positions as described in Section III and proven in Section V-B, we analyzed the dependency of RMSE calculated between compensated results and an ideal gravity vector on the number of iterations for LM and TS algorithms. The iteration denotes a calibration cycle, in which all measured data (in our case in 36 positions) are used for an unknown SEM parameter estimation. This analysis relied on the progress of RMSE with respect to the number of iteration. When the deviation from the steady-state value was less than 1 mg we considered the accuracy of calibration to be sufficient. Fig. 10 shows the RMSE dependency on number of iterations for TS algorithm applied on AHRS M3 accelerometer. The comparison between LM and TS algorithms from the number of iterations point of view is presented in Table IV.

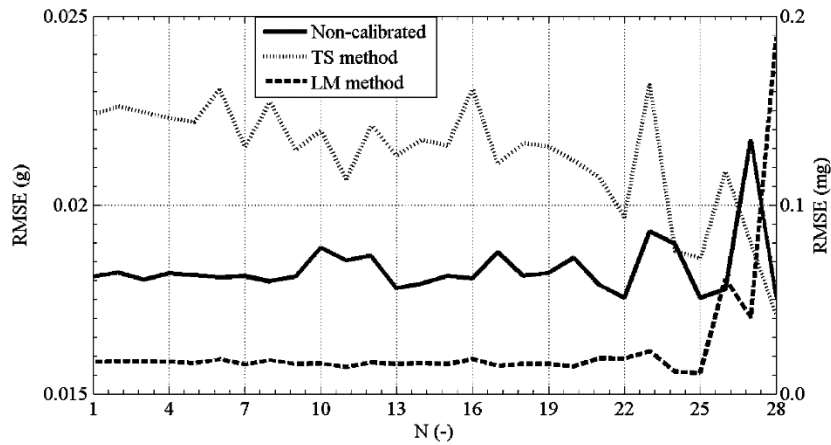


Fig. 7. Dependence of RMSE before (left axis) and after (right axis) calibration on the number of positions using AHRS M3's accelerometer.

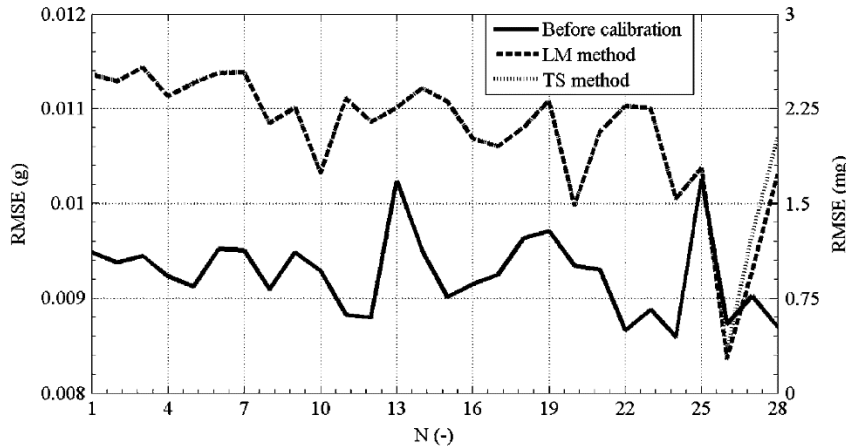


Fig. 8. Dependence of RMSE before (left axis) and after (right axis) calibration on the number of positions using ADIS16405's accelerometer.

#### D. Comparison of SEM During Time Period

We analyzed the variation of SEMs obtained by LM and TS algorithms during a longer time period corresponding to one and half years (the first measurement was taken in April 2009 and the second one was taken in November 2010). We measured 122 positions in both cases with different distributions as shown in Fig. 11. We analyzed the SEMs permutation and their accuracy. The SEMs evaluated based on two data sets using LM and TS calibration algorithms are presented in Table V. In each position the average of 100 data samples was used as in previous analyses.

From Table V it can be seen that parameters are slightly different, which we think was caused by reaching the resolution of the method applied. The influence of different distribution of evaluated positions shown in Fig. 11 is considered as negligible, because the number of evaluated positions was always higher than 21.

#### E. Comparison of Tilt Angles Before and After Calibration

To see the effect of calibration, we performed another analysis in which the tilt angles estimated based on calibration results were compared to the reference ones measured by Rotational-Tilt Platform (RoTiP).

We mounted the accelerometers on RoTiP and tilted them along two axes. A tilt corresponded to pitch ( $\theta$ ) and roll ( $\phi$ ) angles. Specification of RoTiP is listed in Section IV. The pitch angle calculation is defined as (9) and roll angle calculation as (10)

$$\theta = \text{arctg} \left( -f_{by} / \sqrt{f_{bx}^2 + f_{bz}^2} \right) \quad (9)$$

$$\phi = \text{arctg} (f_{bx} / -f_{bz}) \quad (10)$$

where  $\theta$  is the pitch angle;  $\phi$  is the roll angle;  $f_{bx}$ ,  $f_{by}$ ,  $f_{bz}$  are measured accelerations. For computation of  $\text{arctg}$  function, the Matlab function *atan2*, which returns the four-quadrant invert tangent (arctangent) of real parts  $x$  and  $y$ . [2], was used.

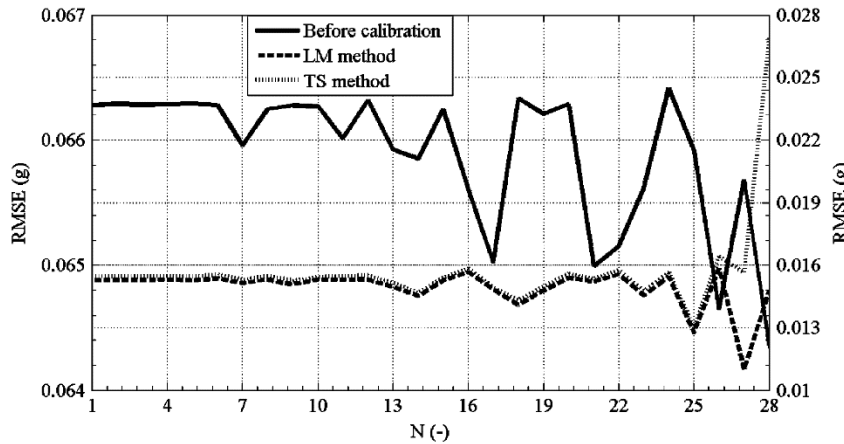


Fig. 9. Dependence of RMSE before (left axis) and after (right axis) calibration on the number of positions using CXL02LF3 accelerometer.

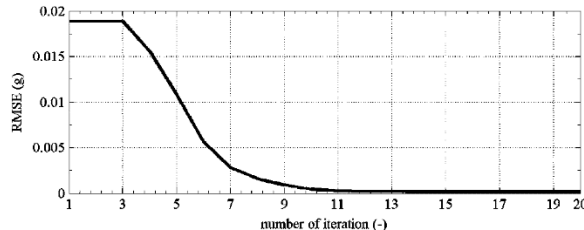


Fig. 10. Dependence of RMSE on the number of iterations for AHRS M3's accelerometer using TS calibration algorithm.

TABLE IV  
NUMBER OF ITERATIONS FOR LM AND TS CALIBRATION ALGORITHMS

	AHRS M3	ADIS16405	CXL02LF3
LM Algorithm	2	1	1
TS Algorithm	9	7	6

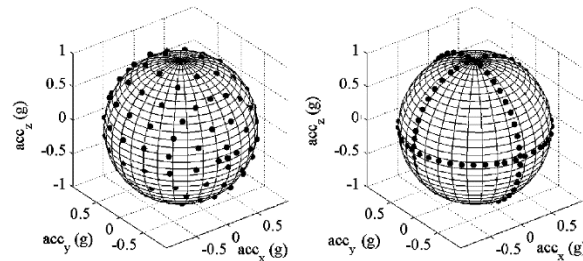


Fig. 11. Evaluated positions in April 2009 (left) and in November 2010 (right).

We analyzed the variation of results when LM and TS algorithms had been applied. The last column of Tables VI–VIII (AHRS M3, ADIS16405, CXL02LF3) describes an Error Percentage Improvement (EPI) which corresponds to the difference between particular deviations (relative errors) related to the maximum angle, i.e., 20 deg. From these tables it can be seen that due to the calibration the tilt angles are more accurate than

TABLE V  
SENSOR ERROR MODELS OBTAINED USING LM ALGORITHM (LM) AND TS ALGORITHM (TS) DURING TIME INTERVAL OF ONE AND HALF YEARS FOR ACCELEROMETER CONTAINED IN AHRS M3

Parameter	LM Apr 2009	LM Nov 2010	TS Apr 2009	TS Nov 2010
$\alpha_{gx}$ (deg)	-0.8769	-0.8758	-0.8830	-0.8760
$\alpha_{ex}$ (deg)	3.0261	3.0286	3.0253	3.0229
$\alpha_{ev}$ (deg)	0.1794	0.1765	0.1818	0.1784
SF <sub>ax</sub> (-)	0.99868	0.99865	0.99902	0.99866
SF <sub>ay</sub> (-)	0.98951	0.98946	0.98828	0.98946
SF <sub>az</sub> (-)	0.98609	0.98611	0.98640	0.98608
b <sub>ax</sub> (g)	0.00153	0.00173	0.00156	0.00172
b <sub>ay</sub> (g)	-0.00541	-0.00602	-0.00527	-0.00598
b <sub>az</sub> (g)	0.01461	0.01440	0.01448	0.01427
RMSE <sup>1</sup>	0.01957	0.01810	0.01957	0.01810
RMSE <sup>2</sup>	0.00014	0.00015	0.00055	0.00017

Superscript 1 denotes RMSE before calibration and 2 after calibration.

TABLE VI  
COMPARISON OF TILT ANGLES BEFORE AND AFTER CALIBRATION USING LM AND TS ALGORITHMS FOR AHRS M3;  $\theta$ —PITCH,  $\phi$ —ROLL

Reference Angle	Without Calibration	LM Algorithm	TS Algorithm	LM EPI
$\theta; \phi$ (deg)	$\theta; \phi$ (deg)	$\theta; \phi$ (deg)	$\theta; \phi$ (deg)	$\theta; \phi$ (%)
0; 0	-0.77; -0.59	-0.70; -0.30	-0.68; -0.26	0.4; 1.5
10; 0	9.18; -0.62	9.61; -0.16	9.62; -0.12	2.2; 2.3
20; 0	19.18; -0.63	20.13; 0.01	20.14; 0.05	3.4; 3.1
0; -10	-0.96; -10.83	-0.90; -10.72	-0.89; -10.69	0.3; 0.6
0; -20	-0.83; -21.10	-0.76; -21.00	-0.75; -21.06	0.4; 0.5
10; -10	9.31; -10.98	9.76; -10.82	9.77; -10.79	2.3; 0.8
20; -20	19.00; -19.62	19.98; -19.76	19.99; -19.72	4.9; 0.7

in case without calibration for all tested sensors and tilt angles.

#### F. Position Determination With and Without Calibration

Furthermore, we analyzed the drift influence on the accuracy of position determination when a compensated model was used. The accelerations were measured for 200 s in a static position with different tilt angles and then two times integrated to get the position. The effect of compensation applied on an

TABLE VII  
COMPARISON OF TILT ANGLES BEFORE AND AFTER CALIBRATION USING LM AND TS ALGORITHMS FOR ADIS16405;  $\theta$ —PITCH,  $\phi$ —ROLL

Reference Angle	Without Calibration	LM Algorithm	TS Algorithm	LM EPI
$0; \phi$ (deg)	$0; \phi$ (deg)	$0; \phi$ (deg)	$0; \phi$ (deg)	$0; \phi$ (%)
0; 0	0.85; -0.29	0.07; 0.10	0.07; 0.10	3.9; 1.0
10; 0	10.80; -0.46	10.09; -0.07	10.09; -0.07	3.6; 2
20; 0	20.66; -0.36	20.04; 0.05	20.04; 0.05	3.1; 1.6
0; -10	1.11; -10.51	0.34; -10.22	0.34; -10.22	3.9; 1.5
0; -20	1.07; -20.35	0.31; -20.15	0.31; -20.15	3.8; 1.5
10; -10	10.92; -10.51	10.23; -10.20	10.23; -10.20	3.5; 1.0
20; -20	20.73; -20.21	20.16; -19.99	20.16; -19.97	2.9; 1.0

TABLE VIII  
COMPARISON OF TILT ANGLES BEFORE AND AFTER CALIBRATION USING LM AND TS ALGORITHMS FOR CXL02LF3;  $\theta$ —PITCH,  $\phi$ —ROLL

Reference Angle	Without Calibration	LM Algorithm	TS Algorithm	LM EPI
$0; \phi$ (deg)	$0; \phi$ (deg)	$0; \phi$ (deg)	$0; \phi$ (deg)	$0; \phi$ (%)
0; 0	4.69; -3.84	-0.43; -0.92	-0.37; -0.75	21.3; 14.6
10; 0	13.48; -3.76	10.71; 0.29	10.54; 0.24	13.9; 17.4
20; 0	21.37; -3.78	20.47; 0.15	20.47; 0.09	4.6; 18.2
0; -10	4.56; -13.25	0.90; 10.37	0.71; -10.31	18.3; 9.4
0; -20	4.63; -22.52	0.94; -20.30	0.74; -20.24	18.5; 11.1
10; -10	13.67; -13.30	10.25; -10.92	10.19; -10.73	17.1; 11.9
20; -20	22.12; -22.37	18.82; -20.75	18.76; -20.54	4.9; 8.2

TABLE IX  
POSITION DETERMINATION IN PLATFORM FRAME BEFORE AND AFTER CALIBRATION USING SEMS GOT FROM LM AND TS ALGORITHMS FOR AHRS M3'S ACCELEROMETER;  $\delta_x, \delta_y, \delta_z$ —DEVIATIONS IN X, Y, Z AXES

Reference Angle	Without Calibration	LM Algorithm	TS Algorithm
$\theta; \phi$ (deg)	$\delta_x, \delta_y, \delta_z$ (m)	$\delta_x, \delta_y, \delta_z$ (m)	$\delta_x, \delta_y, \delta_z$ (m)
0; 0	-239; -56; 5867	7; 2; -160	5; 9; -160
10; 0	-1516; -36; 7224	27; 1; -116	22; 9; -117
20; 0	-3105; 51; 7987	20; -30; -50	10; -22; -54
0; -10	-350; -1078; 6061	-121; 40; -88	-123; 44; -87
0; -20	-721; -2116; 5921	-508; 85; -67	-507; 84; -67
10; -10	-2299; -635; 7555	-674; 828; -30	-680; 832; -31
20; -20	-7555; 1618; 7981	-4553; 5026; 64	-4561; 5025; 22

TABLE X  
POSITION DETERMINATION IN PLATFORM FRAME BEFORE AND AFTER CALIBRATION USING SEMS GOT FROM LM AND TS ALGORITHMS FOR ADIS16405'S ACCELEROMETER;  $\delta_x, \delta_y, \delta_z$ —DEVIATIONS IN X, Y, Z AXES

Reference Angle	Without Calibration	LM Algorithm	TS Algorithm
$\theta; \phi$ (deg)	$\delta_x, \delta_y, \delta_z$ (m)	$\delta_x, \delta_y, \delta_z$ (m)	$\delta_x, \delta_y, \delta_z$ (m)
0; 0	-679; -107; -1825	-30; -1; 136	-27; -4; 135
10; 0	-420; 66; -2403	93; 62; 222	95; 60; 222
20; 0	-2366; 93; -6110	-1157; -70; -3050	-1156; -72; 3051
0; -10	-171; 296; 1618	-44; 156; 821	-42; 153; 821
0; -20	-693; -1492; -4065	-328; -497; -1447	-327; -501; -1423
10; -10	-1629; -548; -2659	-933; 1005; 193	-931; 1002; 194
20; -20	-8276; -1733; -2077	-7422; 6714; -1015	-7120; 6710; -1015

AHRS M3's accelerometer, ADIS16405's accelerometer, and CXL02LF3 can be seen in Tables IX–XI.

Results from Tables IX–XI show that, in most cases, the deviations in position decreased due to the calibration. The devia-

TABLE XI  
POSITION DETERMINATION IN PLATFORM FRAME BEFORE AND AFTER CALIBRATION USING SEMS GOT FROM LM AND TS ALGORITHMS FOR CXL02LF3 ACCELEROMETER;  $\delta_x, \delta_y, \delta_z$ —DEVIATIONS IN X, Y, Z AXES

Reference Angle	Without Calibration	LM Algorithm	TS Algorithm
$\theta; \phi$ (deg)	$\delta_x, \delta_y, \delta_z$ (m)	$\delta_x, \delta_y, \delta_z$ (m)	$\delta_x, \delta_y, \delta_z$ (m)
0; 0	-2951; -339; -586	1668; -169; 15	1683; -190; 40
10; 0	-5867; -3609; -804	-3487; -3541; 32	-3628; -3561; 44
20; 0	-8388; -6863; -794	-6479; -6863; 162	-6534; -6824; 179
0; -10	-6187; 2908; -796	-3224; 3226; 103	-3773; 3198; 164
0; -20	-9345; 5971; 942	-6485; 5481; 210	-7059; -6455; 153
10; -10	-9140; -393; -1022	-1585; -158; 136	-1265; -184; 305
20; -20	-14242; -547; -1202	-1314; -182; 336	-1273; -205; 610

tions in position can be partially caused by imprecise alignment of the compensated sensor frame with respect to the platform frame which lies along main axes of the moving object. Due to imprecise sensor-platform, the alignment measured acceleration deviates from the true one and causes a deviation in position as well. This can be reduced by a successive alignment procedure which was not the subject of this analysis.

## VI. CONCLUSION

The main aim of this paper was to prove the effectiveness of the calibration approach, which does not need to use precise positioning devices and thus is not expensive and time-consuming. These characteristics are the main benefits of the proposed approach. Based on Levenberg–Marquardt (LM) and Thin-Shell (TS) algorithms we evaluated sensor error models (SEMs) for accelerometers of AHRS M3, ADIS16405, CXL02LF3 units and compared them with ones obtained from a Matlab *fminunc* function, which was used as a reference. We provided various analyses to show different aspects of the calibration such as reached values of SEM when LM or TS algorithm was applied, how many taken positions had to be used and how many iterations had to be performed to reach the required precision, or how greatly SEMs changed when they were compared with long-period perspectives. In all cases, the calibration had significant effect on results, e.g., according to Fig. 6 they were approx. 100 times improved. All results proved the suitability of the proposed calibration approach.

## REFERENCES

- [1] D. Jurman, M. Jankovec, R. Kamnik, and M. Topic, "Calibration and data fusion solution for the miniature attitude and heading reference system," *Sens. Actuators A, Phys.*, vol. 138, no. 2, pp. 411–420, Aug. 2007.
- [2] M. Soták, "Coarse alignment algorithm for ADIS16405," *Przeglad elektrotechniczny*, vol. 86, no. 9, pp. 247–251, 2010.
- [3] M. Sipos, P. Paces, M. Reinstein, and J. Rohac, "Flight attitude track reconstruction using two AHRS units under laboratory conditions," in *Proc. IEEE Sensors*, Nov. 2009, vol. 1–3, pp. 630–633.
- [4] M. Reinstein, J. Rohac, and M. Sipos, "Algorithms for heading determination using inertial sensors," *Przeglad Elektrotechniczny*, vol. 86, no. 9, pp. 243–246, 2010.
- [5] N. Barbour and G. Schmid, "Inertial sensor technology trends," *IEEE Sensors J.*, vol. 1, no. 4, pp. 332–339, Dec. 2001.
- [6] J. Včelák, P. Ripka, J. Kubík, A. Platil, and P. Kašpar, "AMR navigation systems and methods of their calibration," *Sens. Actuators A, Phys.*, vol. 123–124, pp. 122–128, 2005.
- [7] Z. Syed, P. Aggarwal, C. Goodall, X. Niu, and N. El-Sheimy, "A new multi-position calibration method for MEMS inertial navigation systems," *Meas., Sci., Technol.*, vol. 18, no. 7, pp. 1897–1907, Jun. 2007.

- [8] S. P. Won and F. Golnaraghi, "A triaxial accelerometer calibration method using a mathematical model," *IEEE Trans. Instrum. Meas.*, vol. 59, no. 8, pp. 2144–2153, Aug. 2010.
- [9] S. Luczak, W. Oleksiuk, and M. Bodnicki, "Sensing tilt with MEMS accelerometers," *IEEE Sensors J.*, vol. 6, no. 6, pp. 1669–1675, Dec. 2006.
- [10] A. Kim and M. F. Golnaraghi, "Initial calibration of an inertial measurement unit using optical position tracking system," in *Proc. PLANS 2004: Position Location and Navigation Symp.*, 2007, pp. 96–101.
- [11] D. H. Titterton and J. L. Weston, *Strapdown Inertial Navigation Technology*. London, U.K.: Peter Peregrinus, 1997, p. 238.
- [12] V. Petručka, P. Kaspar, P. Ripka, and J. M. G. Merayo, "Automated system for the calibration of magnetometers," *J. Appl. Phys.*, vol. 105, no. 7, 2009.
- [13] I. Skog and P. Händel, "Calibration of a MEMS inertial measurement unit," presented at the XVII IMEKO World Congr., Rio de Janeiro, Brazil, 2006.
- [14] T. Pylvänainen, "Automatic and adaptive calibration of 3D field sensors," *Appl. Math. Model.*, vol. 32, no. 4, pp. 575–587, Apr. 2008.
- [15] S. Bonnet, C. Bassompierre, C. Godin, S. Lesecq, and A. Barraud, "Calibration methods for inertial and magnetic sensors," *Sens. Actuators A, Phys.*, vol. 156, no. 2, pp. 302–311, Dec. 2009.
- [16] M. Reinstein, M. Šipos, and J. Rohac, "Error analyses of attitude and heading reference systems," *Przeglad Elektrotechniczny*, vol. 85, no. 8, pp. 114–118, 2009.
- [17] J. Větlák, V. Petručka, and P. Kašpar, "Electronic compass with miniatu-  
re fluxgate sensors," *Sensor Lett.*, vol. 5, no. 1, pp. 279–282, 2007.
- [18] B. M. Wilamowski and H. Yu, "Improved computation for Levenberg & Marquardt training," *IEEE Trans. Neural Netw.*, vol. 21, no. 6, pp. 930–937, Jun., 2010.
- [19] L. S. H. Ngia and J. Sjoberg, "Efficient training of neural nets for non-linear adaptive filtering using a recursive Levenberg–Marquardt algorithm," *IEEE Trans. Signal Process.*, vol. 48, no. 7, pp. 1915–1927, Jul. 2000.
- [20] A. Ranganathan, *The Levenberg–Marquardt Algorithm*. Atlanta, GA, College of Computing, Georgia Inst. Technol., 2004.
- [21] L. M. Saini and M. K. Soni, "Artificial neural network based peak load forecasting using Levenberg–Marquardt and quasi-Newton methods," *Proc. IEEE Proc.*, vol. 149, no. 5, pp. 578–584, 2002, Generation, Transmission and Distribution.
- [22] H. Gavin, "The Levenberg–Marquardt method for nonlinear least squares curve-fitting problems," Dept. Civil and Environmental Engineering, Duke Univ., Durham, NC, 2011.
- [23] K. Madsen, H. B. Nielsen, and O. Tingleff, *Methods for Non-Linear Least Squares Problems*, 2nd ed. Lyngby, Denmark: Tech. Univ. Denmark, 2004, Informatics and Mathematical Modelling.
- [24] M. Soták, M. Sopata, R. Bréda, J. Roháč, and L. Váci, *Navigation System Integration*, Košice: Robert Breda, Košice, Slovak Republic, 2006.
- [25] E. L. Renk, W. Collins, M. Rizzo, F. Lee, and D. S. Bernstein, "Calibrating a triaxial accelerometer-magnetometer—Using robotic actuation for sensor reorientation during data collection," *IEEE Control Syst. Mag.*, vol. 25, no. 6, pp. 86–95, Jun. 2005.
- [26] Find Minimum of Unconstrained Multivariable Function—MATLAB [Online]. Available: <http://www.mathworks.com/help/toolbox/optim/ug/fminunc.html> [Accessed: 29-Apr-2011].
- [27] Attitude and Heading Reference System, Innalabs AHRS M3, Datasheet [Online]. Available: [http://www.galaxynav.com/AHRS\\_M3\\_datasheet\\_2008.10.08.pdf](http://www.galaxynav.com/AHRS_M3_datasheet_2008.10.08.pdf) [Accessed: 29-Apr-2011].
- [28] ADIS16405 | High Precision Tri-Axis Gyroscope, Accelerometer, Magnetometer | Inertial Sensors | Sensors | Analog Devices [Online]. Available: <http://www.analog.com/en/sensors/inertial-sensors/adis16405/products/product.html> [Accessed: 24-Apr-2011].
- [29] Crossbow Accelerometers, High Sensitivity, LF Series [Online]. Available: <http://www.datasheetarchive.com/cxl-datasheet.html> [Accessed: 29-Apr-2011].
- [30] MicroStrain: Inertial Systems—3DM-GX2® [Online]. Available: <http://www.microstrain.com/3dm-gx2.aspx> [Accessed: 29-Apr-2011].
- [31] STEVAL-MKI062V2—STMicroelectronics [Online]. Available: <http://www.st.com/internet/evalboard/product/250367.jsp> [Accessed: 29-Apr-2011].
- [32] J. Veelak, P. Ripka, A. Platil, J. Kubík, and P. Kaspar, "Errors of AMR compass and methods of their compensation," *Sens. Actuators A, Phys.*, vol. 129, no. 1–2, pp. 53–57, 2006.



**Martin Šipoš** was born in Prague, Czech Republic, in 1983. He received the Engineering degree (M.Sc. equivalent) with a specialization in aeronautical instrumentation systems from the Department of Measurement, Faculty of Electrical Engineering, Czech Technical University, Prague, in 2008, where he is currently pursuing the Ph.D. degree in the Laboratory of Aeronautical Information Systems with a dissertation titled "Improvement of INS accuracy using alternative sensors."

His main research activity is INS, GPS, Earth's magnetic field navigation, and adaptive filtering.



**Pavel Pačes** (M'09) was born in Prague, Czech Republic, in 1978. He received the M.Sc. degree in aerospace engineering from the Faculty of Electrical Engineering, Czech Technical University, Prague, in 2005, and the Ph.D. degree from the air traffic control program with two patent applications in 2011.

He gained industrial experience as a programmer and tester of avionics instruments at DevCom, as an HW and SW developer for the Aircraft Research Institute of the Czech Republic, etc.

Dr. Pačes is member of the IEEE Aerospace and Electronic Systems Society and the American Institute of Aeronautics and Astronautics. Currently, he is a National Point of Contact for the Space Generation Advisory Council in support of the United Nations Program on Space Applications.



**Jan Roháč** received the Ing. degree (M.Sc. equivalent) and the Ph.D. degree from the Faculty of Electrical Engineering (FEE), Czech Technical University (CTU), Prague, Czech Republic, in 2000 and 2005, respectively.

He is an Assistant Professor and Researcher with the Department of Measurement, FEE, CTU. He teaches courses concerning aircraft and space systems. His main research interests are in avionics, space technologies, inertial navigation systems, GNSS, AOCS, sensors and their modeling, and data processing methods.

Dr. Roháč is a member of the Czech Aeronautical Society and one of the representatives of the CTU in the PEGASUS Network.



**Petr Nováček** was born in 1983 in Prague, Czech Republic. He received an Ing. degree (M.Sc. equivalent) with a specialization in aeronautical instrumentation systems from the Department of Measurement, Faculty of Electrical Engineering (FEE) Czech Technical University (CTU), Prague, in January 2010. He is currently pursuing the Ph.D. degree under Prof. P. Ripka at the FEE, CTU.

His research interests include sensors (magnetometers and accelerometers), electronics of sensors, digital signal processing, and microcontroller design for low-cost precise navigation systems.

## 4.2. Calibration of Triaxial Gyroscopes

*Proceedings of 10th International Conference "Measurement, Diagnostics, Dependability of Aircraft Systems" 2010*

### Calibration of Tri-axial Angular Rate Sensors

Ing. Martin Šipoš<sup>1)</sup>, Ing. Jan Roháč, Ph.D.<sup>2)</sup>

Czech Technical University in Prague, Faculty of Electrical Engineering

Department of Measurement, Laboratory of Aeronautical Systems and Instrumentation

email: <sup>1)</sup> sipoスマ@fel.cvut.cz, <sup>2)</sup> xrohac@fel.cvut.cz

phone: <sup>1)</sup> +420-22435-2061, <sup>2)</sup> +420-22435-3963

#### Abstract:

*The calibration of angular rate sensors is a complex task, mainly due to the crucial role of defining the reference during the calibration process. Low-cost angular rate sensors, such as MEMS (Micro-Electro-Mechanical-Systems), cannot be used without calibration even in basic precision desired applications. The goal of calibration involves the estimation of the angular rate sensor deterministic error model that consists of the bias vector, matrix of scale factors, matrix of non-orthogonalities, and alignment matrix. In this paper there is proposed a calibration process that does not require either a precise rotational platform or a precise positioning or other reference. The algorithm of tri-axial angular rate sensor calibration is based on a special procedure of angular rate measuring under different setting conditions, Cholesky decomposition, and LU factorization in the angle domain. This calibration algorithm was evaluated using two AHRS (Attitude Heading and Reference System) units 3DM-GX2 (MicroStrain) and AHRS M3 (Innolabs). The calibration process and the deterministic sensor error analyses of angular rate sensors are presented.*

## 1 Introduction

A recent technological progress in the precision and reliability of MEMS (Micro-Electro-Mechanical-Systems) have enabled the usage of inertial sensors based on MEMS in wide range of consumer applications such as Unmanned Aerial Systems (UASs), underwater and indoor navigation, human motion tracking, etc. [1, 2, 3].

The magnetometers and MEMS inertial sensors – accelerometers, and angular rate sensors are contained in the Inertial Measurement Units (IMUs) which is a part of Attitude and Heading Reference Systems (AHRSs). Due to automated process of the sensor manufacturing, parameters of mentioned systems can vary piece to piece. Therefore, the calibration of the tri-axial frame of inertial sensors is necessary for achieving of desired accuracy. The calibration of inertial sensors and magnetometers means the estimation of deterministic sensor error model. The main goal of this paper is to present a method how to calibrate tri-axial angular rate sensors and to point out the results of this calibration. The methodology of the tri-axial accelerometer calibration was described in [4] and results of accelerometer and magnetometer calibration were presented in [5]. We used two different ARHS units 3DM-GX2 (MicroStrain, [6]) and AHRS M3 (Innolabs, [7]) providing raw inertial data from accelerometers with total range  $\pm 5\text{g}$  and  $\pm 2\text{g}$  respectively and from angular rate sensors with range  $\pm 300 \text{ deg/s}$  for the evaluation of calibration algorithm.

## 2 Tri-axial Angular Rate Sensor Error Model

For the sensor's description, the mathematical sensor error model is used. The triad of sensors should be mounted perpendicularly to each other and each triad must be aligned to

the sensor's case. However, this is not usually achieved due to the technology of manufacturing imperfections. This is a problem so the sensor models which cover all these imperfections have to be used. The deterministic sensor error model of tri-axial angular rate sensor that was used in this calibration can be described as [1]:

$$y_g - b_g = S_g T_g M_g u_g = \begin{bmatrix} S_{gx} & 0 & 0 \\ 0 & S_{gy} & 0 \\ 0 & 0 & S_{gz} \end{bmatrix} \begin{bmatrix} 1 & 0 & 0 \\ \alpha_g & 1 & 0 \\ \beta_g & \gamma_g & 1 \end{bmatrix} \begin{bmatrix} r_{g,11} & r_{g,12} & r_{g,13} \\ r_{g,21} & r_{g,22} & r_{g,23} \\ r_{g,31} & r_{g,32} & r_{g,33} \end{bmatrix} \begin{bmatrix} u_{gx} \\ u_{gy} \\ u_{gz} \end{bmatrix}, \quad (2-1)$$

where  $y_g = [y_{gx} \ y_{gy} \ y_{gz}]^T$  is the vector of the measured sensor output;  $b_g = [b_{gx} \ b_{gy} \ b_{gz}]^T$  denotes the vector of sensor biases;  $u_g = [u_{gx} \ u_{gy} \ u_{gz}]^T$  is the vector of referential angular rates;  $S_g = \text{diag}[S_{gx} \ S_{gy} \ S_{gz}]$  is the diagonal matrix containing the scaling factors;  $T_g$  is orthogonalization matrix which transforms the vector expressed in the orthogonal sensor reference frame  $k_o$  into the vector expressed in the non-orthogonal sensor reference frame  $k$  (Fig. 2-1); alignment matrix  $M_g$  is an aerospace sequence Euler angles parameterized rotation matrix, which rotates (aligns) the reference frame to the orthogonal sensor reference frame and this matrix is described by [1, 3]:

$$M_g = \begin{bmatrix} 1 & 0 & 0 \\ 0 & \cos \phi & \sin \phi \\ 0 & -\sin \phi & \cos \phi \end{bmatrix} \begin{bmatrix} \cos \theta & 0 & -\sin \theta \\ 0 & 1 & 0 \\ \sin \theta & 0 & \cos \theta \end{bmatrix} \begin{bmatrix} \cos \psi & \sin \psi & 0 \\ -\sin \psi & \cos \psi & 0 \\ 0 & 0 & 1 \end{bmatrix}, \quad (2-2)$$

where  $\theta$  is pitch,  $\phi$  is roll, and  $\psi$  is yaw Euler angle.

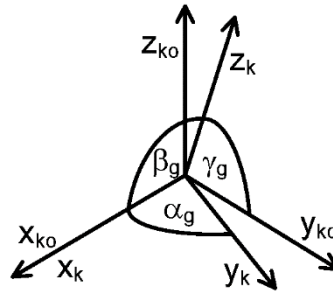


**Fig. 2-1: Orthogonalization of sensor frame  $k$ ;  $k_o$  - orthogonal sensor frame,  $k$  - non-orthogonal sensor frame [1]**

### 3 Calibration Algorithm

The tri-axial angular rate sensor calibration is based on the comparison of angular rates measured by calibrated sensor with reference angular rates. As a reference angular rate is possible to use the Earth rotation but for calibration of MEMS angular rate sensors, there is a problem that the Earth rotation is under the resolution or hidden behind the noise and drift errors. For low-cost angular rate sensors, the calibration tests are typically done using precise rotational platforms that assure constant reference angular rate with corresponding accuracy [8]. Usually, the rotational and positioning platforms are more expensive than calibrated sensors, especially in case of MEMS sensors. Therefore, there was a need to suggest a different access to the calibration of such devices.

Currently, the methods which do not require any precise rotational platforms are developed to obtain the results with comparable accuracy as results obtained using the precise positioning platforms. A possible solution is a calibration procedure based on measurement of angles instead of angular rates [9].

Instead of four measurements as was described in [1], only three measurements were performed. At the beginning of measurements, the AHRS units were kept under standstill conditions and the sensor biases were measured for 30 seconds. The vector of biases  $b_g$  was computed as the mean value of three static data measurements performed at the beginning of rotations. After bias determination, rotations about individual sensitivity axis were done. The measured angular rates are shown in Fig. 3-2a. These angular rates corrected by bias were arranged to the matrix  $v_g$ , where  $r_{ij}$  represent the i-th sensor's output when rotation about the j-th axis was applied [1].

$$v_g = y_g - b_g = \begin{bmatrix} r_{g,xx} & r_{g,xy} & r_{g,xz} \\ r_{g,yx} & r_{g,yy} & r_{g,yz} \\ r_{g,zx} & r_{g,zy} & r_{g,zz} \end{bmatrix}, \quad (3-3)$$

Because of (3-3) is linear and matrices  $S_g$ ,  $T_g$ , and  $M_g$  are constant, the measured angular rates in the matrix  $v_g$  can be integrated and substituted by matrix of angles of rotation  $Y_g$ . After integration the knowledge of reference angular rates is not needed but the angles of rotation need to be known [1]. The reference angular rates were substituted by matrix of reference angles  $A_g$  measured by theodolite (Fig. 3-2b) which was used as a reference with accuracy  $4.17 \times 10^{-3}$  degree. The following calibration procedure is performed only in the angle domain:

$$Y_g = S_g T_g M_g A_g, \quad (3-4)$$

The calibration algorithm is based on assumptions about matrices  $S_g$ ,  $T_g$ , and  $M_g$  [1]:

- a) the scale factor matrix  $S_g$  is a diagonal matrix,
- b) the orthogonalization matrix  $T_g$  is a unit lower triangular matrix,
- c) the alignment matrix  $M_g$  is an orthonormal matrix.

The known matrices are arranged on the left side, the estimated on the right side:

$$Y_g A_g^{-1} = S_g T_g M_g, \quad (3-5)$$

The symmetrical matrices are constructed by right multiplication of each side with its transposition (3-6) and due to orthonormality of  $M_g$ , this matrix can be modified to the form (3-7):

$$(Y_g A_g^{-1})(Y_g A_g^{-1})^T = (S_g T_g M_g)(S_g T_g M_g)^T, \quad (3-6)$$

$$(Y_g A_g^{-1})(Y_g A_g^{-1})^T = (S_g T_g)(S_g T_g)^T, \quad (3-7)$$

Using the Cholesky decomposition, the matrix  $(Y_g A_g^{-1})(Y_g A_g^{-1})^T$  is decomposed into a lower triangular matrix  $S_g T_g$  and its transpose:

$$S_g T_g = \text{chol}\left[(Y_g A_g^{-1})(Y_g A_g^{-1})^T\right]^T, \quad (3-8)$$

The matrices  $S_g$  and  $T_g$  are obtained by LU factorization of the matrix  $S_g T_g$  (3-9) and finally, the alignment matrix  $M_g$  is obtained by (3-10):

$$[T_g S_g] = LU(S_g T_g), \quad (3-9)$$

$$M_g = T_g^{-1} S_g^{-1} Y_g^{-1} A_g^{-1}, \quad (3-10)$$

Complete algorithm is described in [1] and [9].

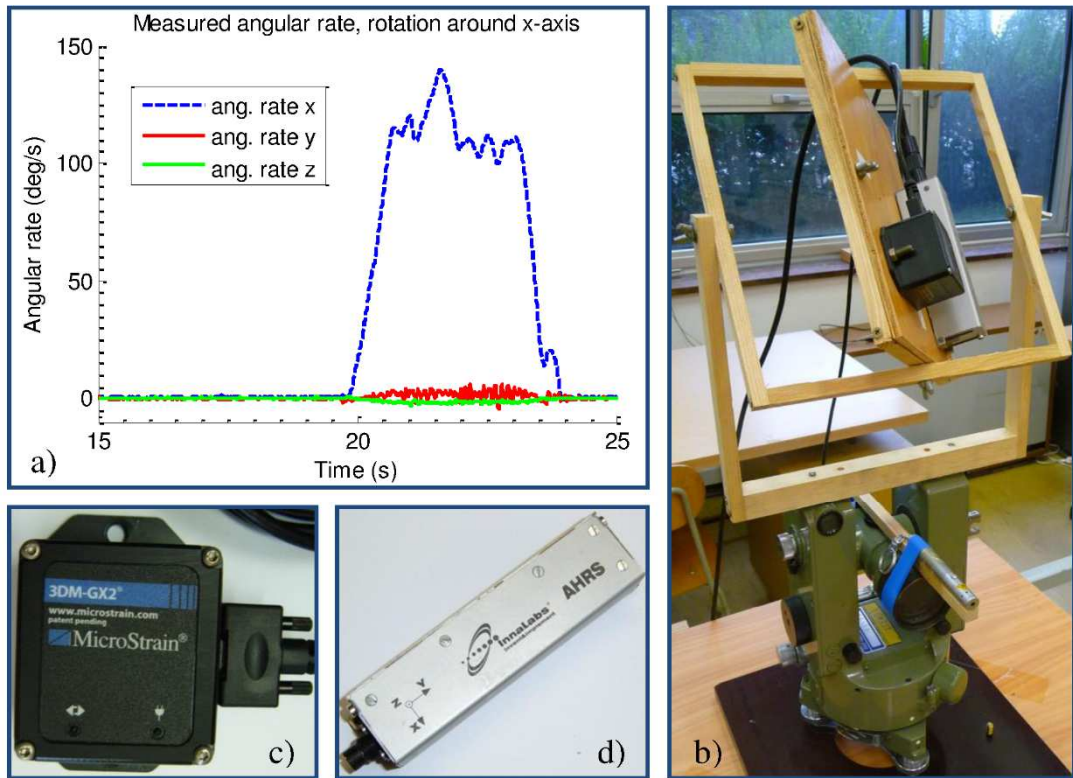


**Fig. 3-2:** a) Measured angular rates, rotation approximately 360 degrees around x-axis; b) Measurement setup with theodolite for calibration of tri-axial angular rate sensors; c) 3DM-GX2; d) AHRS M3

## 4 Experimental Results

The calibration of angular rate sensor was performed for two AHRS units according to the proposed procedure. Parameters of angular rate sensor models are shown in Table 4-1.

AHRS M3 (Innolabs)								
Bias (deg/s)	Scale factors matrix $S$			Orthogonalization matrix $T$			Alignment matrix $M$	
-0.1720	1.0087	0	0	1	0	0	0.9995	0.0287
-0.2985	0	1.0092	0	0.0540	1	0	-0.0289	0.9995
0.0956	0	0	1.0054	0.0231	0.0372	1	-0.0117	-0.0112
3DM-GX2 (MicroStrain)								
Bias (deg/s)	Scale factors matrix $S$			Orthogonalization matrix $T$			Alignment matrix $M$	
-0.3784	1.0119	0	0	1	0	0	0.9996	0.0232
0.1588	0	0.9944	0	0.0372	1	0	-0.0226	0.9997
-0.1309	0	0	1.0013	0.0222	0.0165	1	-0.0159	-0.0037

**Tab. 4-1: Parameters of angular rate sensor error model**

Based on Table 4-1, the biases of angular rates were less than 0.4 deg/s. The deviations of integrated angular rates from reference angles measured by theodolite, were used as a comparison criterion. These deviations between calibrated and non-calibrated sensor triad are shown in Table 4-2.

AHRS M3 (Innalabs)					
Non-calibrated sensor triad $\Delta\alpha$ (deg)			Calibrated sensor triad $\Delta\alpha$ (deg)		
2.9533	10.5255	4.4285	-0.6546	-0.1832	0.0039
9.1152	3.7451	4.2816	-0.0684	0.4167	0.2492
3.7241	9.7039	2.1794	-0.1752	0.1916	0.2436
3DM-GX2 (MicroStrain)					
Non-calibrated sensor triad $\Delta\alpha$ (deg)			Calibrated sensor triad $\Delta\alpha$ (deg)		
4.1306	8.5266	6.0070	-0.4349	0.0395	0.0548
5.1902	-1.7904	1.4082	-0.1134	0.2929	0.2115
2.0931	4.8081	0.5950	-0.1047	0.2143	0.1486

**Tab. 4-2: Deviations of integrated angular rates from reference angles obtained from theodolite for non-calibrated and calibrated sensor triad**

## 5 Conclusion

In this paper, the simple procedure for the low-cost tri-axial angular rate sensors has been introduced. This procedure does not require the usage of any angular standards and any precision rotational platform. Two low-cost AHRS units which contained MEMS tri-axial angular rate sensors were chosen to prove introduced method. The data were measured using only three rotations about sensitivity axes and the calibration algorithm was evaluated in Matlab. As the reference of angles the theodolite was used.

## References

- [1] JURMAN, D.; JANKOVEC, M.; KAMNIK, R.; TOPIČ, M.: Calibration and data fusion solution for the miniature attitude and heading reference system. Elsevier, Sensors and Actuators, 2007, pp 411-420.
- [2] ŠIPOŠ, M.; PAČES, P.; REINŠTEIN, M.; ROHÁČ, J.: Flight Attitude Track Reconstruction Using Two AHRS Units under Laboratory Conditions. Christchurch, New Zealand, IEEE, 2009, pp 675 – 678.
- [3] REINŠTEIN, M.; ŠIPOŠ, M.; ROHÁČ, J.: Error Analyses of Attitude and Heading Reference Systems. Przeglad Elektrotechniczny, 2009, vol. 85, no. 8, p. 114-118.
- [4] ŠIPOŠ, M.; REINŠTEIN, M.; ROHÁČ, J.: Levenberg-Marquardt Algorithm for Accelerometers Calibration. Brno, Univerzita obrany, Fakulta vojenských technologií, 2008, p. 39-45.
- [5] ŠIPOŠ, M.; ROHÁČ, J.: Integration of Low-cost Inertial Navigation Unit with Secondary Navigation Systems. Prague, Czech Technical University in Prague, 2010, pp 146 – 147.
- [6] 3DM-GX2, MicroStrain, 3<sup>rd</sup> September 2010, details: <http://www.microstrain.com/3dm-gx2.aspx>
- [7] AHRS M3 Datasheet, Innalabs, [www.innalabs.com](http://www.innalabs.com), 3<sup>rd</sup> September 2010, datasheet available on page [http://www.galaxynav.com/AHRS\\_M3\\_datasheet\\_2008.10.08.pdf](http://www.galaxynav.com/AHRS_M3_datasheet_2008.10.08.pdf)
- [8] SYED, Z. F.; AGGARWAL, P.; GOODALL, C.; NIU, X.; EL-SHEIMY, N.: A new multi-position calibration methods for MEMS inertial navigation systems. Measurement Science and Technology 10, IOP Publishing LTD., 2007, pp 1897-1907.
- [9] FERRARIS, F.; GORINI, I.; GRIMALDI, U.; PARVIS, M.: Calibration of three-axial rate gyros without angular velocity standards. Sensors and Actuators A, 11-12, 1994, pp 446-449.

## Acknowledgement

This research has been partially supported by Czech Science Foundation project 102/09/H082, partially by the research program No. MSM6840770015 "Research of Methods and Systems for Measurement of Physical Quantities and Measured Data Processing" of the CTU in Prague sponsored by the Ministry of Education, Youth and Sports of the Czech Republic, partially by Grant Agency of the Czech Technical University in Prague grant No. SGS10/288/OHK3/3T/13, and by the Czech Ministry of Education under FRVŠ grant No. 2394/2010/G1.

### 4.3. Improvement of Electronic Compass Accuracy Based on Magnetometer and Accelerometer Calibration

Vol. 121 (2012)

ACTA PHYSICA POLONICA A

No. 4

Proceedings of the SPM11

## Improvement of Electronic Compass Accuracy Based on Magnetometer and Accelerometer Calibration

M. ŠIPOŠ\*, J. ROHÁČ, P. NOVÁČEK

Czech Technical University in Prague, Faculty of Electrical Engineering, Department of Measurement  
Technická 2, 166 27, Prague, Czech Republic

This paper describes the process used for an electronic compass compensation according to accelerometer based tilt evaluation. Tilt angles have to be estimated first for sensed magnetic vector components to be aligned and horizontal components evaluated. Therefore the precision of accelerometer based tilt angles plays a key role in this whole process as well as the magnetometer characteristics. Hence accelerometers plus magnetometers have to be calibrated to improve the accuracy of a tilt and an azimuth angle evaluation. The calibration uses Thin-Shell method to determine sensor error models. Both the effect of calibration and precision of estimated error models have been observed and are presented. The electronic compass consisted of tri-axial magnetometer and tri-axial accelerometer contained in the Inertial Measurement Unit ADIS16405 from Analog Devices manufacturer.

PACS: 85.75.Ss, 91.10.-v, 06.20.fb, 91.25.-r, 07.07.Df

### 1. Introduction

Since 1500 years ago, the mechanical compasses have been used for an azimuth determination and a guidance using Earth magnetic field. Due to the technology development and improvement, current electronic compasses (ECs) have much better parameters which are, of course, influenced by sensor type applied. The most simple low accuracy compasses use Hall sensors. In contrast, more accurate ones use Anisotropic Magneto Resistors (AMR) and the most accurate compasses use the fluxgate sensors [1]. The final accuracy of EC depends not only on used magnetic sensors, but also on tilt sensors, which have to be utilized to mathematically align magnetic sensors (compasses with tilt compensation) into the local navigation frame. Characteristics of tilt sensors also affect the EC accuracy, and therefore they have to be calibrated, which eliminates the sensors imperfections [2]. For low-cost sensors like MEMS (Micro-Electro-Mechanical System) based ones, manufacturers mostly perform only basic calibration and the rest is left on customers. Thus, for better accuracy the system needs to be recalibrated [3]. There exists a wide range of calibration procedures and techniques, e.g. the calibration using redundant heading information computed from rate gyroscopes [4] or the calibration procedure based on ellipsoid fitting problem which does not need heading reference information obtained from redundant sensors [5].

Nowadays, the ECs have become useful in a wide range of consumer applications such as mobile phones, PDAs, robot navigation, human head and hands tracking, attitude determination of inertial navigation systems used in aerospace engineering, etc. [1, 2, 6–8].

In this paper, the EC system and the tilt compensation is briefly described in section 2, the sensor error model (SEM) is further discussed in chapter 3 and Thin-Shell

calibration method is mentioned in section 4. A measurement setup and a measured unit are briefly introduced in section 5. The most important results are summarized in section 6.

### 2. Electronic compass

The simplest electronic compass (EC) can be constructed using only a dual-axis magnetometer. This type of EC can measure accurate only azimuth (yaw angle) in horizontal plane. The resulting azimuth  $\psi$  can be computed using simple eq. (1):

$$\psi = \arctan(f_y/f_x) - D \quad (1)$$

where  $f_x$ ,  $f_y$  are horizontal magnetic field components measured in sensor (body) frame, and  $D$  is a magnetic declination [2].

Although this type of compasses is very simple and easy to manufacture, a main disadvantage of this EC construction is in the obligation to place the sensor accurately into horizontal plane. If it cannot be ensured, the errors are not negligible as was proved by Vcelák in [2]. Generally, it is not possible to ensure this condition providing horizontal mounting of magnetic sensor, so the electronic compass has to be equipped with tilt compensation functionality. The compass with tilt compensation (Fig. 1) usually consists of tri-axial magnetometer and tilt sensor, which can be formed by tri-axial accelerometer [9] or an electronic inclinometer commonly used in Honeywell compasses.

The EC uses magnetometer platform mathematically aligned to the horizontal plane using pitch and roll angles defined by (2) and (3). The azimuth can be then computed using (4).

$$\theta = \arctan\left(-a^{by} / \sqrt{(a^{bx})^2 + (a^{bz})^2}\right), \quad (2)$$

$$\varphi = \arctan(a^{bx} / (-a^{bz})), \quad (3)$$

\* corresponding author; e-mail: [siposmar@fel.cvut.cz](mailto:siposmar@fel.cvut.cz)

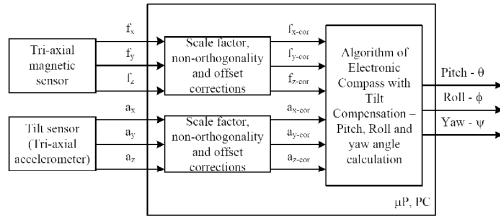


Fig. 1. The block scheme of an EC with a tilt compensation and the compensation of sensor imperfections formed in the sensor error model (5).

$$\psi = \arctan \frac{f_y \cos \varphi + f_z \sin \varphi}{f_x \cos \varphi + f_y \sin \varphi \sin \theta - f_z \cos \varphi \sin \theta} - D, \quad (4)$$

where:  $\theta$ ,  $\varphi$  denote the pitch and roll angle;  $a^{bx}$ ,  $a^{by}$ ,  $a^{bz}$  are measured accelerations in the sensor body frame;  $f_x$ ,  $f_y$ ,  $f_z$  represent magnetic field vector components measured in sensor frame [10].

### 3. Sensor error model

In the chapter 1 it was mentioned that the calibration is necessary to be performed for the elimination of the sensor imperfections. Generally, sensors have many error sources; nevertheless, our sensor error model (SEM) defined by (5) includes the main ones [11]. They correspond to scale factor deflections, axes misalignment described in our case by three non-orthogonality angles [11], and offsets for all three axes. The offset forms a stochastic time-invariant part of the bias; in contrast, a drift characterizes a time-variant part of the bias. Because the calibration process is commonly performed during short-time period, the drift can be considered as zero [11].

$$\begin{aligned} \mathbf{y}_p &= \mathbf{T}_a^p S \mathbf{F}_a (\mathbf{y}_m - \mathbf{b}_a) \begin{pmatrix} 1 & 0 & 0 \\ \alpha_{yx} & 1 & 0 \\ \alpha_{zx} & \alpha_{zy} & 1 \end{pmatrix} \\ &\times \begin{pmatrix} SF_{ax} & 0 & 0 \\ 0 & SF_{ay} & 0 \\ 0 & 0 & SF_{az} \end{pmatrix} \left[ \begin{pmatrix} y_{mx} \\ y_{my} \\ y_{mz} \end{pmatrix} - \begin{pmatrix} b_{ax} \\ b_{ay} \\ b_{az} \end{pmatrix} \right], \end{aligned} \quad (5)$$

where  $\mathbf{y}_p$  represents the compensated vector of either measured acceleration in the case of accelerometers or magnetic field vector in case of magnetometers and is defined in the orthogonal platform frame;  $\mathbf{T}_a^p$  denotes the matrix providing the transformation from the non-orthogonal frame to the orthogonal one with non-diagonal terms  $\alpha_{yx}$ ,  $\alpha_{zx}$ ,  $\alpha_{zy}$  that correspond to the axes misalignment;  $S \mathbf{F}_a$  represents a scale factor matrix;  $\mathbf{b}_a = [b_{ax}, b_{ay}, b_{az}]^T$  is the vector of offsets;  $\mathbf{y}_m = [y_{mx}, y_{my}, y_{mz}]^T$  denotes the vector of measured acceleration/magnetic field vector. The SEM and its derivation are described in more detail in [12].

### 4. Calibration procedure

There already exist several calibration procedures for tri-axial sensors using different principles, e.g. the method using an ellipsoidal-fitting procedure [5, 13], a calibration procedure which uses a robotic arm [14] or a procedure with the usage of 3D optical tracking system that measures the position coordinates of markers attached to a measurement unit [15].

In our case, we used the thin-shell (TS) calibration method. A fundamental principle of the proposed method is based on the fact that the magnitude of measured quantity  $|y|$  (gravity acceleration, magnetic field vector) should be always equal to the constant value when static conditions are ensured and also equal to the square root of the sum of squared vector components (6):

$$y_x^2 + y_y^2 + y_z^2 = |y|^2, \quad (6)$$

where  $y_i$  denotes sensed quantity in direction of  $i$  axis and  $|y|$  is the magnitude of measured quantity. In the case of the gravity vector, it is ideally equal to  $g$  and in the case of the magnetic field vector  $|F|$  it is equal to  $0.48125G$  for the location (area) where the measurements were taken. The value of Earth magnetic field vector was calculated using International Geomagnetic Reference Field model (IGRF 11) which depends on the date of measurement, GPS position, and the altitude [16].

For the calibration purposes, according to [11], 36 positions are recommended to measure, 3 times 12 positions along  $x$ ,  $y$ ,  $z$  axis. The advantage of the method is that the precise knowledge of position orientations is not required. It is only recommended to provide at least 3 positions per each quadrant and each axis. After the measurements are taken, the Thin-Shell algorithm can be applied on the measured data. The TS algorithm is based on a linear minimum mean square error principle minimizing the standard deviation  $\sigma$  defined by (7), which is calculated from compensated vector component estimates and the known number of measurements.

$$\sigma = \sqrt{\frac{\sum_{i=1}^m (\hat{y}_{xi}^2 + \hat{y}_{yi}^2 + \hat{y}_{zi}^2 - |y|^2)^2}{m-1}}, \quad (7)$$

where  $\hat{y}_{xi}$ ,  $\hat{y}_{yi}$ ,  $\hat{y}_{zi}$  are estimations of compensated acceleration/magnetic field vector components and  $|y|$  is the magnitude of the reference value corresponding to measured quantity. The more detailed description of this calibration method is presented in [11, 17].

In each iteration step the interval defines the minimum, maximum, and mean value of the parameter being searched for and these values are then used to update the SEM. Thus, 3 SEMs are obtained corresponding to min., max., and mean values of the given parameter. Based on the updated SEMs new estimates of compensated vector are determined for each position and used for  $\sigma$  calculations. With respect to obtained 3 values of  $\sigma$  the interval is halved to find the local minimum of a standard deviation according to Fig. 2. When  $\sigma_{\text{mean}}$  reaches the smallest value, the interval is halved around  $k_{\text{mean}}$ , where “ $k$ ” rep-

## Improvement of Electronic Compass Accuracy Based on Magnetometer and Accelerometer Calibration 1113

resents the parameter being searched for. Unlike, when other  $\sigma$  reaches the smallest value and  $\sigma_{\text{mean}}$  is the second, the new interval is defined between  $k$ , whose  $\sigma$  was the smallest and  $k_{\text{mean}}$ . For instance, when  $k_{\text{min}}$  has the smallest  $\sigma$ , the  $k_{\text{mean}}$  becomes  $k_{\text{max}}$  for another iteration step and the new  $k_{\text{mean}}$  is calculated as the average of the new  $k_{\text{max}}$  and previous  $k_{\text{min}}$ . The same principle can be applied for the other case [11].

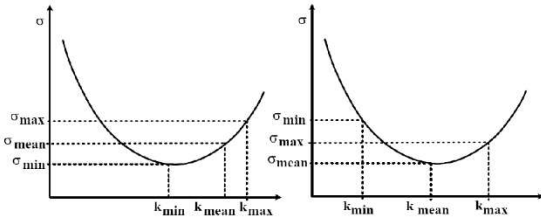


Fig. 2. Criterions for halving the interval, in which the estimated parameters are searched for [11].

### 5. Measurement setup

In our case the measurement setup was built up by the inertial measurement unit (IMU) ADIS16405 [18] (Analog Devices) and the non-magnetic theodolite T1c (Meopta Prague, Czech Republic). The IMU was used to evaluate the EC algorithm with tilt compensation and to prove the improvement of applied calibration procedure. The IMU (Fig. 3) contains the tri-axial magnetometer (MAG), tri-axial accelerometer (ACC), and tri-axial angular rate sensor (ARS). The measurements were performed in the area with minimal magnetic field disturbances in the local time from 18:00 to 19:00 CET when the variations of magnetic field are minimal. For the evaluation of EC accuracy, the IMU was mounted on the non-magnetic theodolite, see Fig. 3, which was used as a reference with an average error  $4.17 \times 10^{-3}$  deg.

In all performed experiments we used for calibration purposes and a final EC evaluation the average of 100 ACC and MAG samples taken in each position under static conditions as a value we consequently calculated with. A main reason for the usage of average values was the elimination of a noise influence.

### 6. Results

#### 6.1. Calibration of Magnetometer and Accelerometer of IMU ADIS16405

From the output data provided by IMU ADIS16405 we used only information from the magnetometer (MAG) and the accelerometer (ACC). After the data had been preprocessed, the calibration was performed using the Thin-Shell algorithm to estimate three misalignment angles (non-orthogonality angles), three scale factor corrections, and three biases, all formed in SEM (5). The



Fig. 3. The Inertial measurement unit ADIS16405 (on the left); theodolite T1c (in the middle); the whole measurement setup (on the right).

parameters of MAG and ACC SEMs are listed in Table I. The deviation between the measured and the ideal vector of applied quantity (corresponds to the magnetic field vector for MAG and to the gravity vector for ACC) is shown in Fig. 4 and Fig. 5. In contrast with the chapter 4, in which 36 positions are recommended for a correct calibration, we used only 21 positions in the case of MAG. The measurement took shorter time and thus we minimized the risk of potential magnetic field variations. In [11] it was proven that 21 positions is a sufficient number without a final accuracy decrease. For ACC calibration, the 36 positions were measured as was recommended.

TABLE I  
Sensor error models obtained using Thin-Shell algorithm for magnetometer (MAG) and accelerometer (ACC) of IMU ADIS16405 (Superscript 1 denotes RMSE before calibration and 2 after calibration)

Parameter	MAG	ACC
$\alpha_{xy}$ [deg]	0.1355	-0.0230
$\alpha_{zx}$ [deg]	-0.6628	0.0351
$\alpha_{zy}$ [deg]	-0.0818	-0.1639
SF <sub>x</sub> [-]	1.0049	0.9996
SF <sub>y</sub> [-]	1.0050	1.0019
SF <sub>z</sub> [-]	1.0004	0.9983
b <sub>x</sub>	-0.71 mG	-13.54 mg
b <sub>y</sub>	-0.83 mG	-6.71 mg
b <sub>z</sub>	0.23 mG	-4.02 mg
RMSE <sup>1</sup>	1.9 mG	9.5 mg
RMSE <sup>2</sup>	0.4 mG	2.5 mg

#### 6.2. Influence of MAG and ACC Calibration to Electronic Compass Accuracy

Finally, we analyzed in previous chapter performed calibration from the final accuracy of realized electronic compass (EC) point of view. We performed four measurements at all. In each measurement the EC was differently tilted in two directions to set values of 0 deg and 20 deg in various combinations. Then, the azimuth was

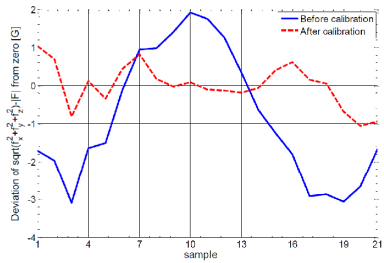


Fig. 4. The dependence of deviations of measured magnetic field vector before and after calibration — MAG of ADIS16405 — 21 evaluated positions.

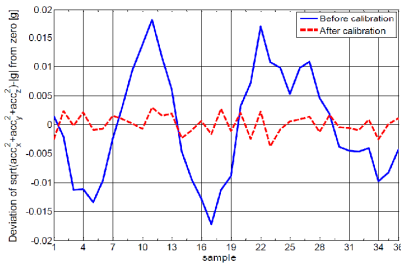


Fig. 5. The dependence of deviations of measured accelerations before and after calibration — ACC of ADIS16405 — 36 evaluated positions.

changing with the step of 22.5 deg and a tilt compensation observed as well as the effect of MAG and ACC calibration on the azimuth accuracy. As a criterion for the azimuth accuracy evaluation the RMSEs were computed and the final values with and without calibration (applied SEM) summarized, see Table II. The table provides the final RMSEs depending on set tilts in two directions (pitch and roll angles). In all four data sets, the application of evaluated SEMs led to the improvement of the final EC accuracy.

TABLE II  
Final accuracy of yaw angle estimation with and without applied ACC and MAG SEM;  $\theta$  - pitch,  $\varphi$  - roll,  $\psi$  - yaw

$\theta$ [deg]	$\varphi$ [deg]	without	with
		calibration	$\Delta\psi_{RMSE}$ [deg]
0	0	1.663	0.534
0	20	1.270	0.462
20	0	2.012	0.567
20	20	1.303	0.563

## 7. Conclusion

This paper deals with an electronic compass (EC) algorithm and procedures needed for its correct functionality.

The EC performance generally depends on used tri-axial magnetometer (MAG) and its parameters as well as on parameters of an aligning system. In our case we used tri-axial accelerometer (ACC) for this purpose. To improve EC performance we applied a calibration procedure Thin-Shell to estimate sensor error models of MAG and ACC. The methods were shortly introduced; nevertheless, a main focus was pointed to present experimental results. We performed the calibration of MAG, which approximately five-times improved its accuracy and in the case of ACC the accuracy was four-times improved. Although the calibration procedure recommended 36 positions to use, we measured data only 21 in the case of MAG which was in accordance to [11]. In contrast, for the ACC calibration we kept 36 positions as was recommended. We analyzed the influence of MAG and ACC calibration on the final EC accuracy by analyzing the differences between the evaluated azimuth and the reference angle obtained from our reference system formed by theodolite T1c. The evaluated azimuth reflected estimated SEMs' parameters, which were: three scale-factors corrections, three non-orthogonality angles, and three offsets. In all tested experiments the application of MAG and ACC SEMs led to improvement of final EC accuracy as was presented.

## Acknowledgement

This research has been partially supported by Czech Science Foundation project 102/09/H082, partially by the research program No. MSM6840770015 "Research of Methods and Systems for Measurement of Physical Quantities and Measured Data Processing" of the CTU in Prague sponsored by the Ministry of Education, Youth and Sports of the Czech Republic and partially by Grant Agency of the Czech Technical University in Prague grant No. SGS10/288/OHK3/3T/13.

## References

- [1] R. Racz, Ch. Schott, S. Huber, *Proceedings of the IEEE sensors 2004*, Vienna, Austria **1-3**, 1446, (2005).
- [2] J. Vcelak, V. Petrucha, P. Kaspar, *Sensor Letters* **5**, 279, (2005).
- [3] Z. Syed, P. Aggarwal, C. Goodall, X. Niu, N. El-Sheemy, *Measurement Science & Technology* **18**, 1897, (2007).
- [4] B. Hoff, R. Azuma, *IEEE and ACM International Symposium on Augmented Reality*, Munich, Germany, 159, (2000).
- [5] X. Hu, Y. Liu, Y. Wang, Y. Hu, D. Yan, *4th IEEE/ACM International Symposium on Mixed and Augmented Reality 2005*, Vienna, Austria, 182-183, (2005).
- [6] V.Y. Skvortsov, HK. Lee, S.W. Bang, YB. Lee, *Proceedings of the 2007 IEEE International Conference on Robotics and Automation* **1-10**, 2963, (2007).
- [7] M. Reinstein, *Przeglad Elektrotechniczny* **87**, 255, (2011).

## Improvement of Electronic Compass Accuracy Based on Magnetometer and Accelerometer Calibration 1115

- [8] M. Reinstein, M. Sipos, J. Rohac, *Przegląd Elektrotechniczny* **85**, 114, (2009).
- [9] J. Včelák, P. Ripka, J. Kubík, A. Platil, P. Kašpar, *Sensors and Actuators A: Physical* **123-124**,, 122, (2005).
- [10] M. Soták, *Przegląd Elektrotechniczny* **86**, 247, (2010).
- [11] M. Sipos, P. Paces, J. Rohac, P. Novacek, *IEEE Sensors Journal*, (2011), accepted for publication.
- [12] I. Skog, P. Händel, *XVII IMEKO World Congress*, Rio de Janeiro, (2006).
- [13] S. Bonnet, C. Bassompierre, C. Godin, S. Lescq, A. Barraud, *Sensors and Actuators A: Physical* **156**, 302, (2009).
- [14] E.L. Renk, M. Rizzo, W. Collins, F. Lee, D.S. Bernstein, *IEEE Control Systems Magazine*, **25**, 86, (2005).
- [15] A. Kim, MF. Golnaraghi, *Plans 2004: Position location and Navigation Symposium*, Monterey, CA, 26, (2004).
- [16] NOAA's Geophysical Data Center - Geomagnetic Online Calculator. Available: <http://www.ngdc.noaa.gov/geomagmodels/IGRFWMM.jsp> [Accessed: 09-Sep-2011].
- [17] M. Soták, M. Sopata, R. Bréda, J. Roháč, L. Váci, *Navigation System Integration*, Košice: Robert Breda, Kosice, the Slovak Republic (2006).
- [18] ADIS16405 High Precision Tri-Axis Gyroscope, Accelerometer, Magnetometer, Inertial Sensors, Sensors, Analog Devices. Available: <http://www.analog.com/en/sensors/inertial-sensors/adis16405/products/product.html> [Accessed: 24-Apr-2011].

#### 4.4. Comparison of Electrolytic Tilt Sensors for Accelerometer Data Correction

*Proceedings of 12th International Conference "Measurement, Diagnostics, Dependability of Aircraft Systems" 2012*

## Porovnání Modulů s Elektrolytickými Senzory Náklonu pro Korekci Polohových Úhlů

### Comparison of Electrolytic Tilt Modules for Attitude Correction

Ing. Martin Šipoš<sup>1)</sup>, Ing. Jan Roháč, Ph.D. <sup>2)</sup>

<sup>1,2)</sup> Czech Technical University in Prague, Faculty of Electrical Engineering

Department of Measurement, Laboratory of Aircraft Instrumentation Systems

E-mail: <sup>1)</sup> siposmar@fel.cvut.cz, <sup>2)</sup> xrohac@fel.cvut.cz

Phone: <sup>1)</sup> +420-22435-2061, <sup>2)</sup> +420-22435-3963

#### **Resumé:**

*Tento příspěvek popisuje analýzy a porovnání různých modulů s elektrolytickými senzory náklonu z hlediska statických a dynamických charakteristik. Pro správné určení polohových úhlů (příčného náklonu a podélného sklonu) vypočtených integrací z úhlových rychlostí je nutné korigovat neomezeně rostoucí chyby těchto naintegrovaných polohových úhlů. Za účelem korekce polohových úhlů navigačního systému jsme analyzovali 5 modulů náklonných senzorů s různými viskozitami elektrolytu. Jednalo se o 2 moduly se senzory se standardní viskozitou a s viskozitou o 50% vyšší (EZ-TILT-2000-008), dva moduly s viskozitou o 15% a 30% vyšší (EZ-TILT-2000-045) než standardní senzor (Advanced Orientation Systems Inc.) a jeden modul Micro 50-D70 se standardním elektrolytem (Spectron Glass and Electronics Inc.). Převodní charakteristiky, hysterese a doba ustálení byly měřeny a analyzovány.*

#### **Abstract:**

*In this paper there are analyzed and compared performances of different electrolytic tilt modules (ETMs) from static and dynamic characteristics point of view. For a correct determination of attitude (roll and pitch angles) evaluated from angular rates by integration, it is generally required to have attitude compensation sources which limit unbound error in this evaluation process and thus they play a key role for a proper function of navigation systems. We analyzed five ETMs with different electrolyte viscosity: EZ-TILT-2000-045 with standard viscosity and with the viscosity of 50% higher (EZ-TILT-2000-008), EZ-TILT-2000-045 with viscosity of 15% and 30% higher than the standard (all types from Advanced Orientation Systems Inc.), and Micro 50-D70 with standard electrolyte viscosity from Spectron Glass and Electronics Inc. The transfer characteristics, hysteresis and settling time on fast angle changes, were measured and analyzed and the results will be presented.*

## 1 Introduction

Over the last decades, the usage of low-cost inertial sensors based on MEMS (Micro-Electro-Mechanical-Systems) technology was increased in many civil and military applications, such as a car, personal, indoor, underwater navigation, navigation of unmanned aerial vehicles [1, 2, 3, 4], etc.

A basic part of inertial navigation systems is an Inertial Measurement Unit (IMU). IMU primarily consists of triaxial accelerometer for translational acceleration measurements and triaxial angular rate sensor for rotational motion measurements. The rotational motion measurements are integrated to evaluate the attitude [5]. For proper attitude evaluation, it is generally required to have attitude correction sources which limit unbound error in this evaluation process.

In this paper, we have analyzed five Electrolytic Tilt Modules (ETMs) suitable for attitude corrections. In comparison to paper [1, 2], in which the ETM was used for correction of triaxial accelerometer imperfection under static conditions, in this paper there are analyzed ETMs from static (transfer characteristics, hysteresis) and dynamic (settling time) characteristics point of view.

In the section 2, the composition of electrolytic tilt modules and the principle of electrolytic tilt sensors are described. The parameters of ETMs EZ-TILT-2000-xxx and Micro 50-D70 with standard viscosity of electrolyte are listed in section 3. The measurement setup with Rotational-Tilt Platform is described in section 4, and measured characteristics are summarized in section 5.

## 2 Principle of Electrolytic Tilt Module

The ETM consists of the single or dual-axis Electrolytic Tilt Sensor (ETS) and conversion module (called by Advanced Orientation Systems Inc.) or signal conditioner (called by Spectron Glass and Electronics Inc.) which controls the sensor excitation and measures and processes the output signal.

In this section, the principle of dual-axis electrolytic tilt sensor is described, a block scheme of electrolytic tilt module is shown plus real measured input and output signals of dual-axis electrolytic tilt sensor are presented.

## 2.1 Principle of Electrolytic Tilt Sensor

The dual-axis electrolytic tilt sensor commonly consists of the cylinder including an electrolyte and five electrodes (see Fig. 1a).

There are two types of cylinders, the first one is made from glass (Fig. 1b), the second one, more robust and more resistant, is made from polymer materials (Fig. 1c).

The pairs of electrodes are connected to a power. The center common electrode is used for measurement of output signal. The output signal changes with the respect to the inclination of sensor. Thus values can be changeable according to the angle of inclination (Fig. 1d).

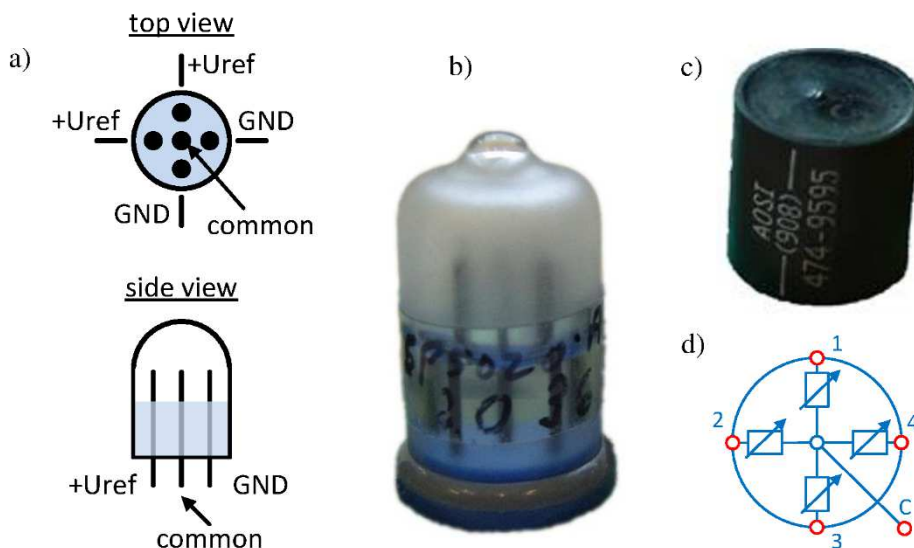


**Fig. 1:** a) The principle scheme of ETS; b) The ETS with glass cylinder; c) The ETS with the cylinder from polymer materials; d) The electric scheme of ETS

## 2.2 Block Scheme of Electrolytic Tilt Module (Conversion Module)

In general, electrolytic tilt sensors require the AC excitation waveform. A block scheme of general purpose dual-axis angle conversion module is shown in Fig. 2 [6]. In the realization of the conversion module, it is necessary to have zero DC offset in excitation waveform, because the usage of even small DC current can permanently polarize the electrolyte and irreversibly damage the sensor.

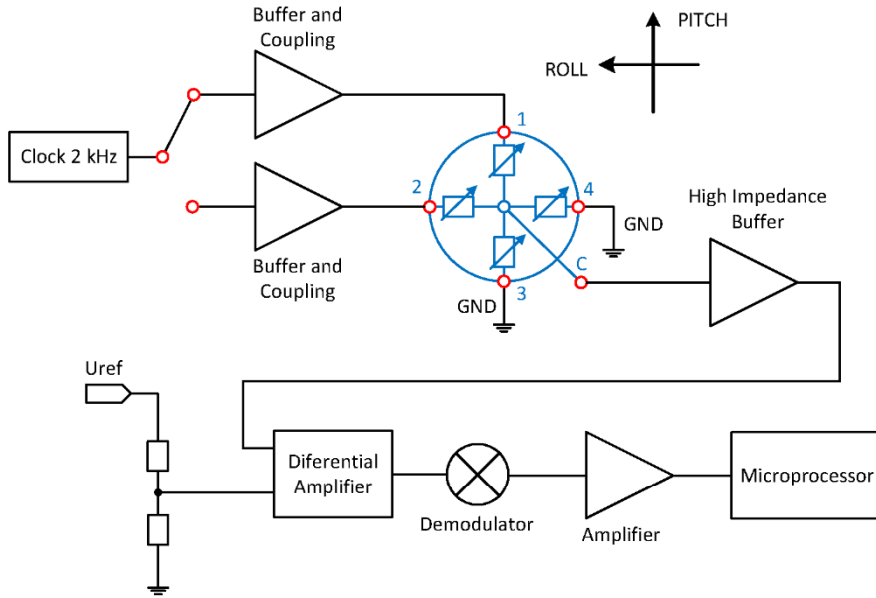


**Fig. 2: The block scheme of electrolytic tilt module [6]**

### 2.3 Measured Input and Output Signals of Dual-Axis Electrolytic Tilt Sensor

First of all, we have connected the input and output pins of electrolytic tilt sensor to oscilloscope and we have analyzed them. The input and output signals in both angles (pitch, roll) of the tilt being zero are shown in Fig. 3. The excitation of ETS was provided by the conversion module. Unlikely, Fig. 4 shows a positive pitch angle output signal and a negative roll angle output signal.

## 3 Parameters of Tested Electrolytic Tilt Modules

In this section, there are listed the basic specifications of electrolytic tilt modules EZ-TILT -2000-008, EZ-TILT-2000-045, and Micro 50-D70, as well as electrolytic tilt sensors used in these ETMs.

The EZ-TILT-2000-xxx modules consist of a multi-output dual axis high resolution conversion module EZ-TILT-2000-xxx and dual-axis electrolytic tilt sensors DX-008/DX-045. In case of ETM Micro 50-D70, the SP 5000-A-000 sensor and the Micro 50 signal conditioner were used.

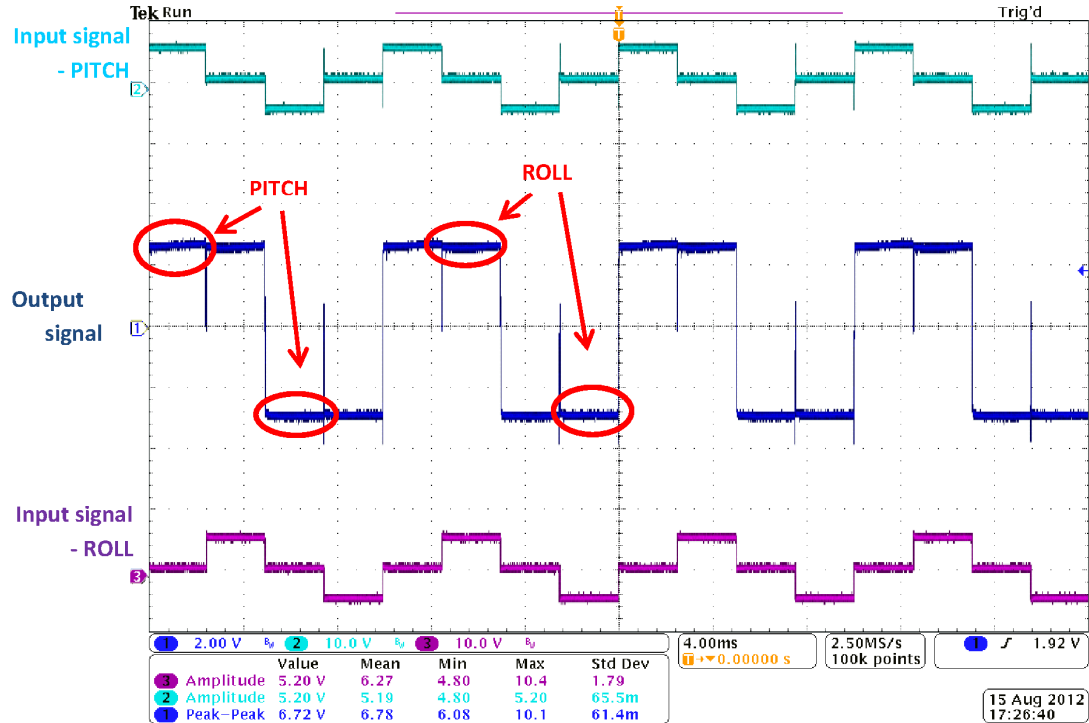


Fig. 3: The input and output signals in zero pitch and roll angles

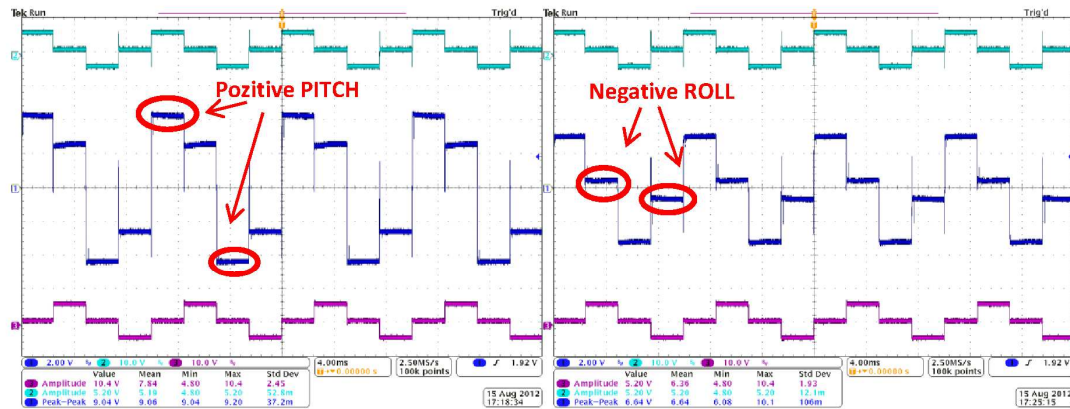


Fig. 4: The input and output signals in positive pitch and negative roll angles

The performances of the electrolytic tilt sensors DX-008, DX-045 [7] and SP 5000-A-000 [8] (all with standard viscosity) are described in Tab. 1, the parameters of conversion modules EZ-TILT-2000-xxx and Micro 50 are listed in Tab. 2.

Parameter	DX-008	DX-045	SP 5000-A-000
Maximal Range (deg)	±20	±70	±45
Linear Range (deg)	±8	±60	-
Resolution (deg)	< 0.0008	< 0.0061	0.02
Repeatability (deg)	< 0.03	< 0.05	0.04
Symmetry	< 2% @ 4 deg	< 2% @ 35 deg	< 5% @ 22.5 deg
Linearity	< 1% @ 8 deg	< 7% @ 60 deg	< 3% @ 22.5 deg
Settling Time (ms)	< 300	< 300	< 160
Temperature Range	-40 to +60 deg C	-40 to +60 deg C	-40 to +80 deg C

**Tab. 1: Performance of Electrolytic Tilt Sensors DX-008, DX-045 and SP 5000-A-000 with Standard Viscosity of Electrolyte [7, 8]**

Parameter	EZ-TILT-2000-xxx	Micro 50
Input Voltage (VDC)	6 to 12	7 to 30
Resolution of A/D Converter	12 bit	12 bit
Repeatability (deg)	< 0.02	< 0.04
Temperature Range	-40 to +60 deg C	-20 to +70 deg C
Output	PWM, Analog, RS-232	RS-232

**Tab. 2: Parameters of ETMs' Conversion Modules**

## 4 The Measurement Setup

All five tested ETMs were measured simultaneously using a modular system for attitude and position estimation [9]. As it was described in [10], the connectivity of modules to the modular system is resolved automatically according to standards IEEE 1451 [11, 12] and IEEE 1588 [12, 13]. In this case, the Micro-50-D70 was used as a primary ETM in the modular system and the four ETMs EZ-TILT-2000-xxx were connected just as additional modules. The whole measurement setup was mounted on a Rotational Tilt Platform (RoTiP). A block scheme of the measurement setup is shown in Fig. 5a and its real look in Fig. 5b. The U1 is the primary ETM connected via RS232 with one conversion module providing access to CAN bus forming the core of the modular system. The CAN bus respects the CAN Aerospace standard. The pair of modules S1 and S2, S3 and S4 are connected the in same way to additional system modules via RS232. The data are converted in all modules according to

CAN Aerospace standard to CAN frame and sent via CAN bus to a master module. The master module receives the data from all sub-modules and resent them to PC via RS232.

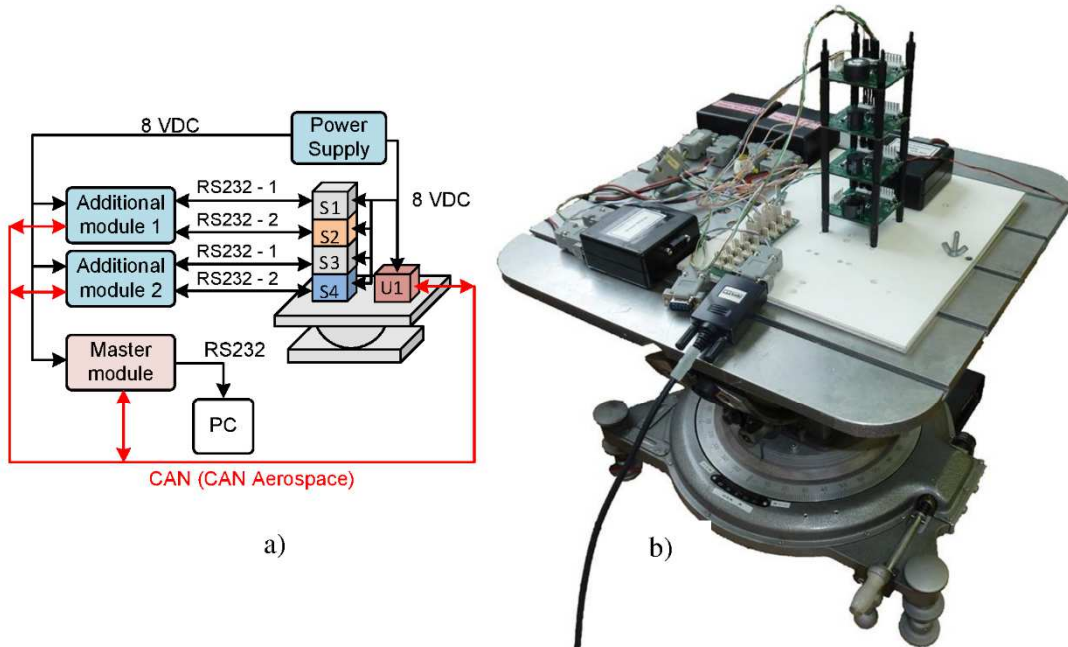


**Fig. 5: a) The block scheme of measurement setup; b) Measurement setup realization**

## 5 Tests and Results

This section provides results of electronic tilt modules measurements which help to analyze the sensors' performances from the accuracy and dynamic characteristics point of view. The tests covered the calibration procedure of ETMs, evaluation of deviations between tilt angles evaluated by upward and downward direction measurements, and settling time evaluation.

During all experiments and analyses the data from all ETMs were sampled and recorded with the frequency of 20 Hz. To eliminate the influence of noise contained in data we made a mean value of 30 seconds for each channel and each position under steady-state conditions. The resultant value was used as a representative for that particular position and channel for static characteristics. For the following tests and results, the range  $\pm 10$  deg covered the linear range of abovementioned sensors and fully satisfied their potential usage requirements for attitude compensation because if roll or pitch angles are higher than  $\pm 10$  deg the airplane is in most cases turning and it is not possible to use ETM for compensation purposes because of centrifugal acceleration.

For result comparison Root Mean Square Error (RMSE) defined by (1) was used.

$$RMSE(x_1, x_2) = \sqrt{\frac{\sum_{i=1}^n (x_{1,i} - x_{2,i})^2}{n}} \quad (1)$$

where:  $x_{1,i}$  is the vector of reference values;  $x_{2,i}$  denotes the vector of measured/estimated values; and  $n$  represents the number of measurements.

## 5.1 Transfer Characteristics

The transfer characteristics of all ETMs were measured using RoTiP platform in the range of  $\pm 10$  deg with the step of 1 deg. As a reference a precise accelerometer Clinotronic Plus with resolution 5 arcsec was used. Measured transfer characteristics of ETM related to reference values were then approximated using 3<sup>rd</sup> order polynomials to get corrections for both pitch (2) and roll angles (3).

$$\theta_{corr} = a \cdot \theta_{nc}^3 + b \cdot \theta_{nc}^2 + c \cdot \theta_{nc} + d, \quad (2)$$

$$\phi_{corr} = e \cdot \phi_{nc}^3 + f \cdot \phi_{nc}^2 + g \cdot \phi_{nc} + h, \quad (3)$$

where:  $\phi$  is the roll angle;  $\theta$  is pitch angle; subscript *corr* represents the angles after the polynomials correction; subscript *nc* corresponds to the measured non-corrected angles;  $a, b, c, d$  are coefficients of pitch angle polynomial;  $e, f, g, h$  are coefficients of roll angle polynomial, where the particular values of  $a - h$  coefficients depend on used ETM.

Figure 6 shows the deviations of pitch and roll angles of all ETMs from reference values before correction.

Transfer characteristics of all ETMs were corrected using the abovementioned polynomials. The worst RMSE values were in the case of EZ-TILT-2000-008-50%; for pitch angle 0.08 deg and for roll angle 0.03 deg. Except the RMSE, the maximal and minimal deviations from reference were observed and as in the previous case the highest deviations were found out in the case of sensor with viscosity about 50% higher. The minimal and maximal values for pitch angle were -0.13 deg and 0.15 deg, in case of roll -0.08 deg and 0.08 deg.

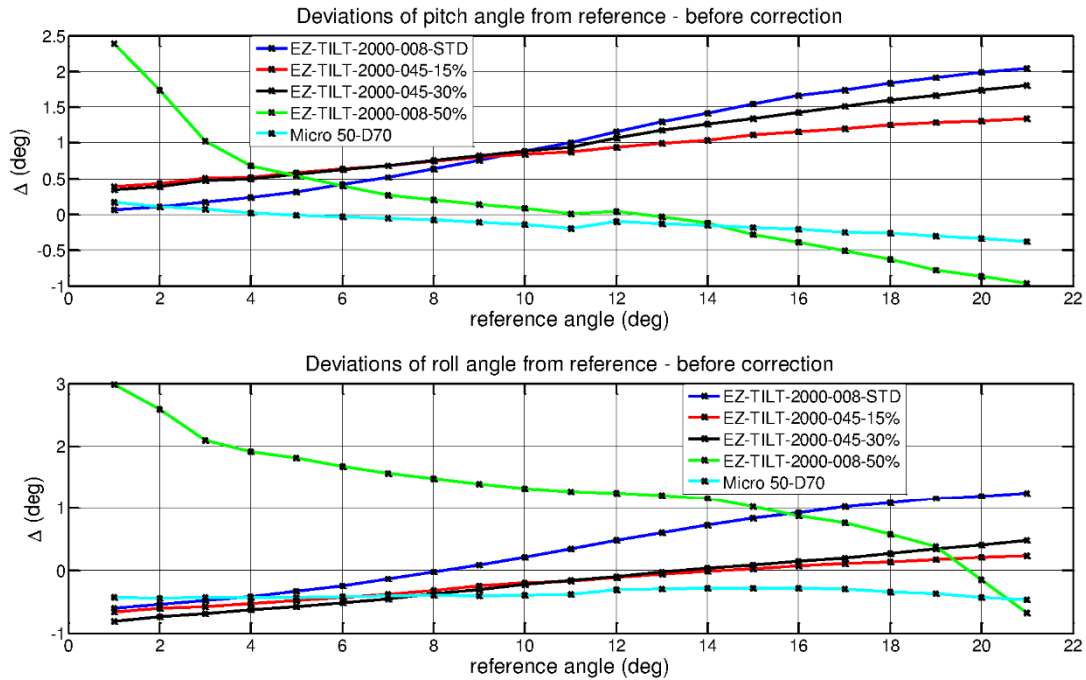


**Fig. 6: Deviations ( $\Delta$ ) of pitch and roll angles from reference values before correction**

## 5.2 Deviation between Tilt Angles Evaluated by Upward and Downward Direction Measurements

Using the same measurement procedure as in the previous section, the data for computation of deviations between tilt angles evaluated by upward and downward direction measurements were evaluated. The measured data were first corrected using the 3<sup>rd</sup> polynomials and after that, the deviations were analyzed. The RMSE, minimal and maximal values of these deviations were computed. The results are summarized in Tab. 3.

Electrolytic Tilt Module	Pitch Angle (deg)			Roll Angle (deg)		
	RMSE	MIN	MAX	RMSE	MIN	MAX
EZ-TILT-2000-008-STD	0.06	-0.11	0.00	0.05	-0.07	0.00
EZ-TILT-2000-008-15%	0.02	-0.05	0.05	0.04	-0.01	0.10
EZ-TILT-2000-008-30%	0.08	-0.12	0.10	0.08	-0.16	0.01
EZ-TILT-2000-008-50%	0.13	-0.43	0.22	0.16	-0.34	0.29
Micro 50-D70	0.05	-0.09	0.11	0.12	0.02	0.24

**Tab. 3: Parameters of ETMs' Conversion Modules**

### 5.3 Settling Time

The settling time is defined by a producer as an elapsed time measured from the end of the tilt disturbance until the sensor output reaches a steady state again [14]. We have measured 8 tilt changes for pitch angle and 8 tilt changes for roll angle with different angular velocities from  $\pm 5$  deg/s to  $\pm 55$  deg/s for both positive and negative directions in range from -6 deg to +6 deg. We have analyzed the settling time for all ETMs and measurements. The differences between particular measurements with different angular velocities were negligible for all ETMs, so as resultant values of settling time we have considered the mean values. The shortest settling time 0.61 second was performed by the EZ-TILT-2000-045-30% and the longest settling time 5.25 second was in the case of EZ-TILT-2000-008-50%. From these analyses it is evident that the EZ-TILT-2000-008-50% is more resistant to vibrations than the EZ-TILT-2000-045-30% and the sensor with viscosity about 50% higher can be substituted by the filter with lower cut-off frequency.

## 6 Conclusion

The main aim of this paper was to describe the function of electrolytic tilt sensors (ETSs) and electrolytic tilt modules (ETMs) and analyze their performances from static and dynamic characteristics point of view. In the paper, we have analyzed five ETMs with different electrolyte viscosity, four ETMs from Advanced Orientation Systems Inc. and one from Spectron Glass and Electronics Inc. First of all the corrections using 3<sup>rd</sup> order polynomials were applied, the resultant accuracy was analyzed and the worst RMSE values were in the case of EZ-TILT-2000-008-50% for pitch angle 0.08 deg and for roll angle 0.03 deg. After that the deviations in tilt angle between upward and downward direction measurements were computed. As in previous characteristics the highest deviations 0.13 deg for pitch and 0.16 deg for roll were determined in the EZ-TILT-2000-008-50% data. The longest settling time was measured in EZ-TILT-2000-008-50% as well and so this sensor is more resistant to vibrations than other sensors with lower viscosity. The deviations from reference 3<sup>rd</sup> after polynomial correction, the hysteresis, settling time will be presented at the conference.

## References

- [1] ŠIPOŠ, M.; ROHÁČ, J.: Usage of Electrolytic Tilt Sensor for Initial Alignment of Tri-axial Accelerometer, ICMT'11 International Conference on Military Technologies 2011, Brno, University of Defence, 2011, p. 685-691, ISBN 978-80-7231-788-2.

- [2] ŠIPOŠ, M.; ROHÁČ, J.; NOVÁČEK, P.: Analyses of Electronic Inclinometer Data for Triaxial Accelerometer's Initial Alignment, *Przeglad Elektrotechniczny*, vol. 88, no. 01a, p. 286-290, ISSN 0033-2097.
- [3] ŠIPOŠ, M.; PAČES, P.; REINŠTEIN, M.; ROHÁČ, J.: Flight Attitude Track Reconstruction Using Two AHRS Units under Laboratory Conditions, *The Eighth IEEE Conference on Sensors 2009*, Christchurch: IEEE Sensors Council, 2009, p. 675-678, ISBN 978-1-4244-5335-1.
- [4] ŠIPOŠ, M.; PAČES, P.; ROHÁČ, J.; NOVÁČEK, P.: Analyses of Triaxial Accelerometer Calibration Algorithms, *IEEE Sensors Journal*, 2012, vol. 12, no. 5, p. 1157-1165, ISSN 1530-437X.
- [5] REINŠTEIN, M.; ROHÁČ, J.; ŠIPOŠ, M.: Algorithms for Heading Determination using Inertial Sensors, *Przeglad Elektrotechniczny*, 2010, vol. 86, no. 9, p. 243-246, ISSN 0033-2097.
- [6] MARIANOVSKY, E.: Advances in Electrolytic Sensor Design and Their Use in the New Generation of Crash Dummies, Advanced Orientation Systems Inc., LINDEN, USA, 2012, online, cited: [2012-08-28], www: <http://www.aositilt.com/Press.htm>
- [7] DX-008 / DX-045 Dual Axis Tilt Sensors, Advanced Orientation Systems Inc., LINDEN, USA, 2012, online, cited: [2012-08-28], www: <http://www.aositilt.com/Dx.htm>
- [8] SP5000 and AU6000 Series, Spectron Glass and Electronics Inc., Hauppauge, USA, 2012, online, cited: [2012-08-28], www: <http://www.spectronsensors.com/datasheets/SDS-117-1409.pdf>
- [9] NOVÁČEK, P.; ŠIPOŠ, M.; PAČES, P.: Modular System for Attitude and Position Determination, *POSTER 2011 - 15th International Student Conference on Electrical Engineering*, CTU in Prague, Faculty of Electrical Engineering, 2011, p. 1-5, ISBN 978-80-01-04806-1.
- [10] ROHÁČ, J.; ŠIPOŠ, M.; NOVÁČEK, P.; PAČES, P.; REINŠTEIN, M.: Modular System for Attitude and Position Estimation, *Workshop 2011*, CTU in Prague, 2011, Czech Republic.
- [11] POPELKA, J.; PAČES, P.: Performance of Smart Sensors Standards for Aerospace Applications, *Przeglad Elektrotechniczny*, 2012, vol. 88, no. 01a, p. 229-232, ISSN 0033-2097.
- [12] PAČES, P.; RAMOS, H. M.; RAMOS, P.: Development of a IEEE 1451 Standard Compliant Smart Transducer Network with Time Synchronization Protocol, *IMTC/2007 IEEE Instrumentation and Measurement Technology Conference Proceedings*, Warsaw, IEEE, 2007, ISBN 1-4244-1080-0.
- [13] PAČES, P.; ŠIPOŠ, M.; VESELÝ, M.: Verification of IEEE1588 Time Synchronization in NASA Agate Data Bus Standard, *IEEE 2009 9th Conference on Electronic Measurement & Instruments*, Beijing, IEEE, 2009, ISBN 978-1-4244-3862-4.
- [14] General Application Notes: Terms and Definitions, Advanced Orientation Systems Inc., LINDEN, USA, 2012, online, cited: [2012-09-04], www: <http://www.aositilt.com/Ap0good.htm>

## Acknowledgement

This research has been partially supported by the research program TA CR Alfa No. TA02011092 “Research and development of technologies for radiolocation mapping and navigation systems”, partially by Grant Agency of the Czech Technical University in Prague grant No. SGS10/288/OHK3/3T/13, and partially by Czech Science Foundation project 102/09/H082.

#### 4.5. Analyses of Electrolytic Tilt Sensor Data for Triaxial Accelerometer's Initial Alignment

Martin ŠIPOŠ, Jan ROHÁČ, Petr NOVÁČEK

Czech Technical University in Prague (1)

## Analyses of Electronic Inclinometer Data for Tri-axial Accelerometer's Initial Alignment

**Abstract.** This paper deals with the usage of a dual-axis electronic inclinometer EZ-TILT-2000-008 to improve an initial alignment of a tri-axial accelerometer, which forms a part of the inertial measurement unit ADIS16405. There were performed several measurements under various initial conditions with the usage of a precise Rotational-Tilt Platform as a reference. Based on measured data the alignment procedure accuracy, null repeatability, stability of initial null angle, hysteresis, and cross-axis dependence were analyzed and the results of these analyses are presented.

**Streszczenie.** Zaprezentowano wykorzystanie dwoosiowego inklinometru EZ-TILT-2000-008 do poprawy ustawiania trzyosiowego przyśpieszeniomierza. Przeprowadzono badania dokładności, powtarzalności zera, histerezy i wpływu osi w opracownym przyśpieszeniomierzu. (Zastosowanie elektronicznego inklinometru do ustawiania trzyosiowego miernika przyśpieszenia).

**Keywords:** electronic inclinometer, tri-axial accelerometer, initial alignment, cross-axis dependence.

**Słowa kluczowe:** inklinometr, przyśpieszeniomierz.

### Introduction

Recently, a technological improvements in the precision and reliability of Micro-Electro-Mechanical-Systems (MEMS) have enabled the usage of low-cost MEMS inertial sensors in wide range of civil and military applications, such as a car navigation, personal navigation, indoor navigation, navigation of unmanned aerial vehicles, underwater navigation, human motion tracking, etc. [1, 2, 3, 4, 5, 6].

A basic part of common navigation systems, which is an Inertial Measurement Unit (IMU), primarily contains accelerometers (ACCs) and angular rate sensors (ARSs) for providing inertial data, and additionally magnetometers (MAGs). These sensors' data are used for various navigation computations such as attitude, velocity and position estimation, initial alignment, etc. In navigation systems, first of all, it is necessary to determine the initial attitude of the navigation system including the determination of initial Euler angles (the roll, pitch, and yaw). They describe the relationship between the sensor frame (SF) and the local navigation frame (LNF) in which the navigation is performed.

For IMUs with low-cost ARSs the initial attitude cannot be determined by a self-alignment procedure using only ARSs them-selves [7, 8], because aforementioned sensors are not able to sense the Earth rotation, which is usually below the noise level [9]. Therefore, the initial attitude has to be determined using the ACCs and MAGs. The procedure of initial attitude determination is called the coarse alignment and its accuracy depends on the level of imperfections of ACCs and MAGs (scale factor corrections, angles of non-orthogonality, biases, etc.). These can be partially compensated using a sensor error model [3, 10]. After the coarse alignment has been done, the Euler angles are initialized and regular Euler angles estimation process, for details see [11], can take place.

This paper extends the analyses presented in [1] and deals with the usage of an electronic inclinometer (EI) EZ-TILT-2000-008 (Advanced Orientation Systems Inc. [12]). The EI is used to improve the initial levelling done based on tri-axial accelerometer, in our case, contained in the IMU ADIS16405 (Analog Devices [13]). The levelling procedure forms the part of initial attitude determination, in which the pitch and roll angles are estimated. The accuracy of initial attitude determination depends on biases of ACCs which cause non-negligible errors in pitch and roll estimates and vary with each system turning-on. This mentioned imperfection of accelerometers was a motivation for using other system with a different principle of angles estimation. In our case, the EI was used, which enabled the estimation

of accelerometer biases. There were performed several measurements under various initial conditions with the usage of the Rotational-Tilt Platform (RoTiP) as the reference. Based on the measured data the accuracy analyses were performed.

### Initial Attitude Determination

The initial attitude determination is a procedure, in which Euler angles are estimated. There exist various algorithms for initial attitude determination, e.g. a coarse/fine alignment, static/in-motion alignment, analytic alignment and so on [9]. In this paper, the initial attitude is evaluated using the coarse alignment procedure only. This procedure can be divided into two steps. First one includes the levelling procedure to determine the pitch and roll angles. The following one is named a course alignment and determines the yaw angle [8]. For IMUs consisted of tri-axial MAG as well as ACC and ARS, the yaw angle can be determined easily. In the following part only the levelling procedure is described.

### Levelling procedure

A main aim of the levelling is determine the pitch (1) and roll (2) angles according to the gravity vector measured by tri-axial ACC under static conditions [7, 8].

$$(1) \quad \theta = \arctg \left( -f^{by} / \sqrt{(f^{bx})^2 + (f^{bz})^2} \right)$$

$$(2) \quad \phi = \arctg \left( f^{bx} / -f^{bz} \right)$$

where:  $\theta$  is the pitch angle,  $\phi$  denotes the roll angle,  $f^{bx}$ ,  $f^{by}$ ,  $f^{bz}$  are measured accelerations in the sensor frame.

The procedures of the levelling and course alignment were described in detail by Soták in [7, 8]. Based on the real tests performed by Soták it can be seen that the estimated values of pitch and roll angles are not identical with the reference ones due to the influence of accelerometer biases. Based on the specifications of ADIS16405 the initial bias error is up to  $\pm 50$  mg (for  $1\sigma$  corresponding 68% probability) and thus can cause the error of  $\pm 2.9$  degree in zero tilt. This error negatively influences the final accuracy of estimated initial attitude as well as the following position evaluation. This imperfection of the process was the motivation for a usage of a different system to measure and correct the pitch and roll angles determined from the accelerometer during the coarse alignment procedure [1].

### Applied Systems and Measurement Setup

This section describes basic specifications of applied measurement systems. The performance of the ADIS16405's tri-axial ACC (Analog Devices [13]) is provided in Table 1. In the case of the electronic inclinometer (EI) EZ-TILT-2000-008 (Advanced Orientation Systems Inc. [12]) it is in Table 2.

Table 1. The parameters of the ADIS16405's accelerometer [13]

Accelerometer's parameter	Typical value
Dynamic range	$\pm 18 \text{ g}$
Initial sensitivity	3.33 mg/LSB
Initial bias error ( $\pm 1\sigma$ )	$\pm 50 \text{ mg}$
In-run bias error ( $\pm 1\sigma$ )	0.2 mg
Velocity random walk ( $\pm 1\sigma$ )	0.2 m/s/ $\sqrt{\text{hr}}$
Output noise (no filtering, rms)	9 mg
Noise density (no filtering)	0.5 mg/ $\sqrt{\text{Hz}}$

Table 2. The parameters of the EZ-TILT-2000-008 [12]

EI's parameter	Typical value
Range	$\pm 8 \text{ deg}$
Analog output	1 to 4 VDC
Power supply	6 to 12 VDC
Resolution of A/D convertor	12 bit
Response (10% - 90%)	40 ms
Repeatability	<0.02 deg
Temperature range	-40 to +60 degC

The EI (Fig. 1a) is an advanced programmable dual-axis linear analog/digital module with CMOS microprocessor which includes a dual-axis polymer based electrolytic tilt sensor (ETS) DX-008. The EI module provides analog, PWM, and RS-232 tilt information in two axes. Full description is specified in [12]. In our case, the viscosity of ETS was about 50% higher than viscosity of standard ETS.

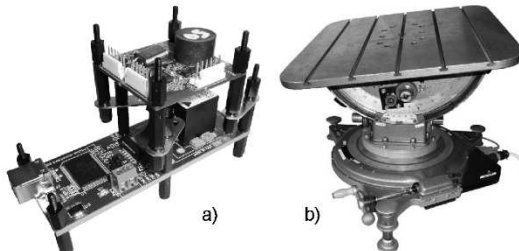


Fig.1. a) ADIS16405 board with EZ-TILT-2000-008 mounted on; b) Rotational-Tilt Platform

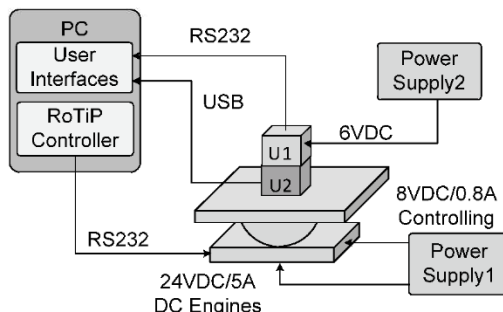


Fig.2. A block scheme of measurement setup; U1 – electronic inclinometer EZ-TILT-2000-008, U2 – IMU ADIS16405

As a reference system for the results comparison and analyses we used the Rotational-Tilt Platform (RoTiP), see Fig. 1b. The RoTiP is capable to set positions with required attitude and speed along three axes. The specification of RoTiP is provided in Table 3.

Table 3. The parameters of Rotational-Tilt Platform

Parameter	Range	Speed of motion	Resolution
Pitch	$\pm 45 \text{ deg}$	$\pm 42 \text{ deg/s}$	0.00033 deg
Roll	$\pm 25 \text{ deg}$	$\pm 60 \text{ deg/s}$	0.00065 deg
Heading	0 to 360 deg	$\pm 310 \text{ deg/s}$	0.00074 deg

A block scheme of measurement setup is shown in Fig. 2. It includes the RoTiP with its power supply, two measurement systems (EI, IMU) powered by other DC power supply and USB, and a PC control station. The PC software controls the RoTiP position via RS232 bus and collects the data from the measurement systems.

### Tests and Results

This chapter provides the results of EI and ACCs tests which helped to analyse the measurements system performances from their accuracy point of view. The tests covered the effect of EI correction on the final accuracy, the correction of ACC's transfer characteristics, a null repeatability, the stability of the initial null angle, the hysteresis, and cross-axis dependence.

During all experiments and analyses the data from ADIS16405 were sampled and recorded with the frequency 100 Hz and the data from EZ-TILT-2000-008 with 14 Hz. To eliminate the influence of a noise contained in the data we made a mean value of 100 samples for each channel and each position under steady-state conditions and a resultant averaged value was used as a representative for that particular position and channel.

For a result comparison Root Mean Square Error (RMSE) defined by (3) was used.

$$(3) \quad RMSE(x_1, x_2) = \sqrt{\frac{\sum_{i=1}^n (x_{1,i} - x_{2,i})^2}{n}}$$

where:  $x_{1,i}$  is the vector of reference values,  $x_{2,i}$  denotes the vector of measured/estimated values, and  $n$  represents the number of measurements.

### Transfer Characteristics

The transfer characteristics of both measurement systems were measured using RoTiP platform in the range approximately  $\pm 8 \text{ deg}$  with the step of 1 deg. The systems were consequently tilted among steady-state positions with angular velocity 2 deg/s. Measured transfer characteristics of EI related to the reference values were then approximated using 2<sup>nd</sup> order polynomials to get corrections for both pitch (4) and roll (5) angles.

$$(4) \quad \theta_{cor} = 0.001761 \cdot \theta_{nc}^2 + 1.031 \cdot \theta_{nc} + 0.6138$$

$$(5) \quad \phi_{cor} = 0.001761 \cdot \phi_{nc}^2 + 1.033 \cdot \phi_{nc} + 0.2546$$

where:  $\theta$  is the pitch angle,  $\phi$  denotes the roll angle, subscript  $cor$  represents the angles after the polynomial correction, subscript  $nc$  corresponds to the measured non-corrected angles.

The deviations of EI transfer characteristics from the reference values before and after the correction are shown in Fig. 3. The effect of EI transfer characteristics correction on the precision of ACC biases estimation and consecutive ACC based angles estimation can be seen in Fig. 4. The experiment in each position considered that based on corrected value of EI ACCs were newly initialized, which means that the biases of ACCs were newly estimated and corrected. The RMSE and variance values from Fig. 3 and Fig. 4 are listed in Table 4.

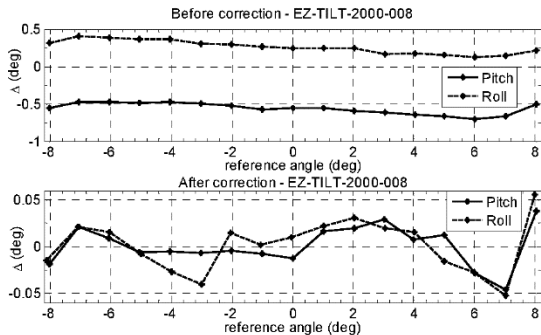


Fig.3. Deviations ( $\Delta$ ) of pitch and roll angles from the reference values before and after corrections using 2<sup>nd</sup> order polynomials – electronic inclinometer EZ-TILT-2000-008

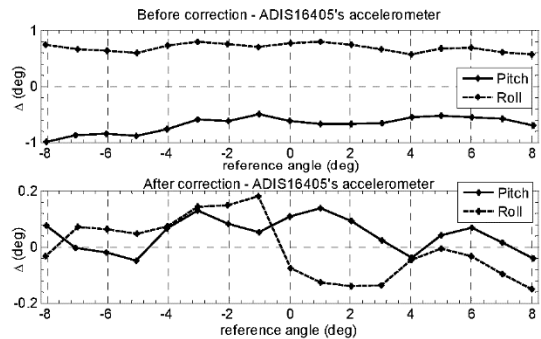


Fig.4. Deviations ( $\Delta$ ) of pitch and roll angles from the reference values before and after bias corrections using corrected data of electronic inclinometer – ACC of IMU ADIS16405

Table 4. The RMSE and variance values before and after correction for EI and ACC (according to Figs. 3-4)

	EI (deg)		ACC (deg)	
	Pitch	Roll	Pitch	Roll
RMSE before correction	0.57	0.27	0.69	0.70
RMSE after correction	0.04	0.05	0.07	0.10
Variance before corr.	0.0057	0.0077	0.0213	0.0053
Variance after corr.	0.0005	0.0005	0.0114	0.0034

#### Null Repeatability

The repeatability is defined as an angular error calculated from angle deviations when the measurement system is repeatedly placed in the same position and consequently replaced from it. A special angle of importance is the null angle, which is characterized by the null repeatability characteristics [14]. As in the previous case, the RoTiP was used to set the positions and to refer the angles. The ACC and EI were tilted within the range of  $\pm 8$  deg along combined directions (positive pitch and negative roll and conversely). The angular rate between subsequent positions was kept at the value of 2 deg/s in all cases. For each channel of EI and ACC and steady-state conditions the average of 100 samples was calculated. Fifty times the null angle position was subsequently set up. The performances of EI and ACC are shown in Fig. 5.

Based on obtained data from the null repeatability experiment the RMSE of EI performance was 0.12 deg for the pitch and 0.09 deg for the roll angle. In the case of ACC the RMSE was higher in both cases, i.e. 0.81 deg for the pitch and 0.40 deg for the roll angle. From Fig. 5 it is clear that the null repeatability of ACC is influenced by the initial bias error, which can be compensated using the bias correction obtained from EI.

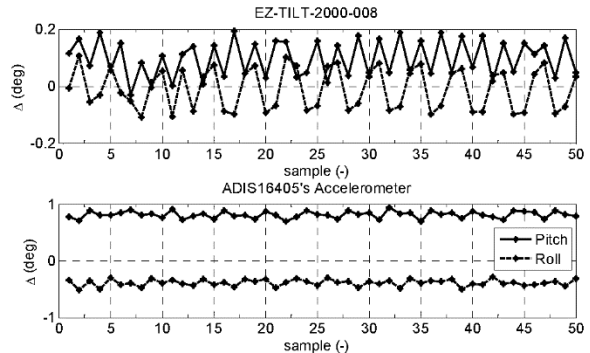


Fig.5. The Null repeatability of pitch and roll angles for the EI and the ACC, where “ $\Delta$ ” means a deviation between measured angle and the reference angle equal to 0 deg

#### Stability of Initial Null Angle

The stability of an initial null angle, which corresponds to an initial bias error defined by Analog Devices [13], was also observed. For both systems there were performed 20 measurements during 4 days. Each measurement was performed after the power was 60 seconds switched-on to stabilize the system operating conditions. As well as in previous cases in each position and steady-state conditions 100 data samples were averaged to obtain the value we then worked with.

The RMSE for the pitch and roll angles of EI was 0.05 deg in both axes. The RMSE for the pitch and roll of ACC was 0.87 deg and 0.25 deg, respectively. The stability of initial null angle characteristics for both EI and ACC is shown in Fig. 6. From the ACC characteristics it can be seen that the pitch and roll angles were again influenced by an initial bias error, unlike the EI. According to Fig. 6, the initial bias error has smaller influence on EI than on ACC. It proves the EI to be suitable for initial ACC corrections from the null angle stability point of view.

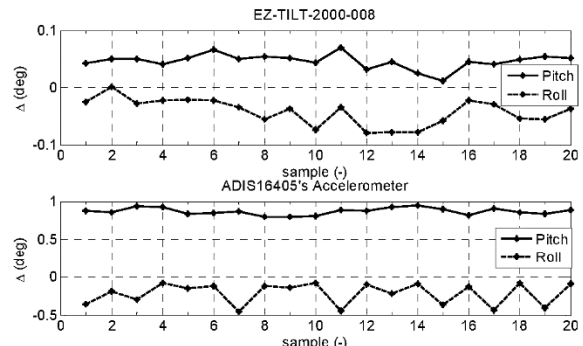


Fig.6. The Stability of an initial null angle for EI and ACC, where “ $\Delta$ ” represents a deviation between a measured angle and a reference angle equal to 0 deg

#### Hysteresis

The hysteresis characteristics were measured in the range of  $\pm 8$  deg forward and backward for both angles of tilt. As in previous measurements, the average of 100 samples was taken as a representative value of particular steady-state position. The hysteresis was observed on the sensor data already compensated for the nonlinearity and initial offset. According to tilt angles evaluated based on measured data when the RoTiP was tilted from -8 deg up to +8 deg and back, we evaluated differences between obtained angles of both directions and a particular reference angle of RoTiP. The progresses of those

differences for both sensors are presented in Fig. 7. The hysteresis  $\delta_H$  can be then calculated according to (6).

$$(6) \quad \delta_H = \left( \frac{y_{up} - y_{down}}{y_{max} - y_{min}} \right)_{max} .100 (\%)$$

where  $y_{up}$  denotes an evaluated value from a forward measurement (tilt being increased),  $y_{down}$  corresponds to a backward measurement (tilt being decreased), and  $y_{min}, y_{max}$  are the minimal and maximal values of the measurement.

With respect to (6) and measured data the EI hysteresis was 0.51 % for the pitch and 0.43 % for the roll angle. The hysteresis for ACC was 0.71 % for the pitch and 1.19 % for the roll angle.

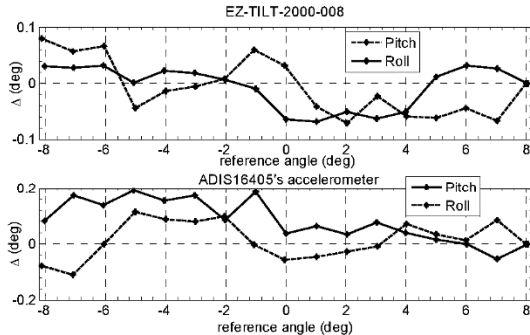


Fig.7. The progress of differences “ $\Delta$ ” defined between tilt angles evaluated from measurements in which the RoTiP was tilted from -8 deg up to +8 deg and in backward direction. The differences correspond to the same reference angle of RoTiP set within a forward and backward direction of the measurement

#### Cross-axis Dependence

The cross-axis dependence was measured for both systems using the same procedure and the same number of samples to be averaged for representing values as in previous cases. In the cases of the pitch angles being changed, the roll angle deviations were measured. In the other case, the roll angles were changed and pitch angle deviations were measured. The measured data for both systems were analysed. The cross-axis dependencies for ACC are shown in Fig. 8. The RMSE was 0.08 deg for the pitch and 0.06 deg for the roll angle.

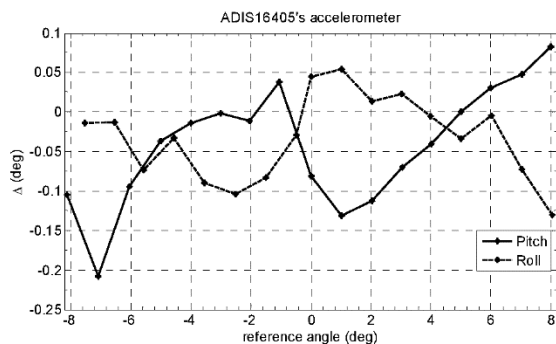


Fig.8. Cross-axis dependence of ACC where “ $\Delta$ ” represents cross-axis deviation

According to measured characteristics of ACC it can be seen that the cross-axis error is negligible with respect to other error sources. Unfortunately, performed analyses of EI showed the strong cross-axis dependence and the additional measurements had to be performed. The cross-

axis dependencies for the pitch and roll angles of EI are shown in Fig. 9 and Fig. 10, respectively.

The measured characteristics were analysed and approximated by two-variable polynomials. We analysed different order of polynomials from the computational cost and the accuracy points of view. The RMSEs which were computed from deviations between measured and reference angles before and after cross-axis correction using different order polynomials are shown in Table 5.

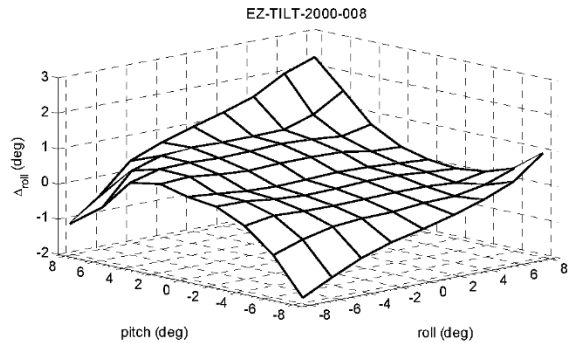


Fig.9. Cross-axis dependence of EI – pitch angle tilted, roll angle deviations observed

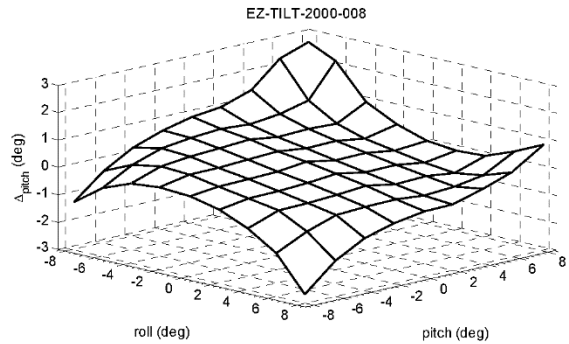


Fig.10. Cross-axis dependence of EI – roll angle tilted, pitch angle deviations observed

Furthermore, we performed the correction using other mathematical algorithm – LOcally WEighted Scatterplot Smoothing (LOWESS), but the application of this algorithm did not lead to well-marked improvement of the accuracy. Finally, we chose 3<sup>rd</sup> order polynomials described by (7) and (8) for pitch and roll correction, respectively.

$$(7) \quad \Delta\theta = 0.093 - 0.081\theta - 0.082\phi - 0.002\theta^2 - 0.003\theta\phi + 0.001\theta^3 + 0.003\theta\phi^2 - 0.0001\phi^3$$

$$(8) \quad \Delta\phi = 0.273 + 0.077\theta - 0.050\phi - 0.001\theta^2 + 0.001\theta\phi - 0.001\phi^2 + 0.0003\theta^3 + 0.003\theta^2\phi + 0.0005\phi^3$$

where:  $\Delta\theta, \Delta\phi$  are the pitch and roll corrections,  $\theta, \phi$  are estimated pitch and roll angles.

Table 5. The RMSEs of applied polynomials for EI cross-axis correction

Applied polynomial	RMSE (deg)	
	Pitch	Roll
No correction	0.67	0.77
Correction using 1 <sup>st</sup> order polynomial	0.44	0.39
Correction using 2 <sup>nd</sup> order polynomial	0.43	0.38
Correction using 3 <sup>rd</sup> order polynomial	0.13	0.14
Correction using 4 <sup>th</sup> order polynomial	0.12	0.12
Correction using 5 <sup>th</sup> order polynomial	0.09	0.10

### Conclusion

This paper concerns a levelling procedure of navigation systems using tri-axial accelerometer (ACC) and electronic inclinometer (EI). The levelling forms the part of coarse alignment process which is needed to be performed within the initialization of inertial navigation systems. The levelling is generally done by ACCs; however, ACC biases negatively affect its precision. Due to this reason other system is required and thus we analysed how the precision can be improved by EI utilization and what weak points the system has.

In our case we used ACCs of IMU ADIS16405 and electrolytic tilt sensor of EZ-TILT-2000-008 EI system. Both systems belong to the low-cost category. The main aim was to analyse different effects of their characteristics on the levelling precision. For both systems we analysed the transfer characteristics, null repeatability, stability of initial null angle, hysteresis, and cross-axis dependence. All these characteristics were measured in the range of  $\pm 8$  deg using a Rotational-Tilt Platform (RoTiP) which provided us with reference values of tilt. These values were related with ACC and EI data and used for analyses.

The RMSEs of performed analyses are summarized in Table 6. From this table, it can be seen that the main error affecting accuracy of the EI was caused by a cross-axis dependence with the RMSE equal to 0.13 deg for the pitch angle and 0.14 deg for the roll angle. These errors can be further reduced by using higher order polynomials or using other correction algorithms, such as aforementioned LOWESS. Nevertheless, with more and more complicated functions applied the computation cost will increase and the accuracy improvement will not change so much.

The measured characteristics of EI were slightly different from values specified by manufacturer. It was probably caused by using an electrolyte with higher viscosity than the one generally used in standard EI systems. However, according to measured data and performed analyses we proved that the corrections based on EI data led to the improvement of the levelling accuracy, which was our main purpose.

Table 6. The results of performed analyses for EI EZ-TILT-2000-008 and ACC ADIS16405's

Performed analyses	EI		ACC	
	Pitch	Roll	Pitch	Roll
No correction: RMSE (deg)	0.57	0.27	0.69	0.70
After correction: RMSE (deg)	0.04	0.05	0.07	0.10
Null repeatability: RMSE (deg)	0.12	0.09	0.81	0.40
Init. null angle stability: RMSE (deg)	0.05	0.05	0.87	0.25
Hysteresis (%)	0.51	0.43	0.71	1.19
Cross-axis dependence: RMSE (deg)	0.13	0.14	0.08	0.06

This research has been partially supported by Czech Science Foundation project 102/09/H082, partially by the research program No. MSM6840770015 "Research of Methods and Systems for Measurement of Physical Quantities and Measured Data Processing" of the CTU in Prague.

Prague sponsored by the Ministry of Education, Youth and Sports of the Czech Republic and partially by Grant Agency of the Czech Technical University in Prague grant No. SGS10/288/OHK3/3T/13.

### REFERENCES

- [1] Šipoš M., Roháč J., Usage of Electrolytic Tilt Sensors for Initial Alignment of Tri-axial Accelerometer, *ICMT11 International Conference on Military Technologies 2011*, 2011, Brno, Czech Republic, 685-691
- [2] Šipoš M., Roháč J., Calibration of Tri-axial Angular Rate Sensors, *MDS2010 - Measurement, Diagnostics, Dependability of Aircraft Systems*, 2010, Brno, Czech Republic, 148-152
- [3] Reinstein M., Šipoš M., Roháč J., Error Analyses of Altitude and Heading Reference Systems, *Przegląd Elektrotechniczny*, 85 (2009), nr 8, 114-118
- [4] Sipos M., Paces P., Reinstein M., Roháč J., Flight Attitude Track Reconstruction Using Two AHRS Units under Laboratory Conditions, *IEEE Sensors 2009, Christchurch, New Zealand*, 2009, 675-678
- [5] Jurman D., Jankovec M., Kamnik R., Topic M., Calibration and Data Fusion Solution for the Miniature Attitude and Heading Reference System, *Sensors and Actuators A-Physical*, 138 (2007), 411-420
- [6] Reinstein M., Roháč J., Šipoš M., Algorithms for Heading Determination Using Inertial Sensors, *Przegląd Elektrotechniczny*, 86 (2010), nr 9, 243-246
- [7] Soták M., Testing the coarse alignment algorithm using rotation platform, *Acta Polytechnica Hungarica*, ISSN 1785-8860, 7 (2010), nr 5, 87-107
- [8] Soták M., Coarse alignment algorithm for ADIS16405, *Przegląd elektrotechniczny*, ISSN 0033-2097, 86 (2010), nr 9, 247-251
- [9] Reinstein M., Evaluation of Fine Alignment Algorithm for Inertial Navigation, *Przegląd Elektrotechniczny*, 87 (2011), nr 7, 255-258
- [10] Šipoš M., Pačes P., Roháč J., Nováček P., Analyses of Triaxial Accelerometer Calibration Algorithms, *IEEE Sensors Journal*, 2011, accepted for publication.
- [11] Jalovecký R., Janů P., Computation Method Analysis of Turn Angle, *International Conference on Military Technologies 2010*, Bratislava, Slovak Republic, 2010.
- [12] EZ-TILT-2000-008-rev2 Multi-Output Dual Axis High Res. Conversion Module w/RS232, *Advanced Orientation Systems*, Linden, USA, 2009, URL: <<http://www.aositilt.com/Ez208.htm>>, [cit. 2011-07-20]
- [13] Triaxial Inertial Sensor with Magnetometer ADIS16400/ADIS16405, *Analog Devices*, Norwood, USA 2009, URL: <[http://www.analog.com/static/imported-files/data\\_sheets/ADIS16400\\_16405.pdf](http://www.analog.com/static/imported-files/data_sheets/ADIS16400_16405.pdf)>, [cit. 2011-07-20]
- [14] General Application Notes, *Advanced Orientation Systems*, Linden, USA, 2009, URL: <<http://www.aositilt.com/Ap0good.htm>>, [cit. 2011-07-20]

**Authors:** Ing. Martin Šipoš\*, E-mail: [siposmar@fel.cvut.cz](mailto:siposmar@fel.cvut.cz), Ing. Jan Roháč\*, Ph.D., E-mail: [xrohac@fel.cvut.cz](mailto:xrohac@fel.cvut.cz), Ing. Petr Nováček\*, E-mail: [petr.novacek@fel.cvut.cz](mailto:petr.novacek@fel.cvut.cz) \*Czech Technical University in Prague, Technická 2, Prague, Czech Republic.

#### 4.6. Practical Approaches to Attitude Estimation in Aerial Applications

Hindawi Publishing Corporation  
International Journal of Aerospace Engineering

### Research Article

## Practical Approaches to Attitude Estimation in Aerial Applications

**Martin Sipos, Jakub Simanek, Jan Rohac**

*Department of Measurement, Faculty of Electrical Engineering, Czech Technical University in Prague, Technicka 2, Prague, Czech Republic*

Correspondence should be addressed to Martin Sipos, [siposmar@fel.cvut.cz](mailto:siposmar@fel.cvut.cz)

This paper focuses on practical approaches to attitude estimation suitable for aerial applications. A main concern is in the comparison of their performances based on real flight experiments. All covered approaches are theoretically described and then applied to evaluate flight data with respect to a referential attitude obtained by a multi-antenna GPS receiver. The first approach uses a complementary filter providing estimates based only on inertial data measured by a low-cost inertial measurement unit (IMU). The second approach implements an IMU/GPS integration scheme using extended Kalman filter (EKF) evaluating the attitude and position based on inertial data supplemented by the position obtained from a single-antenna GPS receiver. The third approach fuses data from an IMU, magnetometer, and electrolytic tilt sensor via the EKF, which is further extended by the Gauss-Newton minimization method. These three approaches were implemented and compared based on measured real flight data which suffer from vibration impacts varying according to a flight phase. Reducing the vibration impacts on the accuracy of the attitude estimation was a main motivation. Results of attitude estimation performed with these three approaches are provided to confirm their accuracy and suitability in aerial applications.

### 1. Introduction

Generally, the usage of low-cost Inertial Measurement Units (IMUs) is broad nowadays. Of course, the objective "low-cost" has a crucial meaning in sense of potential applications. As long as low-cost IMUs use MEMS (Micro-Electro-Mechanical Systems) based inertial sensors they are small in dimensions, light, low power consuming and thus their presence can be found for instance in mobile phones, terrestrial vehicles, robots, stabilized platforms as well as in Unmanned Aerial Vehicles (UAVs), small aircrafts, and satellites. Even if the applications are cost-effective, the performance commonly requires data fusion from various sources due to the inertial sensors' imperfections, such as insufficient resolution for navigation purposes, bias instabilities, noise etc. Therefore, a special data treatment needs to be involved. In sense of aerial applications the usage of UAVs has increased rapidly in recent years. UAVs can be employed in many military and civil applications [1], [2] fulfilling a broad spectrum of assignments in fields of reconnaissance, surveillance, search and rescue, remote sensing for atmospheric measurements, traffic monitoring, natural disaster, damage assessment, inspection of power lines, or for aerial photography [2], [3]. These applications generally require navigation to be

carried out which includes the attitude, velocity, and position estimation [4] and thus cost-effective solutions have been commonly studied and implemented with advantage.

A current research and development in the area of low-cost navigation systems are focused on small scale and as cheap as possible solutions [5]. As mentioned, as long as MEMS based IMUs are used the evaluation process requires data fusion from available aiding sources. These sources stabilize errors in navigation solutions and thus increase navigation accuracy. Over last few years, a solution of vehicle navigation without absolute position measurements provided by GPS or radio frequency beacons has become very popular. For indoor or low altitude navigation it can use for example cameras, laser scanners, or odometers in terrestrial navigation [6], [7]. However, the solutions fusing inertial measurements aided by GPS are still preferable for aerial vehicles operating outside in large areas simply because of unblocked GPS signals. The implementation of other aiding sensors, such as magnetometer or pressure sensors, can further enhance the overall accuracy, reliability, and robustness of a navigation system [8], [9]. An attention is also paid to data processing algorithms used for attitude and position estimation, so there can be found many literature sources dealing with filtering techniques using for instance complementary filters [10].

particle filters [11], or Kalman filters (KFs) [12], [13]. In the last named case the extended KF (EKF) is used most of the time since it provides an acceptable accuracy with a reasonable computational load. Therefore, KF represents one of the most used algorithms for UAV attitude estimation (see comprehensive survey of estimation techniques done by authors in [14]) and is often complemented by other algorithms and decision-based aiding [15]. However, most of the state estimation algorithms are evaluated in simulations, or with respect to other techniques utilizing inertial and magnetic sensors.

Applied navigation solutions also need to deal with vehicle vibrations which affect inertial measurements them-selves. The vibrations can have different frequency content and thus the solutions require particular tuning of fusion parameters. This paper contribution is in a tuning of these parameters as well as in a performance comparison of different approaches to attitude estimation suitable for aerial applications respecting harsh environment with high vibration impacts. For the purpose of obtaining real flight synchronous data with the possibility of various fusion schemes a modular navigation system was used [16]. It consisted of a MEMS based IMU, single-antenna GPS receiver, magnetometer, and electrolytic tilt sensors (ETSs) with a different electrolyte viscosity. Different attitude estimation approaches were applied on the obtained data: using the IMU data only, which provided elementary level of independence, which was in contrast to other approaches using the IMU data aided by a magnetometer, ETS, and GPS receiver. The approaches studied in this paper fuse the data via a complementary filter and EKF. In one case the EKF is further extended by the Gauss-Newton Minimization (GNM) algorithm.

All studied approaches are tuned to satisfy a certain level of accuracy and applied on real flight data. The results are compared to an accurate referential attitude obtained from a multi-antenna GPS receiver. Such comparison with an independent referential system provides a thorough overview of performances of studied approaches and shows their capabilities to handle sensors' imperfections and vibration impacts of harsh environment on the accuracy of attitude estimation in aerial applications.

## 2. Attitude Estimation Approaches

This section describes the attitude (i.e., Euler angles - roll, pitch, and yaw ( $\phi, \theta, \psi$ ), or quaternion representation) estimation approaches relying on measured data from IMU, magnetometer, electrolytic tilt sensor (ETS), and GPS receiver.

### 2.1. Attitude Estimation Based on Accelerometer and Gyroscope Data

An IMU commonly consists of a triaxial accelerometer (ACC) and triaxial gyroscope providing acceleration and angular rate measurements in the direction along all three sensitivity axes. The ACCs measure the components of translational and gravitational acceleration. The gyroscopes measure

inertial angular rates along their sensitivity axes including also the Earth's rotation. However, in the case of MEMS based low-cost gyroscopes the Earth rotation is under the resolution; therefore, it is not necessary to consider it in calculations.

The attitude can be estimated solely from ACC and gyroscope data, but the final accuracy is not sufficient in any case due to limiting factors. The attitude from ACCs can be used only under steady-state conditions, e.g., for determination of initial roll and pitch angles or in flight phases when the vehicle is not maneuvering or accelerating. On the other hand, the gyroscopes can be used for standalone attitude estimation, but the final accuracy strongly depends on their parameters and due to the integration of angular rates the errors are unbounded and often grow rapidly. This fact limits their usage only for short periods of time.

The ACC readings can be used for determination of roll and pitch angles using (1), also referred to as coarse alignment, which is commonly used to initialize the roll and pitch angles before taking off [17]:

$$\begin{bmatrix} \phi_{ACC}(k) \\ \theta_{ACC}(k) \end{bmatrix} = \begin{bmatrix} \text{atan2}(a_y^b(k), a_z^b(k)) \\ \text{atan2}\left(-a_x^b(k), \sqrt{a_y^b(k)^2 + a_z^b(k)^2}\right) \end{bmatrix} \quad (1)$$

where subscript *ACC* denotes that the angles are based on accelerations;  $(a_x^b, a_y^b, a_z^b)$  are accelerations measured by triaxial ACC and atan2 is a four-quadrant arctangent function. These roll and pitch estimates are valid only under aforementioned steady-state conditions.

Estimation of the Euler angles is primarily based on angular rates integration as described by (2-4):

$$\begin{bmatrix} \Delta\phi_{GYR}(k) \\ \Delta\theta_{GYR}(k) \\ \Delta\psi_{GYR}(k) \end{bmatrix} = \begin{bmatrix} 1 & \sin\phi \tan\theta & \cos\phi \tan\theta \\ 0 & \cos\phi & -\sin\phi \\ 0 & \sin\phi \sec\theta & \cos\phi \sec\theta \end{bmatrix}_{(k-1)} \cdot (\boldsymbol{\omega}^b(k) - \bar{\boldsymbol{\omega}}) T_s \quad (2)$$

where  $\Delta$  is an angle increment; subscript *k* denotes the discrete time; subscript *GYR* denotes that the angles are based on gyroscope readings;  $\boldsymbol{\omega}^b$  is the vector of measured angular rates;  $T_s$  is a sampling period; and  $\bar{\boldsymbol{\omega}}$  is the vector of biases estimated as:

$$\bar{\boldsymbol{\omega}} = \frac{1}{m} \sum_{k=1}^m \boldsymbol{\omega}^b(k) \quad (3)$$

where  $m$  is the number of measured samples under static conditions during initialization phase (ranges typically from few seconds up to few minutes of averaging under static conditions).

The final attitude based on gyroscope data is computed using following equation:

$$\begin{bmatrix} \phi_{GYR}(k) \\ \theta_{GYR}(k) \\ \psi_{GYR}(k) \end{bmatrix} = \begin{bmatrix} \phi_{GYR}(k-1) \\ \theta_{GYR}(k-1) \\ \psi_{GYR}(k-1) \end{bmatrix} + \begin{bmatrix} \Delta\phi_{GYR}(k) \\ \Delta\theta_{GYR}(k) \\ \Delta\psi_{GYR}(k) \end{bmatrix} \quad (4)$$

where  $\phi_{GYR}(0)$  and  $\theta_{GYR}(0)$  are initialized using (1).

## 2.2. Attitude Estimation Using Aiding Systems

Since the attitude is primarily based only on angular rates integration it diverges rapidly from true values. When ACCs are considered as an aiding source, gravity measurements allow compensation only in the roll and pitch channels under steady-state conditions. To overcome this limitation other approaches might be used. Therefore, this section presents potential approaches using aiding sources and suitable for attitude estimation in aerial applications. This section thus presents two different approaches to yaw estimation, and two EKF algorithms, one standard and second one extended by GNM algorithm.

### 2.2.1. Yaw Estimation

A common way to estimate yaw angle is by using magnetometer (MAG) or GPS measurements. When a MAG is used the simplest way is using only horizontal vector components of the magnetic field measured by dual-axis magnetometer. This way requires the MAG being placed always in the horizontal plane which might be done by a gimbal system. However, Strapdown navigation systems are preferred nowadays which means that a triaxial magnetometer needs to be used and tightly mounted in the navigated object. In this case, the horizontal levelling is done mathematically. The yaw angle is computed using (5), where the information about roll and pitch angle is necessary [18, p. 357], [19]:

$$\psi_{MAG} = -\text{atan}2\left(\frac{m_y^b c_\phi - m_z^b s_\phi}{m_x^b c_\theta + m_y^b s_\phi s_\theta + m_z^b s_\theta c_\phi}\right) - D \quad (5)$$

where subscript *MAG* denotes that the yaw angle is based on magnetometer data;  $(m_x^b, m_y^b, m_z^b)$  are measured magnetic vector components; and  $D$  is the magnetic declination;  $c_\phi = \cos \phi$ ,  $s_\phi = \sin \phi$ , etc.

When the UAV is equipped with a GPS receiver, the approximate yaw angle can be determined using consecutive measurements of position and triangulation in the horizontal plane:

$$\psi_{GPS}(k) = \text{atan}2(p_E(k) - p_E(k-1), p_N(k) - p_N(k-1)) \quad (6)$$

where  $(p_E, p_N)$  are positions in the direction of north and east coordinates;  $\text{atan}2$  is the four-quadrant arctangent function.

There are some drawbacks of the GPS-based yaw angle determination in aerial applications. First, the GPS-based yaw angle includes the effect of sideslip and wind disturbance, so it can differ from the real yaw angle. Second, due to the uncertainty of GPS position it is recommended to determine  $\psi_{GPS}$  only when the forward velocity passes certain threshold in order to avoid large uncertainty before the take-off. Better accuracy can be also achieved by averaging the estimates across a longer time interval.

### 2.2.2. Complementary Filter for Attitude Determination

An efficient way of evaluating attitude by using an IMU data only is to combine a long-term stability of roll

and pitch angles estimated based on gravity measurements and a short-term stability of integrated angular rates. This fact characterizes data fusion to respect the dynamic changes observed by gyros and steady-state conditions allowing to correct the roll and pitch angles based on ACC measurements. The complementary filter (CF) is such a combination of the ACC for the low frequency attitude estimation and gyroscope output for the high frequency estimation [20]. One of the straightforward realizations of a CF is described by:

$$\begin{bmatrix} \phi_{CF}(k) \\ \theta_{CF}(k) \\ \psi_{CF}(k) \end{bmatrix} = L \begin{pmatrix} \begin{bmatrix} \phi_{CF}(k-1) \\ \theta_{CF}(k-1) \\ \psi_{CF}(k-1) \end{bmatrix} + \begin{bmatrix} \Delta\phi_{GYR}(k) \\ \Delta\theta_{GYR}(k) \\ \Delta\psi_{GYR}(k) \end{bmatrix} \\ + (I - L) \begin{bmatrix} \phi_{ACC}(k) \\ \theta_{ACC}(k) \\ \psi_{MAG}(k) \end{bmatrix} \end{pmatrix} \quad (7)$$

where subscripts *GYR*, *ACC*, and *MAG* denote angles based on gyroscope, ACC and MAG data, as previously defined in eq. (1-5);  $L$  is a diagonal matrix of constant weighting coefficients and  $I$  is a identity matrix with the same size as  $L$ .

This kind of attitude estimation overcomes the problem of slowly degrading gyroscope based attitude via corrections from ACC and MAG. Despite the solution is not computationally demanding, it works well in many situations. ACC do not provide sufficient corrections in many dynamic systems (e.g., aircraft stands no longer undisturbed on the ground or no longer flies in a steady straight flight) and degrade the attitude output during rapid maneuvers or when exposed to severe vibration. Therefore, the CF can be modified by dynamics detection criteria, as described in Section 2.2.4. The resulting attitude is then determined using (7) during low UAV dynamics and using (4) under other conditions. The same issue comes when a magnetometer is integrated and environment magnetic field changes occur. However, it rarely occurs in the aerial applications during the flight, since the influence of the aircraft body is generally compensated.

### 2.2.3. IMU/GPS Extended Kalman Filter

The first approach, shown in Fig. 1, implements the IMU/GPS integration scheme done by EKF (see [21, p. 178] for details about the EKF algorithm) and estimates a 12-dimensional state vector (8) containing position, velocity, attitude, and gyroscope biases. The measurement vector (9) is 3-dimmensional and includes GPS position converted to the local navigation coordinate system. The process and measurement models are in the form of following differential functions (10) and (11) (for details see [22] for implementation without the gyroscope bias estimates):

$$\dot{x} = [p_N \ p_E \ p_D \ v_x \ v_y \ v_z \ \phi \ \theta \ \psi \ b_{ox} \ b_{oy} \ b_{oz}]^T \quad (8)$$

$$y = [p_N \ p_E \ p_D]^T \quad (9)$$

where  $\mathbf{x}$  is the state vector;  $(p_N, p_E, p_D)$  are components of the position vector  $\mathbf{p}^n$  in the local navigation (North-East-Down) coordinate frame;  $(v_x, v_y, v_z)$  are the body frame components of velocity vector  $\mathbf{v}^b$ ;  $(\phi, \theta, \psi)$  are roll, pitch, and yaw angles;  $(b_{\omega x}, b_{\omega y}, b_{\omega z})$  are gyroscope biases; and  $\mathbf{y}$  is the measurement vector.

The system function  $f(\mathbf{x}, \mathbf{u})$  propagates the state  $\mathbf{x}$  and input  $\mathbf{u}$  (i.e., accelerations and angular rates) and the measurement function  $h(\mathbf{x})$  is used to update the EKF state with measurements (i.e., GPS position). They are defined as:

$$f(\mathbf{x}, \mathbf{u}) = \begin{bmatrix} \mathbf{C}_b^n \mathbf{v}^b \\ \mathbf{a}^b + \mathbf{v}^b \times (\mathbf{\omega}^b - \mathbf{b}_\omega) + \mathbf{C}_b^n \mathbf{g}^n \\ 1 & \sin \phi \tan \theta & \cos \phi \tan \theta \\ 0 & \cos \phi & -\sin \phi \\ 0 & \sin \phi \sec \theta & \cos \phi \sec \theta \\ \mathbf{0} \end{bmatrix} \quad (10)$$

$$h(\mathbf{x}) = \mathbf{p}^n \quad (11)$$

where  $\mathbf{a}^b$  is a vector of accelerations measured by triaxial ACC,  $\mathbf{0}$  is a vector of zeros,  $\mathbf{g}^n = [0 \ 0 \ g]^T$  is the gravity vector; symbol  $\times$  represents the vector cross product, and  $\mathbf{C}_b^n$  is the body to navigation frame rotational matrix:

$$\mathbf{C}_b^n = \begin{bmatrix} c_\theta c_\psi & -c_\phi s_\psi + s_\phi s_\theta c_\psi & s_\phi s_\psi + c_\phi s_\theta c_\psi \\ c_\theta s_\psi & c_\phi c_\psi + s_\phi s_\theta s_\psi & -s_\phi c_\psi + c_\phi s_\theta s_\psi \\ -s_\theta & s_\phi c_\theta & c_\phi c_\theta \end{bmatrix} \quad (12)$$

where  $c_\phi = \cos \phi$ ,  $s_\phi = \sin \phi$ , etc.

The process and measurement noise covariance matrices  $\mathbf{Q}$  and  $\mathbf{R}$  for the models defined in (10) and (11) are described as follows:

$$\mathbf{Q} = \text{diag}(\sigma_v^2, \sigma_\omega^2, \sigma_{b_\omega}^2) \quad (13)$$

$$\mathbf{R} = \text{diag}(\sigma_p^2) \quad (14)$$

where diag denotes a diagonal matrix and  $\sigma^2$  are vectors of element-wise squared standard deviations for velocity, angular rates, gyroscope biases and GPS position, respectively, and are specified in Table 2.

The advantage of this approach is a straightforward implementation and satisfactory navigation performance. The motion model is corrected for the centrifugal force; therefore, it is highly preferable for applications where this force occurs frequently, e.g. during a turn. However, even when properly tuned, the estimates strongly rely on the GPS signal availability. In the case of blocked or lost GPS signal the estimates begin to diverge quickly and results may become unstable as long as the filter parameters are not adjusted. This approach is implemented to estimate the attitude, position, and velocity, but the position and velocity are not the subject of this paper.

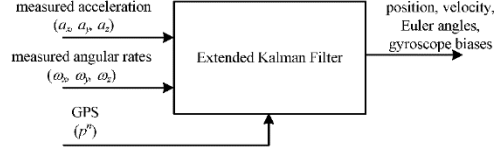


Fig. 1: IMU/GPS EKF

#### 2.2.4. Extended Kalman Filter with Gauss-Newton Minimization

The second EKF approach with the Gauss-Newton Minimization (GNM) algorithm uses data measured by a tri-axial gyroscope, ACC, MAG, and roll and pitch angles measured by an electrolytic tilt sensor (ETS). A main advantage of this approach is that it does not depend on any external source of information, e.g. on the GPS signal.

In this case, the state vector defined in (15) is 10-dimensional and consists of angular rates ( $\omega_x, \omega_y, \omega_z$ ), components of quaternion attitude representation ( $q_0, q_1, q_2, q_3$ ) [23], and gyroscope biases ( $b_{\omega x}, b_{\omega y}, b_{\omega z}$ ). The measurement vector is then defined as a triad of angular rates ( $\omega_x^{bm}, \omega_y^{bm}, \omega_z^{bm}$ ) and four components of quaternion  $\mathbf{q}_b^n = (q_0^m, q_1^m, q_2^m, q_3^m)$  rotating the vector from the body to navigation frame (further referred as  $\mathbf{q}$ ) (16).

$$\mathbf{x} = [\omega_x^b \ \omega_y^b \ \omega_z^b \ q_0 \ q_1 \ q_2 \ q_3 \ b_{\omega x} \ b_{\omega y} \ b_{\omega z}]^T \quad (15)$$

$$\mathbf{y} = [\omega_x^{bm} \ \omega_y^{bm} \ \omega_z^{bm} \ q_0^m \ q_1^m \ q_2^m \ q_3^m]^T \quad (16)$$

The triads of angular rates and biases are modeled as the output of Gauss-Markov process with white noise vector  $\mathbf{w}_\omega$ . The vector  $\mathbf{\omega}_q = (0 \ \omega_x^{bm} \ \omega_y^{bm} \ \omega_z^{bm})$  formed as the quaternion with zero scalar part is related with quaternion derivative  $\dot{\mathbf{q}}$  as [24]:

$$\dot{\mathbf{q}} = \frac{1}{2} \hat{\mathbf{q}} \otimes \mathbf{\omega}_q \quad (17)$$

where  $\otimes$  represents quaternion multiplication.

The quaternion derivative is integrated and the resultant quaternion is normalized to unit magnitude using equation (18):

$$\hat{\mathbf{q}} = \frac{\mathbf{q}}{|\mathbf{q}|} \quad (18)$$

The process model is shown in Fig. 2 and defined as:

$$f(\mathbf{x}, \mathbf{u}) = \begin{bmatrix} -\frac{1}{\tau} \mathbf{\omega}^b + \frac{1}{\tau} \mathbf{w}_\omega \\ \frac{1}{2} \hat{\mathbf{q}} \otimes \mathbf{\omega}_q \\ \frac{1}{\tau_b} \mathbf{b}_\omega + \frac{1}{\tau_b} \mathbf{w}_\omega \end{bmatrix} \quad (19)$$

The measurement function (20) is used to update the EKF state with the vector consisted of three gyroscope measurements and by four components of the quaternion, which are computed using ACC, ETS, and MAG

measurements. The advantage of a quaternion approach lies in the linearity of the output equations which significantly simplifies the filter design and reduces computational requirements [24], [25].

$$h(\mathbf{x}) = \begin{bmatrix} \omega^b \\ q \end{bmatrix} \quad (20)$$

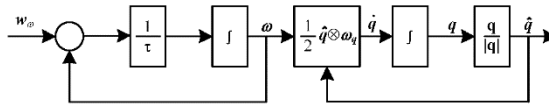


Fig. 2: Process Model for Angular Rates and Quaternions [26]

The process and measurement noise covariance matrices  $\mathbf{Q}$  and  $\mathbf{R}$  for the models defined in (19) and (20) are described as:

$$\mathbf{Q} = \text{diag}(\sigma_{\omega}^2, \sigma_q^2, \sigma_{b_{\omega}}^2) \quad (21)$$

$$\mathbf{R} = \text{diag}(\sigma_{\omega m}^2, \sigma_{q m}^2) \quad (22)$$

where diag denotes a diagonal matrix and  $\sigma$  are vectors of the standard deviations for angular rates, quaternion components, gyroscope biases, respectively,  $m$  denotes measured data and are further specified in Table 2.

To estimate the quaternion vector based on ACC, ETS, and MAG measurements the weighting of ACC and ETS data and Gauss-Newton Minimization method was utilized. The minimization is based on following assumptions:

- ACC and MAG are 3-dimentional measuring systems;
- ETS, ACC, and MAG axes are aligned and deterministic sensor errors are compensated;
- magnitudes of the gravity vector and magnetic field vector are known and given for a particular local geographical area.

Ideally, the result of minimization should be the best fit of quaternion which is used for rotation of the measurements in body frame into known reference values (in the local navigation frame). However, the ACC and MAG measurements are burdened by several sources of errors as:

- ACC attitude is influenced by the components of translational acceleration instead of only gravity;
- variations of the Earth's magnetic and gravity fields [27].

First of all, the compensation of ACC biases is necessary. To reduce initial bias errors, ETSs, which have commonly under static conditions better accuracy than ACCs, can be utilized. For analyses of ETS suitability for bias compensations see [28].

After the bias initial compensation, the ETS data are used to aid the ACC data to reach better stability of corrections for attitude estimation in cases of low dynamic flight. The acceleration components evaluated

with respect to the ETS based roll and pitch angles are fused with data from the ACC through weighting coefficient matrix  $\mathbf{W}_{ETS} = \text{diag}(w_{ETS_x}, w_{ETS_y}, w_{ETS_z})$ :

$$\begin{bmatrix} a_{(ACC+ETS)_x} \\ a_{(ACC+ETS)_y} \\ a_{(ACC+ETS)_z} \end{bmatrix} = \mathbf{W}_{ETS} \begin{bmatrix} a_{ACC_x} \\ a_{ACC_y} \\ a_{ACC_z} \end{bmatrix} + [\mathbf{I} - \mathbf{W}_{ETS}] \begin{bmatrix} a_{ETS_x} \\ a_{ETS_y} \\ a_{ETS_z} \end{bmatrix} \quad (23)$$

where subscripts  $ACC+ETS$ ,  $ACC$ ,  $ETS$  denote the resulting acceleration after the fusion, acceleration measured by ACC, and the one evaluated based on ETS data.

Then the error function for Gauss-Newton minimization algorithm is defined as

$$\varepsilon(\hat{\mathbf{q}}) = \mathbf{y}^n - \mathbf{R}(\hat{\mathbf{q}})\mathbf{y}^b = \mathbf{y}^n - \begin{bmatrix} C_b^n & 0 \\ 0 & C_b^n \end{bmatrix} \mathbf{y}^b \quad (24)$$

where  $\varepsilon(\hat{\mathbf{q}}) = [\varepsilon_1, \varepsilon_2, \varepsilon_3, \varepsilon_4, \varepsilon_5, \varepsilon_6]^T$  is the vector of "error function";  $\hat{\mathbf{q}}$  is the current quaternion vector estimate;  $\mathbf{y}^n = [a_x^n, a_y^n, a_z^n, m_x^n, m_y^n, m_z^n]^T$  is the vector composed of known gravity and Earth's magnetic field vector components expressed in the local navigation frame;  $\mathbf{y}^b = [a_x^b, a_y^b, a_z^b, m_x^b, m_y^b, m_z^b]^T$  is the vector of measured ACC and MAG data rotated using the matrix  $\mathbf{R}(\hat{\mathbf{q}})$  where the rotation matrix  $C_b^n$  utilizing a current quaternion estimate  $\hat{\mathbf{q}}$  is defined as:

$$\begin{aligned} C_b^n &= \mathbf{R}(\hat{\mathbf{q}}) = \\ &= \begin{bmatrix} \hat{q}_0^2 + \hat{q}_1^2 - \hat{q}_2^2 - \hat{q}_3^2 & 2(\hat{q}_1\hat{q}_2 + \hat{q}_3\hat{q}_0) & 2(\hat{q}_1\hat{q}_3 - \hat{q}_2\hat{q}_0) \\ 2(\hat{q}_1\hat{q}_2 - \hat{q}_3\hat{q}_0) & \hat{q}_0^2 - \hat{q}_1^2 + \hat{q}_2^2 - \hat{q}_3^2 & 2(\hat{q}_2\hat{q}_3 + \hat{q}_0\hat{q}_1) \\ 2(\hat{q}_1\hat{q}_3 + \hat{q}_2\hat{q}_0) & 2(\hat{q}_2\hat{q}_3 - \hat{q}_0\hat{q}_1) & \hat{q}_0^2 - \hat{q}_1^2 - \hat{q}_2^2 + \hat{q}_3^2 \end{bmatrix} \end{aligned} \quad (25)$$

A nonlinear minimization problem is stated as:

$$\min_{\mathbf{q}} f(\hat{\mathbf{q}}) = \frac{1}{2} \varepsilon(\hat{\mathbf{q}})^T \varepsilon(\hat{\mathbf{q}}) \quad (26)$$

where  $f(\hat{\mathbf{q}})$  is a "cost function".

By applying the GNM algorithm, the new quaternion estimate  $\hat{\mathbf{q}}_+$  is computed as current estimate  $\hat{\mathbf{q}}$  deducted by the correction corresponding to the error function  $\varepsilon(\hat{\mathbf{q}})$  as:

$$\hat{\mathbf{q}}_+ = \hat{\mathbf{q}} - (\mathbf{J}^T(\hat{\mathbf{q}})\mathbf{J}(\hat{\mathbf{q}}))^{-1} \mathbf{J}^T(\hat{\mathbf{q}}) \varepsilon(\hat{\mathbf{q}}) \quad (27)$$

where  $\mathbf{J}(\hat{\mathbf{q}})$  is the Jacobian of the error function  $\varepsilon(\hat{\mathbf{q}})$  defined as [29]:

$$\begin{aligned} \mathbf{J}(\hat{\mathbf{q}}) &= \frac{\partial \varepsilon(\mathbf{q})}{\partial \mathbf{q}} \Big|_{\mathbf{q}=\hat{\mathbf{q}}} = -\frac{\partial \mathbf{R}(\mathbf{q})}{\partial \mathbf{q}} \mathbf{y}^b \Big|_{\mathbf{q}=\hat{\mathbf{q}}} = \\ &= -\left[ \frac{\partial \mathbf{R}(\mathbf{q})}{\partial q_1} \mathbf{y}^b \quad \frac{\partial \mathbf{R}(\mathbf{q})}{\partial q_2} \mathbf{y}^b \quad \frac{\partial \mathbf{R}(\mathbf{q})}{\partial q_3} \mathbf{y}^b \quad \frac{\partial \mathbf{R}(\mathbf{q})}{\partial q_4} \mathbf{y}^b \right] \end{aligned} \quad (28)$$

As aforementioned, during the flight measured acceleration corresponds to the total acceleration minus gravity so it contains also translational acceleration which can cause significant errors of attitude determination. To avoid the degradation of the accuracy by ACC, ETS, and

MAG corrections from GNM, it is convenient to use these corrections only under steady-state conditions when zero or low UAV dynamics is detected. The following detection criterions are used:

$$|\omega| < \omega_{dyn} \& \left( |\alpha| < (g + a_{dyn}) \& |\alpha| > (g - a_{dyn}) \right) \quad (29)$$

where  $|\omega| = \sqrt{\omega_x^2 + \omega_y^2 + \omega_z^2}$  is the magnitude of angular rate vector;  $\omega_{dyn}$  is its predetermined limit value;  $|\alpha| = \sqrt{a_x^2 + a_y^2 + a_z^2}$  is the magnitude of acceleration vector in the body frame;  $a_{dyn}$  is its predetermined limit value;  $g$  is the magnitude of gravity vector. The experimentally estimated values of  $\omega_{dyn}$  and  $a_{dyn}$  are presented in Section 3.

A block scheme of all data processing covering the corrections of ACC by ETS and the EKF with the GNM algorithm is shown in Fig. 3.

### 3. Measurement Setup and Experimental Results

This section describes the measurement setup which was mounted in the UAV and utilized to obtain the data. Besides the results of attitude estimation for all of aforementioned approaches, the analyses of EKF with GNM are presented at the end of this section.

#### 3.1. Measurement Setup

A modular navigation system (described in details in [16]) consists of following sensors and systems connected via CAN bus (CANaerospace protocol) with a defined sampling frequency  $F_s$ :

- IMU ADIS16405 (Analog Devices) – accelerations and angular rates ( $F_{s,IMU} = 50$  Hz), temperature compensated and internally filtered (digital filter reducing the sensor bandwidth to about 16 Hz);
- Electrolytic tilt sensors EZ-TILT-2000 (Advanced Orientation Systems Inc.) - roll and pitch angles ( $F_{s,ETS} = 10$  Hz); four sensors with different electrolyte viscosity (ETS-STD: standard viscosity defining the response time of 40 ms, ETS-15: viscosity 15% higher than the standard, ETS-30: viscosity 30% higher, ETS-50: viscosity 50% higher), the first three EZ-TILT-2000 modules use DX-045 sensor with range  $\pm 70^\circ$ ; in case of ETS-50, the DX-008 sensor with range  $\pm 15^\circ$  was used;
- Magnetometer HMR2300 (Honeywell) - components of a magnetic field ( $F_{s,MAG} = 50$  Hz);
- GPS receiver Garmin 18x-5Hz - latitude, longitude, altitude, speed ( $F_{s,GPS} = 5$  Hz);
- 3-antenna GPS receiver Polar X2@e (Septentrio) – the reference for attitude estimation - roll, pitch, and yaw angles ( $F_{s,REF} = 10$  Hz).

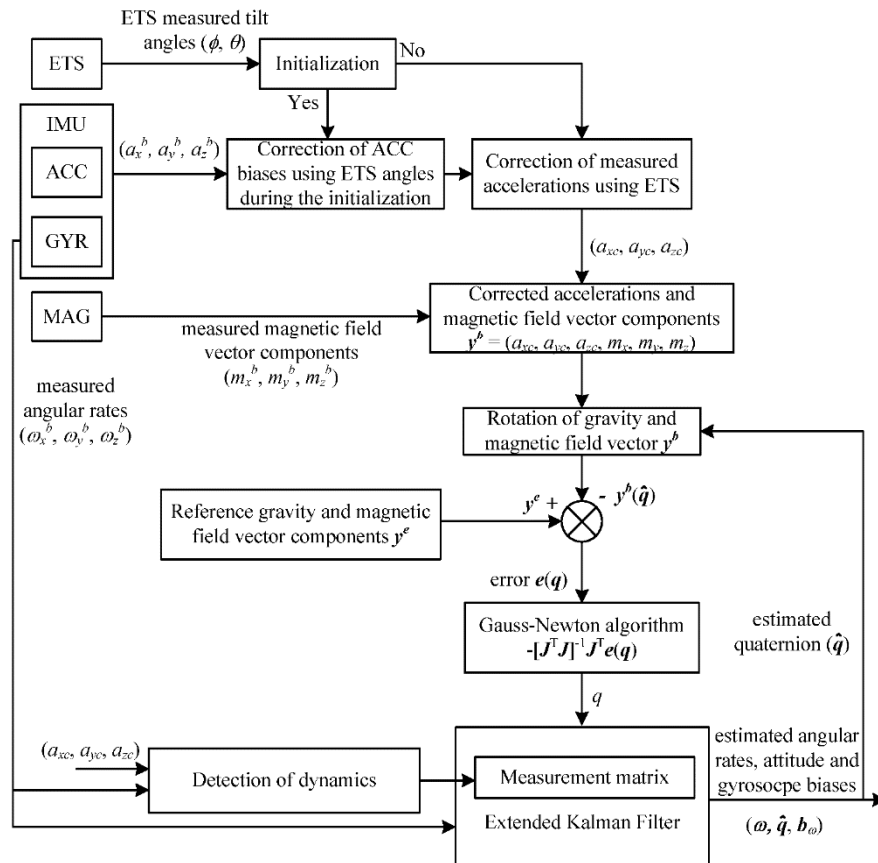


Fig. 3: EKF with Gauss-Newton Minimization Algorithm

The modular navigation system was mounted in Bellanca Super Decathlon XXL UAV (see Fig. 4) with 60 ccm combustion engine, 3 meter wing span, and weight of 20 kg including payload. The UAV was remotely controlled above a small airport and performed various flight patterns including rectangular, eight-pattern, circular, rapid altitude changes flight mode (see Fig. 5). The experiment took about 23 minutes (including take-off, flight, and landing). During the flight, there were the phases with high dynamics reaching angular rates of  $\pm 65^\circ/\text{s}$  and the measuring system was exposed to vibration affecting the ACC readings with values up to  $20 \text{ m/s}^2$  caused by the harsh environment.



Fig. 4: Bellanca Super Decathlon XXL

The attitude reference was provided by the 3-antenna GPS receiver Polar X2@e (Septentrio). Accuracy of the reference system was evaluated based on the distances among three antennae and manufacturer documentation. The resulting accuracy of  $1\sigma$  was then  $0.2^\circ$  in roll angle,  $0.6^\circ$  in pitch angle and  $0.3^\circ$  in yaw angle.

### 3.2. Experimental results

Data preprocessing includes the compensation of triaxial ACC [30] and gyroscope [31], [32] for deterministic errors, the sensor error models were presented in [16]. The ETSs with different viscosities of electrolyte (standard, about 15%, 30% and 50% higher than standard) were corrected using 3<sup>rd</sup> order polynomials [33]. After these corrections the alignment of MAG and ETSs coordinate systems to the IMU coordinate frame was done. As a last step of data preprocessing accelerations, angular rates, and MAG readings were pre-filtered using a 5<sup>th</sup> order low-pass filter with the cut-off frequency of 5 Hz. According to Fig. 6, such a bandwidth is sufficient for a small UAV to reduce noise and high frequency vibrations present in the data without interfering with the UAV dynamics.

The preprocessed data were used for attitude estimation using algorithms described in Section 2. All results are accompanied by the root mean square error (RMSE) allowing results comparison with respect to the reference attitude from 3-antenna GPS receiver. The RMSE is defined as:

$$\text{RMSE} = \sqrt{\frac{1}{n} \sum_{i=1}^n (\hat{x}_i - x_i)^2} \quad (30)$$

where  $\hat{x}$  denotes the estimate,  $x_i$  the reference value, and  $n$  is the number of observed samples.

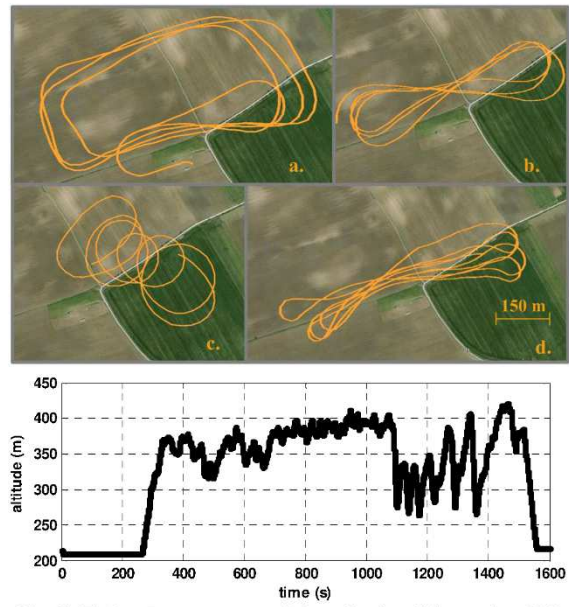


Fig. 5: Flying Patterns - position obtained from the GPS; (Top) a) Rectangular; b) Eight-pattern; c) Circular; d) Rapid Altitude Changes; (Bottom) Altitude during the flight

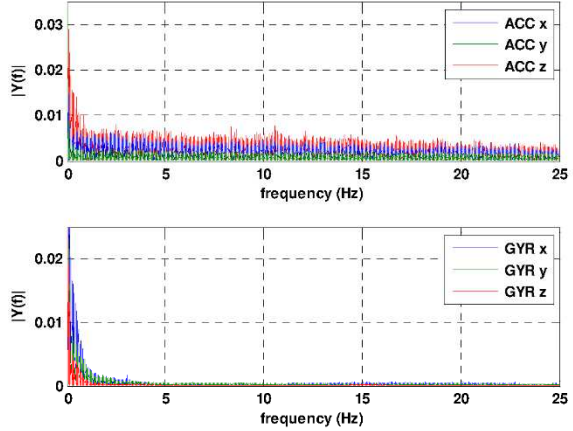


Fig. 6: Amplitude spectrum of the IMU measurements from the UAV flight. (Top) Accelerometers. (Bottom) Gyroscopes

To provide all potential aspects, results provided in Table 1 also include attitude estimated only from gyro data and ACC data which were just pre-filtered. Furthermore, the yaw angle obtained based on GPS and MAG data is also provided. All this provides an understanding about the efficiency of aforementioned more sophisticated approaches compared to the simplest way of attitude evaluation. To evaluate the progression of  $\psi_{MAG}$  the estimates of roll and pitch angles from the EKF were used under the belief of their correctness.

Table 1. Attitude RMSE

Attitude estimation approach	Roll (°)	Pitch (°)	Yaw (°)
Gyroscopes only	5.9	5.0	110.8
Accelerometers only	24.0	9.67	-
GPS	-	-	13.3
Magnetometer	-	-	7.3
Complementary filter	22.2	5.5	35.2
CF with dynamics constraints	16.8	4.9	35.2
IMU/GPS EKF	1.2	2.0	4.3
GNM	4.8	5.1	42.1
EKF+GNM	1.9	2.7	5.3

The approach utilizing the complementary filter showed unsufficient accuracy of attitude estimation even after experimental tuning of the weighting parameter matrix  $L$  especially in the roll and yaw channels. The lowest RMSE was reached for  $L = diag(0.98 \ 0.98 \ 0.5)$ , results are denoted in Table 1. Its performance is not notably improved even with the dynamics constraint (29) restricting the influence of non-gravitational accelerations for  $a_{dyn} = 1 \text{ m/s}^2$ . In comparison with previous approaches, the EKF based on IMU/GPS integration provides satisfying accuracy of the attitude estimation, but at the cost of GPS data availability. The last evaluated approach utilizing the EKF extended by the GNM algorithm provides comparable results as previous EKF approach, but its main advantage is in the independency of the algorithm on external source of information, i.e. on the GPS signal. Results when only GNM based attitude is estimated are also denoted for a complete overview. The EKF+GNM results correspond to the situation in which the approach parameters were already tuned and under this “final settings” conditions this approach reached the best performance. The tuning and “final settings” conditions are closely described in the following section.

### 3.3. Analyses of the Extended Kalman Filter with Gauss Newton Minimization

This section describes the analyses of the EKF extended by the GNM algorithm performed according to different updating schemes covering ACC and ETS with different electrolyte viscosities and when deterministic error models for ACCs and gyros, obtained by the calibration, were applied. The results of EKF+GNM performance for different updating settings are summarized in Table 3 and Table 4. The best performance of the EKF+GNM with a particular updating scheme was reached under “final settings” conditions which are closely described in Section 3.3.2.

#### 3.3.1. Correction of ACC Initial Bias Error

As stated in Section 2.2.4., initial ACC bias error needs to be corrected. The ACC initial bias error ( $1\sigma$ ) for the IMU ADIS16405 can vary in the range of  $\pm 0.49 \text{ m/s}^2$  which can induce the attitude error up to  $\pm 2.9^\circ$ . This initial error negatively influences the accuracy of estimated attitude. Usage of ETS is a convenient way to mitigate the ACC initial bias. This fact was confirmed

during laboratory tests, see [28]. During the initialization phase of flight on the ground, the ACC and ETS data are compared and the initial bias error is corrected. With respect to the performed experiment the values of initial biases were evaluated as  $[0.08 \ 0.09 \ 0.05] \text{ m/s}^2$ .

#### 3.3.2. Tuning of EKF+GNM

To achieve the final RMSE results denoted in Table 1, the EKF+GNM needed to be tuned. First, the  $Q$  and  $R$  matrices of EKF were set to their initial values and a successive tuning aimed for minimizing the sum of the RMSE corresponding to the progressions of roll, pitch and yaw estimates and the reference. Second, the boundaries of dynamics  $\omega_{dyn}$  and  $a_{dyn}$  were tuned. The highest accuracy was achieved when the ACC+ETS+MAG updating scheme was applied and boundaries  $\omega_{dyn} = 3.3^\circ/\text{s}$  and  $a_{dyn} = 1.9 \text{ m/s}^2$  were used. The values were obtained in accordance to the RMSE progressions shown in Fig. 7 and Fig. 8. Using these boundaries, high dynamics was detected in 83.2% of the flight and thus the ACC, ETS, MAG corrections were applied only in 16.8% of the flight. After that the  $Q$  and  $R$  matrices were tuned. In all cases, the convergence of GNM algorithm was ensured and up to 5 its iterations within a measurement update were sufficient for quaternion update estimation. The final values of  $Q$  and  $R$  are listed in Table 2.

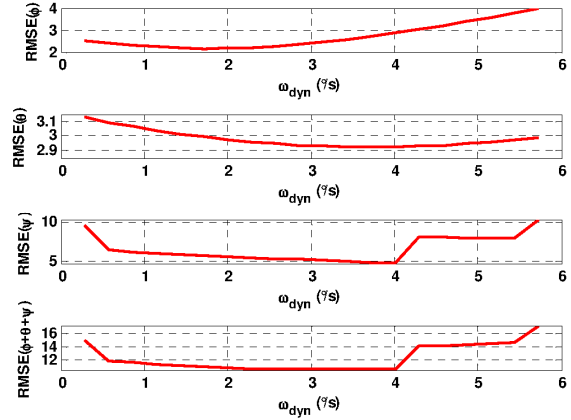


Fig. 7: Tuning of dynamics limit  $\omega_{dyn}$  from angular rate measurements

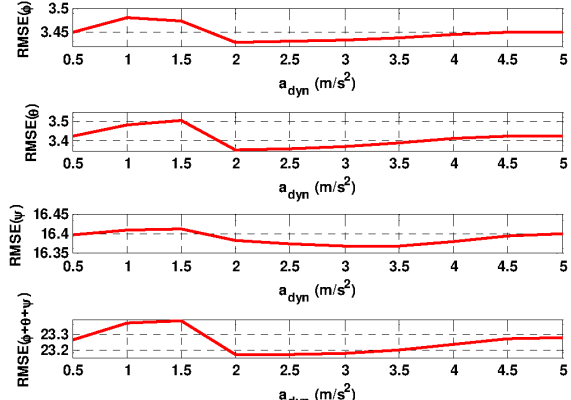


Fig. 8: Tuning of dynamics limit  $a_{dyn}$  from accelerations

### 3.3.3. Usage of ETS for ACC Corrections

The suitability of usage of ETS for correcting ACC data were confirmed under laboratory conditions in [28]. Several performance analyses of four different ETSs were performed and evaluated in [33]. The analyses included aspects such as hysteresis, settling time, immunity of ETSs to vibrations, and static accuracy. Results can be found in [26]; however, the most suitable sensor was evaluated as the ETS-15 followed by the ETS-30. These experiments suffered from the absence of dynamics. To evaluate the behavior of ETSs under the dynamics in harsh environment as well as their suitability for ACC corrections, all four ETSs were mounted into the UAV and the corrections according to (23) were applied. The attitude RMSE of the EKF+GNM with usage of different ETSs are provided in Table 3. For the analyses, the EKF+GNM with parameters of “final settings”, which corresponds to the smallest attitude RMSE obtained within the whole evaluation, were used.

The “final settings” covered:

- determined values of  $\mathbf{Q}$  and  $\mathbf{R}$  matrices listed in Table 2,
- the compensation of ACC and gyroscope by predetermined Sensor Error Models (SEMs),
- estimation of gyroscope biases within the EKF initialization,
- correction of acceleration based on ETS data with a weighting coefficient  $\mathbf{W}_{ETS}$ ,
- determined thresholds  $\omega_{dyn}$  and  $a_{dyn}$ .

In Table 3 and Table 4, the  $\Delta$  values in the brackets correspond to the differences of the RMSE with “final settings” and particular RMSE with studied settings.

The updating scheme reflects the situation denoted in the first columns of Table 3 and Table 4. The rest of parameters corresponded to their parallel in “final settings”.

In Table 3 the influence of ACC and ETS corrections were analyzed separately and also combined via weighting coefficient vector  $\mathbf{W}_{ETS} = \text{diag}(0.46 \ 0.56 \ 0.50)$ . The values in brackets show differences of particular updating scheme and the one corresponding to the “final settings”. The ETS-15 was picked up as the most convenient one for ACC corrections based on carried out comparison provided by the first row vs. the last three rows. Those differences might be understood as small and negligible; however, it needs to have in mind that the correction of ACC by ETS was applied just in 16.8% of the flight due to the determined dynamic boundaries.

### 3.3.4. Improvement of the Accuracy Based on ACC and Gyroscope SEM Compensation

To confirm the suitability of applying ACC and gyro deterministic error models (SEMs) [30], [32], Table 4 summarizes the analyses focused on the effect of applying SEMs on the accuracy of attitude estimation. The analyses cover cases when SEMs were not applied separately and both together, which all can be compared with the case of “final setting” conditions. Only the case, when ACC SEM was applied and gyroscope SEM compensation was not, has a comparable performance as the “final settings” case. This situation is caused by reducing the gyroscope errors’ effect on the accuracy with ACC+ETS corrections from long-term perspectives. In all other cases, the attitude RMSE was improved by application of the SEMs under real flight experiment.

Table 2. Standard deviations for the EKF approaches

IMU/GPS EKF									
$\sigma_v$ (m/s)	$\sigma_\omega$ (°/s)			$\sigma_{b_\omega}$ (°/s)			$\sigma_p$ (m)		
3.1	1.6			10 <sup>-6</sup>			3.8		
EKF+GNM									
$\sigma_\omega$ (°/s)			$\sigma_q$ (-)			$\sigma_{b_\omega}$ (°/s)			
$\sigma_{\omega_x}$ (°/s)	$\sigma_{\omega_y}$ (°/s)	$\sigma_{\omega_z}$ (°/s)	$\sigma_{q_0}$ (-)	$\sigma_{q_1}$ (-)	$\sigma_{q_2}$ (-)	$\sigma_{q_4}$ (-)	$\sigma_{b_{\omega_x}}$ (°/s)	$\sigma_{b_{\omega_y}}$ (°/s)	$\sigma_{b_{\omega_z}}$ (°/s)
1.53	1.22	1.16	0.0029	0.0029	0.0030	0.0032	0.0018	0.0018	0.0018
$\sigma_\omega$ (°/s)									
$\sigma_{\omega_x}^b$ (°/s)	$\sigma_{\omega_y}^b$ (°/s)	$\sigma_{\omega_z}^b$ (°/s)	$\sigma_{\omega_x}^b$ (°/s)	$\sigma_{\omega_y}^b$ (°/s)	$\sigma_{\omega_z}^b$ (°/s)	$\sigma_{q_0}^b$ (-)	$\sigma_{q_1}^b$ (-)	$\sigma_{q_2}^b$ (-)	$\sigma_{q_3}^b$ (-)
0.04	0.03		0.02			0.0002	0.0002	0.0005	0.0002

Table 3. Attitude RMSE of EKF+GNM with ACC+ETS Different Settings

EKF+GNM corrected by	Roll/(ΔRoll) (°)	Pitch/(ΔPitch) (°)	Yaw/(ΔYaw) (°)
ACC+ETS-15 with “final settings”	1.87	2.67	5.32
ACC	1.91/(0.04)	2.82/(0.15)	5.49/(0.17)
ETS-15	2.06/(0.19)	3.08/(0.41)	6.14/(0.82)
ACC+ETS-STD	2.03/(0.16)	3.08/(0.41)	6.12/(0.80)
ACC+ETS-30	1.91/(0.04)	2.75/(0.08)	5.50/(0.18)
ACC+ETS-50	1.92/(0.05)	2.80/(0.13)	5.62/(0.30)

### 3.3.5. Summary of EKF+GNM Analyses

It is clear from Table 3 and Table 4 that in all cases except one the attitude RMSEs were improved when SEMs were applied. Even if the resulting differences might seem negligible it needs to have in mind that the experiment included a real flight and slight differences in RMSEs do not unambiguously provide a measure of behavior during dynamic changes. During the performed experiment only 16.8% of ACC+ETS corrections were possible to use.

Details of the attitude progressions estimated by aforementioned approaches are shown in Fig. 9, Fig. 10, and Fig. 11. The results compare angles from GNM, EKF+GNM, integrated angular rates, and the reference angles. Unfortunately, there were several inconveniences

which caused outages of the GPS data because of the wing vibration, and changes in a satellite view. Nevertheless, these outages do not play important role in analyses of studied approaches. As it can be seen in Fig. 9–Fig. 11, the reference angles were provided in the majority of time. There can be seen that the minimal differences are between the reference angles and angles from EKF+GNM. The GNM based angles are computed only from ACC and MAG data and these angles are strongly influenced by high dynamics. On the other hand, gyroscope based angles suffer from higher deviations from the reference which is caused by uncorrected bias drift and its instability. The estimated angular rate biases, which improved the final accuracy of EKF+GNM are shown in Fig. 12.

Table 4. Attitude RMSE of EKF+GNM without Error Compensation

EKF+GNM	Roll/(ΔRoll) (°)	Pitch/(ΔPitch) (°)	Yaw/(ΔYaw) (°)
ACC+ETS-15 with "final settings"	1.87	2.67	5.32
without ACC SEM & with gyro SEM	1.89/(0.02)	2.88/(0.21)	6.00/(0.68)
without gyroscope SEM & with ACC SEM	1.87/(0.00)	2.65/(-0.02)	5.46/(0.14)
without ACC and gyroscope SEMs	1.87/(0.00)	2.81/(0.14)	6.14/(0.82)

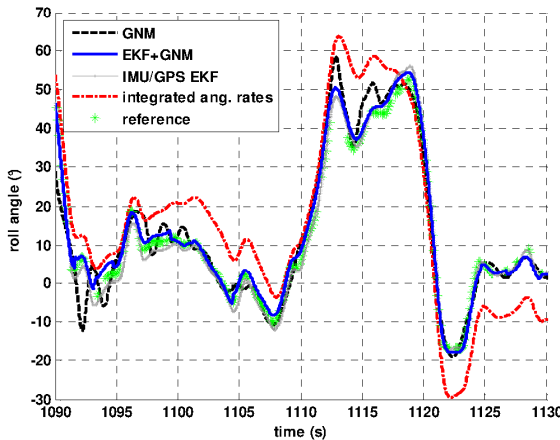


Fig. 9: Estimation of the roll angle

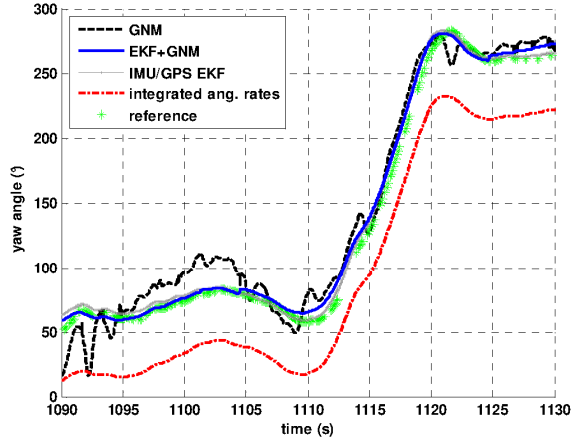


Fig. 11: Estimation of the yaw angle

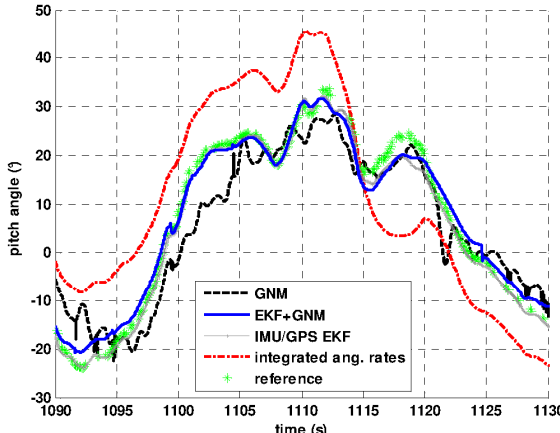


Fig. 10: Estimation of the pitch angle

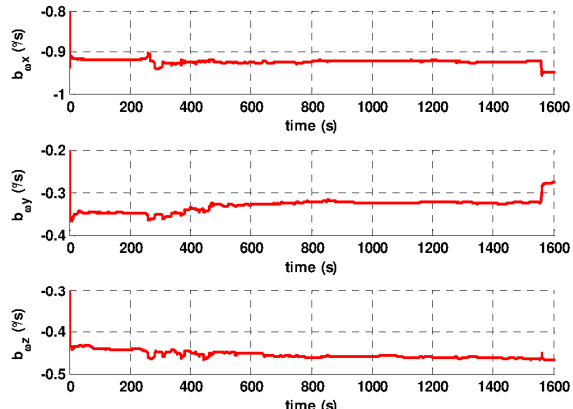


Fig. 12: Estimation of angular rate biases (please note that the sudden changes in the bias estimates around 1550 s were caused by hard landing)

#### 4. Conclusions

This paper focuses on different attitude estimation approaches exploiting inertial measurements aided by various sensors and systems and compares their performances. The paper covers: a straightforward method of attitude evaluation using accelerometers or gyroscope measurements only and their fusion by means of a complementary filter, an IMU/GPS fusion scheme Extended Kalman Filter (EKF), and the EKF extended by the Gauss-Newton minimization algorithm. All studied approaches are compared based on real-flight experiment carried out with a UAV. The paper provides an inside view of studied approaches and their behaviors with respect to dynamics of flight and harsh environment which aerial vehicles generally produce. According to presented results the best attitude estimation was achieved using inertial measurements combined with an external GPS measurements using an IMU/GPS EKF, or using inertial measurements aided by the magnetometer and electrolytic tilt sensors and fused by the EKF extended by GNM algorithm. Thorough analyses of the experiment confirmed that the EKF+GNM approach gives comparable results as the IMU/GPS EKF which is commonly used. In contrast to the IMU/GPS EKF the EKF+GNM approach is independent on GPS which brings a big advantage from attitude point of view mainly in indoor areas or areas with blocked GPS signals. Moreover, the real-flight experiment confirmed previously performed laboratory experiments and their results about the electrolytic tilt sensors and sensor calibration presented in [28], [30], [32], [33] under real flight conditions inducing high dynamic changes during the UAV maneuvering and strong vibrations coming from the UAV harsh environment.

#### Acknowledgments

This work was supported partially by the research program TA CR Alfa under the grant No. TA02011092 "Research and development of technologies for radiolocation mapping and navigation systems" and by the Grant Agency of the Czech Technical University in Prague grant No. SGS13/144/OHK3/2T/13.

#### References

- [1] B. Liu, Z. Chen, X. Liu and F. Yang, "An efficient nonlinear filter for spacecraft attitude estimation," *International Journal of Aerospace Engineering*, pp. 1-11, 2014.
- [2] M. Tarhan and E. Altug, "EKF based attitude estimation and stabilization of a quadrotor UAV using vanishing points in catadioptric images," *Journal of Intelligent & Robotic Systems*, vol. 62, no. 3-4, pp. 587-607, 2011.
- [3] D. B. Kingston and R. W. Beard, "Real-time attitude and position estimation for small UAVs using low-cost sensors," in *AIAA 3rd "Unmanned Unlimited" Technical Conference, Workshop and exhibit*, 2004.
- [4] Y. S. Suh, "Attitude estimation by multiple-mode Kalman filters," *IEEE Transactions on industrial electronics*, vol. 53, no. 4, pp. 1386-1389, 2006.
- [5] S. Leutenegger and R. Siegwart, "A low-cost and fail-safe Inertial Navigation System for airplanes," in *Robotics and Automation, IEEE International Conference on*, 2012.
- [6] A. Bry, A. Bachrach and N. Roy, "State estimation for aggressive flight in GPS-denied environments using onboard sensing," in *Proc. IEEE Int Robotics and Automation Conf*, 2012.
- [7] S. Weiss, M. Achtelik, M. Chli and R. Siegwart, "Versatile distributed pose estimation and sensor self-calibration for an autonomous MAV," in *Robotics and Automation, IEEE International Conference on*, 2012.
- [8] J. Calusdian, X. Yun and E. Bachmann, "Adaptive-gain complementary filter of inertial and magnetic data for orientation estimation," in *Robotics and Automation, IEEE International Conference on*, 2011.
- [9] D. Zachariah and M. Jansson, "Self-motion and wind velocity estimation for small-scale UAVs," in *Robotics and Automation, IEEE International Conference on*, 2011.
- [10] M. Euston, P. Coote, R. Mahony, J. Kim and T. Hamel, "A complementary filter for attitude estimation of a fixed-wing UAV," in *Intelligent Robots and Systems, IEEE/RSJ International Conference on*, 2008.
- [11] M. Sotak, M. Sopata and F. Kmec, "Navigation systems using Monte Carlo method," in *Guidance, Navigation and Control Systems*, 2006.
- [12] A. Bachrach, S. Prentice, R. He and N. Roy, "RANGE - Robust autonomous navigation in GPS-denied environments," *Journal of Field Robotics*, vol. 28, no. 5, pp. 644-666, 2011.
- [13] J. L. Crassidis, F. L. Markley and Y. Cheng, "Survey of nonlinear attitude estimation methods," *Journal of Guidance Control and Dynamics*, vol. 30, no. 1, pp. 12-28, 2007.
- [14] R. Munguia and A. Grau, "A Practical Method for Implementing an Attitude and Heading Reference System," *Int. J. Adv. Robot. Syst.*, vol. 11, p. 62, 2014.
- [15] H. G. de Marina, F. J. Pereda, J. M. Giron-Sierra and F. Espinosa, "UAV attitude estimation using unscented kalman filter and TRIAD," *Industrial Electronics, IEEE Transactions on*, vol. 59, no. 11, pp. 4465-4474, 2012.
- [16] M. Sipos, J. Simanek, P. Novacek, J. Popelka and J. Rohac, "Modular navigation system for unmanned aerial vehicles," in *International Conference on Military Technologies*, 2013.
- [17] M. Sotak, "Coarse alignment algorithm for ADIS16405," *Przeglad elektrotechniczny*, vol. 86, pp. 247-251, 2010.
- [18] J. A. Farrell, *Aided Navigation: GPS with High Rate Sensors*, McGraw-Hill, 2008.
- [19] M. Sipos, J. Rohac and P. Novacek, "Improvement of electronic compass accuracy based on magnetometer and accelerometer calibration," *Acta Physica Polonica A*, vol. 121, no. 4, pp. 945-949, 2012.
- [20] V. Kubelka and M. Reinstein, "Complementary filtering approach to orientation estimation using inertial sensors only," in *Robotics and Automation, IEEE International Conference on*, 2012.
- [21] M. S. Grewal and A. P. Andrews, *Kalman filtering: theory and practice using MATLAB*, John Wiley & Sons, 2011.
- [22] A. Nemra and N. Aouf, "Robust INS/GPS sensor fusion for UAV localization using SDRE nonlinear filtering," *IEEE Sensors Journal*, vol. 10, no. 4, pp. 789-798, 2010.
- [23] J. Diebel, "Representing Attitude: Euler Angles, Unit Quaternions, and Rotation Vectors," Stanford University, Stanford, California, 2006.
- [24] X. Yun, M. Lizarraga, E. Bachmann and R. McGhee, "An improved quaternion-based Kalman filter for real-time tracking of rigid body orientation," in *Intelligent Robots and Systems, IEEE/RSJ International Conference on*, 2003.
- [25] X. Yun and E. R. Bachmann, "Design, Implementation, and Experimental Results of a Quaternion-Based Kalman Filter for Human Body Motion Tracking," *IEEE TRANSACTIONS ON*

- ROBOTICS, VOL. 22, NO. 6, pp. 1216 - 1227, 2006.
- [26] X. Yun, C. Aparicio, E. Bachmann and R. McGhee, "Implementation and Experimental Results of a Quaternion-Based Kalman Filter for Human Body Motion Tracking," in *Proceedings of the 2005 IEEE International Conference on Robotics and Automation*, Barcelona, Spain, 2005.
  - [27] E. R. Bachmann, Y. Xiaoping and A. Brumfield, "Limitations of Attitude Estimation Algorithms for Inertial/Magnetic Sensor Modules," *IEEE Robotics & Automation Magazine*, vol. 14, no. 3, pp. 76 - 87 , 2007.
  - [28] M. Sipos and P. Rohac J. and Novacek, "Analyses of electronic inclinometer data for tri-axial accelerometer's initial alignment," *Przeglad Elektrotechniczny*, vol. 88, pp. 286-290, 2012.
  - [29] J. Cordova Alarcon, H. Rodriguez Cortes and E. Vivas, "Extended Kalman Filter tuning in attitude estimation from inertial and magnetic field measurements," in *Electrical Engineering, Computing Science and Automatic Control, CCE, 2009 6th International Conference on* , Toluca, 2009.
  - [30] M. Sipos, P. Paces, J. Rohac and P. Novacek, "Analyses of Triaxial Accelerometer Calibration Algorithms," *IEEE Sensors Journal*, vol. 12, no. 5, pp. 1157-1165, 2012.
  - [31] D. Jurman, M. Jankovec, R. Kamnik and M. Topic, "Calibration and data fusion solution for the miniature attitude and heading reference system," *Sensors and Actuators A: Physical*, vol. 138, pp. 411-420, 2007.
  - [32] M. Sipos and J. Rohac, "Calibration of tri-axial angular rate sensors," in *Measurement, Diagnostics, Dependability of Aircraft Systems, International Conference on*, Brno, 2010.
  - [33] M. Sipos and J. Rohac, "Comparison of electrolytic tilt modules for attitude correction," in *Measurement, Diagnostics, Dependability of Aircraft Systems, International Conference on*, 2012.

## 5. Unpublished Results Related to the Thesis

In chapter 4, the results related to the author's thesis are presented through selected journal and conference papers. Due to the limited number of pages in the published papers and due to progressive development in the thesis objectives further results unpublished are present in details in following subchapters.

### 5.1. Results Related to Triaxial Gyroscope Calibration

A main goal of the proposed gyroscope calibration as already described in details in chapter 4.2 involves the estimation of deterministic errors (in form of the SEM) such as non-orthogonalities, scale factor errors, offsets, and gyroscope framework misalignments. The calibration process is based on three consecutive rotations of gyroscope along all sensitivity axes. For parameter estimation, measured angular rates are numerically integrated to obtain the angles of performed rotation. The reference angles of the rotation can be obtained by means of a theodolite [28], FOG based measurement system (Fig. 1) [74], or already calibrated accelerometers [75]. Based on the minimization criterion considering deviations between gyroscope based data and the reference data the SEM is estimated. The algorithm applied for the SEM estimation is based on Cholesky decomposition and LU (Lower-Upper) factorization. For calibration purposes two AHRS units, 3DM-GX2 (Microstrain) and AHRS M3 (Innalabs) were used.

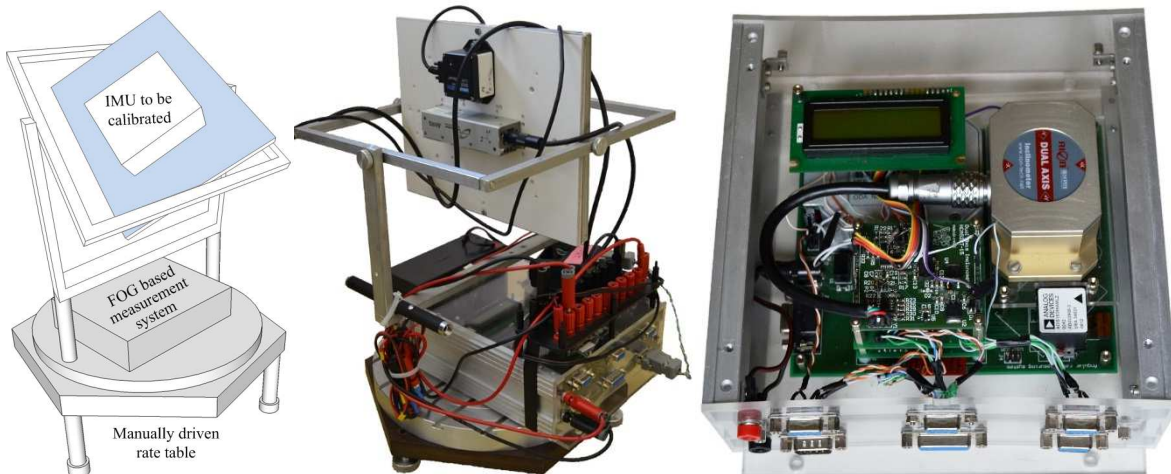


Fig. 1: Concept scheme of measurement setup (on the left); measurement setup with two AHRS units (AHRS M3, 3DM-GX2) mounted on (center); FOG based measurement system used for triaxial gyroscope calibration (right)

The main advantage of this calibration approach is that it does not require any precise rotational or positioning platform. The other advantage is that the calibration process requires only angles of rotation as a reference which means that referential angular rates are not needed.

When already calibrated accelerometers are used as a reference, the calibration procedure assumes that the accelerometer frame coincides with gyroscope frame, because the compensated accelerometer readings are used to align gyroscope's axis to the plane in which the rotation is performed with the accuracy better than  $\pm 1^\circ$  [75]. When this alignment angle error is less than  $\pm 1^\circ$ , the error caused in the angular rate is about 0.02% which can be assumed as negligible.

### 5.1.1. Verification of Gyroscope Calibration

The parameters of SEMs were estimated for gyroscopes of 3DM-GX2 and AHRS M3 (Fig. 1). The resultant accuracy of both gyroscope's SEMs were verified on seven independent data sets. As an evaluation criterion, the RMSE via a deviation matrix is defined and used as a criterion for calibration compensation efficiency following (1).

$$\mathbf{e}_{i,j} = \begin{bmatrix} e_{x,x} & e_{y,x} & e_{z,x} \\ e_{x,y} & e_{y,y} & e_{z,y} \\ e_{x,z} & e_{y,z} & e_{z,z} \end{bmatrix}, \quad (1)$$

where  $e_{i,j}$  reflects a residual deviation of an integrated angle projected to the  $j$ -axis when an angular rate was applied along the  $i$ -axis [76].

To verify the final accuracy of the integrated angles from those seven different datasets a combined matrix was needed to form. The matrix was formed in a way that each element was calculated as the RMSE of all specific elements belonging to the specified position in the already evaluated deviation matrices from (1). The final combined matrix is presented in Table 1 for 3DM-GX2 and in Table 2 for AHRS M3.

TABLE 1: EVALUATION OF ESTIMATED GYROSCOPE SEMS, RMSE OF DEVIATION MATRICES BEFORE/AFTER COMPENSATIONS - 3DM-GX2

RSME of deviation matrices before compensation $\Delta\alpha$ (°)			RSME of deviation matrices after compensation $\Delta\alpha$ (°)		
7.53	7.34	6.85	0.40	0.13	0.47
4.03	0.61	47.02	0.33	0.42	0.21
5.48	3.04	1.55	0.63	0.34	0.75

TABLE 2: EVALUATION OF ESTIMATED GYROSCOPE SEMS, RMSE OF DEVIATION MATRICES BEFORE/AFTER COMPENSATION - AHRS M3

RSME of deviation matrices before compensation $\Delta\alpha$ (°)			RSME of deviation matrices after compensation $\Delta\alpha$ (°)		
3.74	8.97	8.22	0.88	0.73	1.08
1.11	0.63	4.31	0.28	0.63	0.84
13.89	3.68	2.04	0.42	0.43	1.30

The results presented in Table 1 and Table 2 confirm the suitability and efficiency of sensor errors compensation. The application of SEMs improved the accuracy of angle determination based on gyroscopes angular rates. Based on 30 second long experiments, the average error of angle determination was 2.6% before compensation and 0.1% after compensation for 3DM-GX2 gyroscope framework and was 1.4% before and 0.2% after compensation for AHRS M3.

### 5.1.2. Angular Rate Domain Approach of Gyroscope Calibration

Even if a proposed methodology for gyroscope calibration uses an angle domain approach, a calibration in angular rate domain is also possible. There are two possible ways how to calibrate the gyroscopes in the angular rate domain.

First approach requires the calibration platform capable of constant and known rotation. The values of reference and measured angular rates are then processed by any calibration algorithm to determine sensor errors. Unfortunately, this approach mostly relies on precise and expensive rotational platforms which limit its common usage.

Second approach assumes that the reference and measured angular rates are recorded and then processed by any calibration algorithm. Nevertheless, this approach is limited by precision of reference system which should be able to measure the angular rate with at least 10 times better accuracy than the calibrated sensor. This condition is ensured for example when systems such as RLGs, FOGs are employed for calibration of low-cost MEMS-based gyroscopes.

The second approach for the calibration in angular rate domain was evaluated in [76]. For the calibration purposes the combination of the FOG based measurement system [74] and a simple manually-driven platform was utilized (Fig. 1). The measured and reference angular rates were recorded and synchronized using a correlation function. Afterwards the parameters of gyroscope's SEM were estimated by the same algorithm as in the case of calibration in angle domain. The results were evaluated based on accuracy analyses, it showed that the calibration performed in the angular rate domain has approximately 3.7 times worse RMSE of residual deviations for both calibrated IMUs than the calibration performed in the angle domain [76].

## 5.2. Analyses of Electrolytic Tilt Sensors for Accelerometer Data Correction

The motivation for this work was to analyze and evaluate data of five ETSs with different electrolyte viscosity: standard, 15%, 30%, 50% (Advanced Orientation System, Inc. - Fig. 2) and standard from Spectron Glass and Electronic Incorporated (Fig. 2). Finally the most convenient electrolytic tilt sensor which can be used for corrections of triaxial accelerometer's imperfections such as initial bias error, null repeatability and so on was determined. Since the initial bias error of triaxial accelerometer can vary in the range up to  $\pm 50 \text{ mg} \approx \pm 2.9^\circ$  for ADIS16405 (based on manufacturer's specifications), the ETS can be used as an suitable aiding source for improvement of accelerometer performance and thus for improvement of the overall accuracy of attitude estimation.

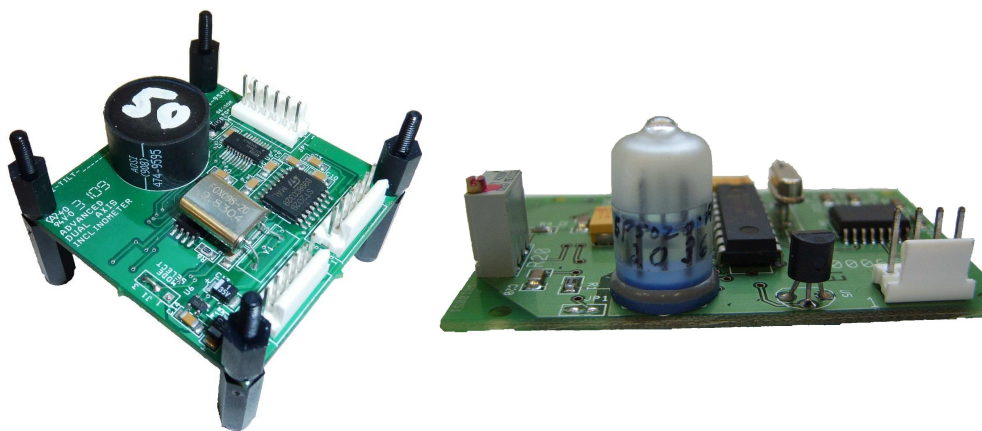


Fig. 2: Module with electrolytic tilt sensor EZ-TILT-2000-008-50% (on the left); module Micro 50-D70 with electrolytic tilt sensor (on the right)

The overview of ETS's principle of operation and typical parameters of five ETSs with different electrolyte viscosity was introduced in chapter 4.4 and the suitability of corrections based on ETS data were confirmed in chapter 4.5. In the following subchapters the performance of five ETSs was evaluated under static and dynamic conditions based on particular experiments.

### 5.2.1. Transfer Characteristics of Electrolytic Tilt Sensors

The biaxial electrolytic tilt sensors measure the angles of tilt in direction of two sensitivity axes  $X$  and  $Y$  (the direction of  $X$  and  $Y$  axes generally then corresponds to axes in navigation frame North-East-Down). The angle measured in direction of  $X$  axis is called pitch angle ( $\theta$ ) and in direction of  $Y$  axis is called roll angle ( $\phi$ ).

First of all, the transfer characteristics of all ETSs were measured for in both axes of tilt (Fig. 3). Based on measured and reference data the 3<sup>rd</sup> order polynomial functions were obtained to get corrections for pitch and roll angles. The corrections were applied on the measured characteristics, the deviations after corrections are shown in Fig. 4. The minimal, maximal and RMSE values of all ETSs are listed in Table 3.

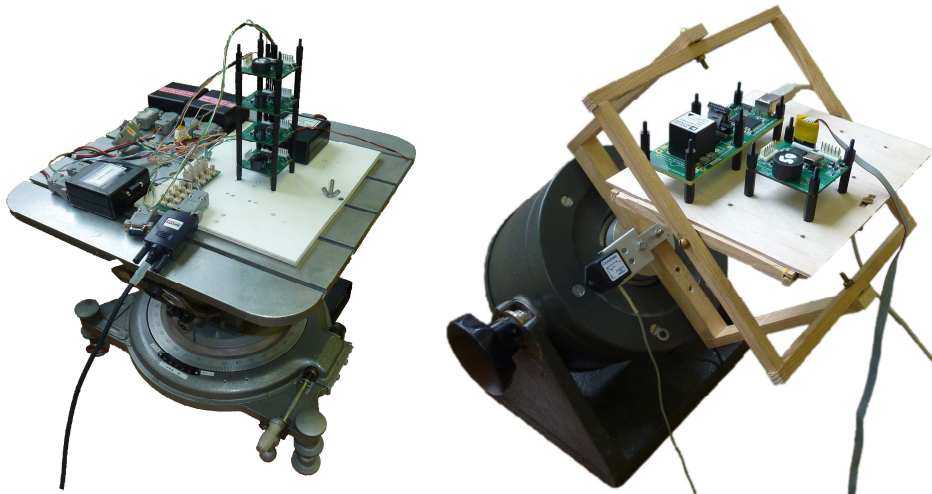


Fig. 3: Measurement setup with five electrolytic tilt sensors (on the left); measurement setup for testing of influence of vibrations on ETSs (on the right)

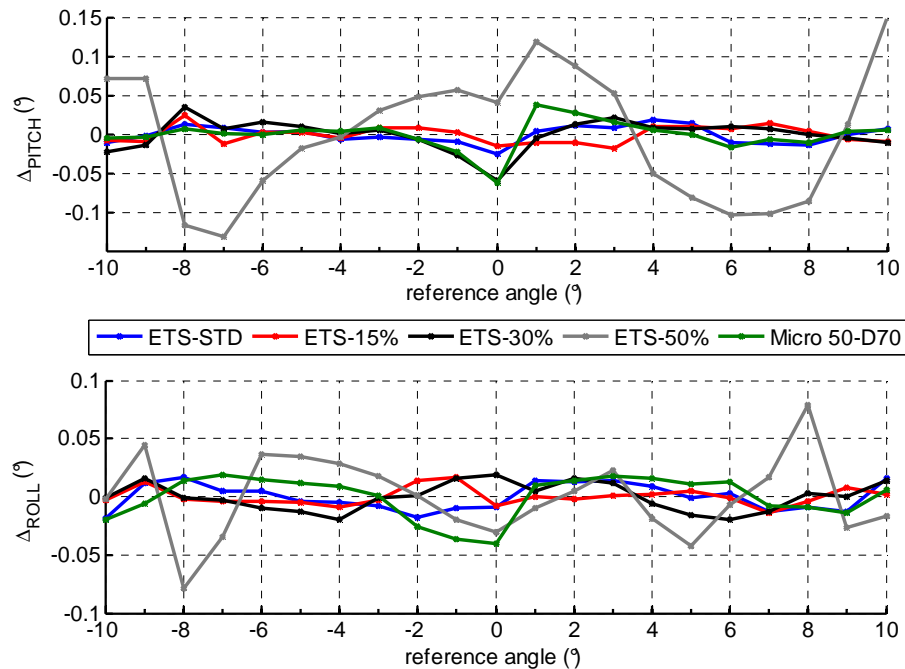


Fig. 4: Deviations ( $\Delta$ ) of pitch and roll angles from reference values after correction

TABLE 3: DEVIATIONS OF PITCH AND ROLL ANGLES FROM REFERENCE VALUES BEFORE AND AFTER CORRECTION

Micro 50D-70			EZ-TILT-2000-045-STD			EZ-TILT-2000-045-15%				
	Min	Max	RMSE	Min	Max	RMSE	Min	Max	RMSE	
$\theta$ (°)	Before	-0.38	0.17	0.19	0.07	2.04	1.23	0.39	1.34	0.94
	After	-0.06	0.04	0.02	-0.03	0.02	0.01	-0.02	0.03	0.01
$\phi$ (°)	Before	-0.47	-0.27	0.38	-0.60	1.25	0.71	-0.67	0.24	0.34
	After	-0.04	0.02	0.02	-0.02	0.02	0.01	-0.01	0.02	0.01

EZ-TILT-2000-045-30%			EZ-TILT-2000-008-50%				
	Min	Max	RMSE	Min	Max	RMSE	
$\theta$ (°)	Before	0.35	1.81	1.13	-0.97	2.39	0.82
	After	-0.06	0.04	0.02	-0.13	0.15	0.08
$\phi$ (°)	Before	-0.81	0.48	0.43	-0.67	2.98	1.50
	After	-0.02	0.02	0.01	-0.08	0.08	0.03

The worst case based on minimal, maximal, and RMSE values was found out in the case of EZ-TILT-2000-008-50%; on the other hand as the most accurate sensor the EZ-TILT-2000-045-15% was determined based on the lowest RMSE value.

### 5.2.2. Deviations of Tilt Angles Evaluated by Electrolytic Tilt Sensors

The measured data were corrected using 3<sup>rd</sup> order polynomial functions and the deviations of tilt angles were evaluated based on data measured according the following procedure: the sensors were tilted from -10° up to +10° with steps of 1° along pitch axis. Afterwards they were tilted back from +10° to -10° with the same step along the pitch axis again. The same procedure was used also along roll axis. The deviations within position pairs of both directions were analyzed and are shown in Fig. 5. The RMSE, minimal and maximal values of these deviations were computed and summarized in Table 4. From these analyses, the most convenient ETS EZ-TILT-2000-045-15% is chosen based on the lowest RMSE value.

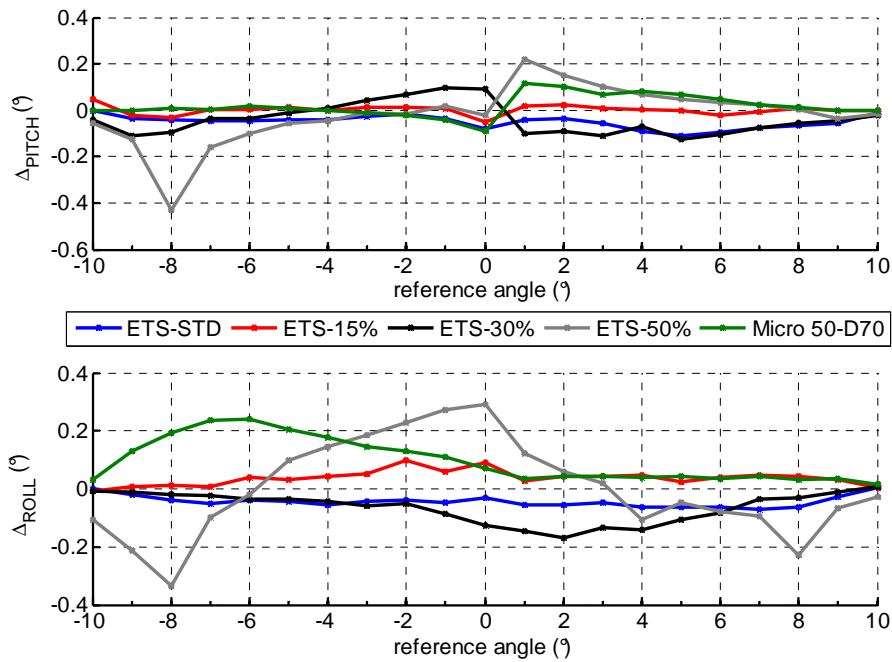
Fig. 5: Deviations ( $\Delta$ ) of pitch and roll angles evaluated by upward and downward direction measurements

TABLE 4: DEVIATIONS BETWEEN TILT ANGLES EVALUATED BY UPWARD AND DOWNWARD DIRECTION OF MEASUREMENTS

Electrolytic Tilt Sensor	Pitch Angle (°)			Roll Angle (°)		
	RMSE	MIN	MAX	RMSE	MIN	MAX
EZ-TILT-2000-045-STD	0.06	-0.11	0.00	0.05	-0.07	0.00
EZ-TILT-2000-045-15%	0.02	-0.05	0.05	0.04	-0.01	0.10
EZ-TILT-2000-045-30%	0.08	-0.12	0.10	0.08	-0.16	0.01
EZ-TILT-2000-008-50%	0.13	-0.43	0.22	0.16	-0.34	0.29
Micro 50-D70	0.05	-0.09	0.11	0.12	0.02	0.24

### 5.2.3. Analyses of Settling Time

The settling time defined by a producer is the time elapsed from the end of the tilt disturbance until the sensor output reaches a steady state with boundaries  $\pm 1 \sigma$  ( $\sigma$  is standard deviation obtained from data under static conditions). All ETSS were mounted on rotational and tilt platform and the data were measured for 8 preset positions that were reached by a ramp with positive and negative angular velocities in the range from  $5^\circ/\text{s}$  to  $55^\circ/\text{s}$ . Since evaluated settling times for individual ETSS did not vary more than 10% a mean value for each sensor was evaluated. Their values are denoted in Table 5. Moreover, examples of settling progressions are shown in Fig. 6. It can be seen that ETS EZ-TILT-2000-045-30% has the lowest settling time. As such, considering the minimum settling time ETS EZ-TILT-2000-045-30% is the most suitable sensor from this point of view.

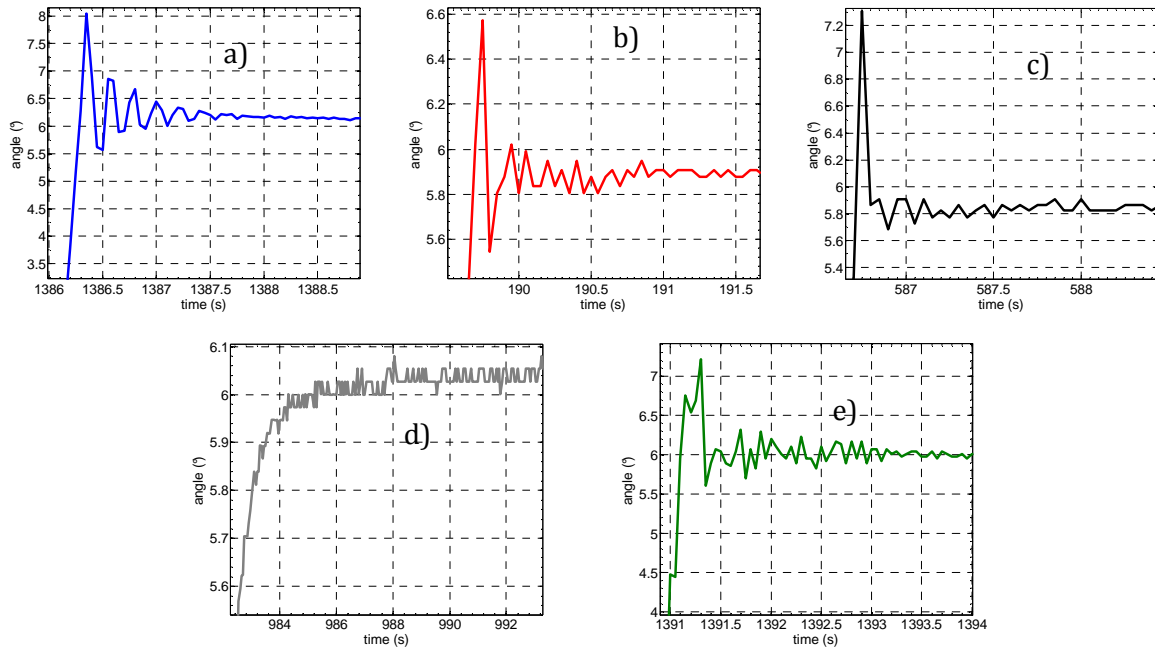


Fig. 6: Settling time: a) EZ-TILT-2000-045-STD; b) EZ-TILT-2000-045-15%; c) EZ-TILT-2000-045-30%; d) EZ-TILT-2000-008-50%; e) Micro 50-D70

TABLE 5: SETTLING TIME OF ALL EVALUATED ELECTROLYTIC TILT SENSORS

Electrolytic Tilt Sensor	T <sub>s</sub> (s)
EZ-TILT-2000-045-STD	2.41
EZ-TILT-2000-045-15%	1.28
EZ-TILT-2000-045-30%	0.61
EZ-TILT-2000-008-50%	5.25
Micro 50-D70	1.88

### 5.2.4. Influence of Vibrations on Attitude Determined by Electrolytic Tilt Sensors

The influence of vibrations was tested using the system for vibration testing (Fig. 3) which is described in details in [77]. Based on real flight data and vibration characteristics, the amplitude of vibrations  $a = 0.05g$  was chosen and with respect to the sampling frequency of the system, the frequency range from 5 Hz to 10 Hz was evaluated. The frequencies below 5 Hz could not be tested due to the platform limitation. For the comparison of results, the standard deviations  $\sigma$  is used as a criterion. The values of  $\sigma$  for all 5 tested ETSs are listed in Table 6. From the table, it can be seen that the most resistant ETS to the vibration is with 50% viscosity of electrolyte, followed by 30% viscosity. There is a slight difference between sensors with standard and 15% viscosity of electrolyte. The worst immunity of vibrations is observed in case of sensor Micro 50-D70.

Table 6: INFLUENCE OF VIBRATIONS TO FIVE ELECTROLYTIC TILT SENSORS

a=0.05 g		Micro 50-D70	EZ-TILT-2000-045-STD		EZ-TILT-2000-045-15%	
f (Hz)	$\sigma_\theta$ (°)	$\sigma_\phi$ (°)	$\sigma_\theta$ (°)	$\sigma_\phi$ (°)	$\sigma_\theta$ (°)	$\sigma_\phi$ (°)
5	1.52	0.72	0.24	0.43	0.16	0.32
6	1.19	0.77	0.09	0.23	0.11	0.24
7	1.67	1.26	0.12	0.16	0.16	0.36
8	1.21	0.96	0.16	0.22	0.14	0.33
9	1.01	0.73	0.05	0.11	0.10	0.24
10	0.45	0.41	0.03	0.09	0.07	0.17

a=0.05 g		EZ-TILT-2000-045-30%		EZ-TILT-2000-008-50%	
f (Hz)	$\sigma_\theta$ (°)	$\sigma_\phi$ (°)	$\sigma_\theta$ (°)	$\sigma_\phi$ (°)	
5	0.15	0.33	0.02	0.02	
6	0.10	0.25	0.02	0.02	
7	0.15	0.37	0.02	0.02	
8	0.12	0.33	0.02	0.02	
9	0.09	0.23	0.02	0.02	
10	0.06	0.17	0.02	0.02	

Considering the all measured characteristics, the following order of electrolytic tilt sensors was determined (the most convenient is the first one):

- EZ-TILT-2000-045-15%,
- EZ-TILT-2000-045-30%,
- EZ-TILT-2000-045-STD%,
- Micro 50-D70,
- EZ-TILT-2000-008-50%.

All tested sensors were also mounted on the UAV and tested for the improvement of INS accuracy in harsh environment are presented in [46] and in chapter 4.6.

### 5.2.5. Triaxial Accelerometer Initial Bias Estimation based on Electrolytic Tilt Sensor Data

The results published in paper [48] confirm that the ETS data are useful for triaxial accelerometer initial bias estimation and can significantly improve the accuracy of initial attitude determination.

From measured pitch and roll angles by biaxial electrolytic tilt sensor the accelerations can be computed using (2) [78]. The vector of accelerometer initial biases is possible to estimate using (3).

$$\begin{aligned} a_{ETSX} &= -G \sin(\theta_{ETS}), \\ a_{ETSY} &= G \sin(\phi_{ETS}) \cos(\theta_{ETS}), \\ a_{ETSZ} &= G \cos(\phi_{ETS}) \cos(\theta_{ETS}). \end{aligned} \quad (2)$$

$$\begin{aligned} b_{ACCX} &= a_{ACCX} - a_{ETSX}, \\ b_{ACCY} &= a_{ACCY} - a_{ETSY}, \\ b_{ACCZ} &= a_{ACCZ} - a_{ETSZ}, \end{aligned} \quad (3)$$

where  $\phi_{ETS}, \theta_{ETS}$  are pitch and roll angles measured by biaxial electrolytic tilt sensor;  $G = 1g = 9.80665 m/s^2$  is the value of gravity vector;  $(a_{ETSX}, a_{ETSY}, a_{ETSZ})^T$  is the vector of accelerations obtained from electrolytic tilt sensor data;  $(a_{ACCX}, a_{ACCY}, a_{ACCZ})^T$  is the vector of accelerations measured by triaxial accelerometer;  $(b_{ACCX}, b_{ACCY}, b_{ACCZ})^T$  is the estimated vector of initial biases.

## 6. Conclusion

### 6.1. Summary and Contribution

This doctoral thesis is primarily dedicated to the improvement of low-cost INS overall accuracy from attitude point of view by means such as usage of alternative sensors, estimation of sensor errors and usage of adaptive attitude estimation approaches. This kind of INS generally consists of MEMS based low-cost inertial navigation unit in which gyroscopes are aided by accelerometer and electrolytic tilt sensor. Since the intention is paid just to attitude, the objectives included a design and development of low-cost INS with algorithms for attitude evaluation and excluding GPS. The final low-cost INS realization was primarily developed for usage on UAVs or small aircrafts.

To increase the final accuracy of roll, pitch and yaw angles estimation, several steps were taken improving the performance of the sensors. Firstly the parameters of accelerometer, gyroscope and magnetometer deterministic SEMs were estimated providing means for consecutive error compensation.

The suitability of accelerometer SEMs compensation was verified for three evaluated accelerometers ADIS16405, AHRS M3 and CXL02LF3. As long as manufactures provide just basic calibration of low-cost inertial sensors additional is generally needed. The improvement can vary manufacturer to manufacturer and piece by piece. In the case of ADIS16405 and AHRS M3 the original accuracy was improved about 2% in average. The better improvement was achieved in the case of CXL02LF3 about 13% (for details see chapter 4.1).

To evaluate the gyroscope errors compensation suitability, the approximately 30 second long experiments were done and the measured angular rates were integrated to obtain roll, pitch and yaw angles for gyroscopes of AHRS M3 and 3DM-GX2 units. The average error of angle determination was 2.6% before and 0.1% after compensation for 3DM-GX2 gyroscope framework and was 1.4% before and 0.2% after compensation for AHRS M3. The detailed analyses were presented in chapters 4.2 and 5.1.

The influence of magnetometer errors compensation was also analyzed in chapter 4.3. The verification was based on different 64 combinations of roll, pitch and yaw angles under static conditions. The average error of yaw angle determination was before compensation 6.9% and after it 2.4%.

Although the triaxial accelerometer is calibrated, its performance can be further improved using an electrolytic tilt sensor. Based on several static tests, the ETS with a viscosity about 15% higher than standard was assumed as the most convenient sensor for initial bias estimation under static conditions. The vector of ADIS16405 accelerometer initial biases was determined as (0.008g, 0.009g, 0.005g). This vector has reduced the error of accelerometer-based initial pitch and roll angles about approximately 0.5°.

Finally, the adaptive data processing approach for attitude estimation was designed and implemented in quaternion form. The Gauss-Newton method was utilized for data fusion of accelerometer, magnetometer and electrolytic tilt sensor. The quaternion obtained from GNM was then aided with gyroscope data via an extended Kalman filter. The implemented algorithms were evaluated using data set obtained from UAV Bellanca Super Decathlon XXL. The final accuracy of EKF with GNM attitude estimation represented by RMSE values was compared to other attitude estimation approaches such as attitude determination based on gyroscopes, accelerometers, complementary filter, IMU/GPS EKF

and so on. The minimal RMSE values of roll, pitch and yaw angles ( $1.2^\circ$ ,  $2.0^\circ$ ,  $4.3^\circ$ ) were reached in case of IMU/GPS EKF, nevertheless in this approach position obtained from GPS receiver was used and thus it is not independent on external sources. In case of GNM+EKF, the RMSE values were ( $1.8^\circ$ ,  $2.6^\circ$ ,  $5.3^\circ$ ) and thus it reached the minimal RMSE values from all evaluated approaches which were independent on external sources of information.

The improvement of attitude determination accuracy based on sensor error compensations was confirmed under static conditions in chapters 4 and 5. The applying of accelerometer's and gyroscope's SEMs was also evaluated using real flight data. The overall accuracy of roll, pitch and yaw angles was improved about 0.1%, 5.2% and 15%, respectively.

The other analyses were focused on usage of ETS for accelerometer data corrections. The final accuracy of attitude estimation was verified for accelerometer only and for accelerometer aided by ETS. The usage of ETS improved the overall accuracy of roll, pitch and yaw angles about 2.2%, 6.0% and 3.2%, respectively. Even if the final accuracy improvement might seem negligible it needs to have in mind that the experiment included a real flight data and slight differences in RMSEs do not unambiguously provide a measure of behavior during dynamic changes. During the performed experiment only 16.8% of ACC+ETS corrections were possible to use. The detailed analyses and results were presented in chapter 4.6.

In this doctoral thesis, it was confirmed that the overall accuracy of attitude estimation was improved by usage of calibration techniques of all used sensors, by usage of electrolytic tilt sensor and by adaptive data processing approach. The objectives of the thesis were also successfully fulfilled.

## 6.2. Future Work

Even though the objectives of doctoral thesis are fulfilled, there are still tasks and challenges in navigation systems which need to be solved and further can improve the attitude estimation accuracy.

- The calibration procedures for inertial sensors were proposed in the thesis. Nevertheless, these procedures were primarily proposed for calibration of MEMS sensors with respect their typical resolution. For calibration of accelerometers and gyroscopes with resolution at least 100 times better than in case of MEMS sensors (sensors in tactical grade category and higher), the calibration procedures are not good enough and thus the more sophisticated approaches need to be developed.
- The accelerometers and gyroscopes used on UAV and small airplanes are strongly influenced by vibrations which degrade the final attitude determination. During the different flight modes, the different character, amplitudes and frequencies of vibrations are present. Therefore, to minimize the impact of vibrations, the algorithms for data denoising need to be designed and realized to improve the accuracy of attitude estimation in harsh environment conditions. The suppression of vibrations plays a key role when inertial navigation data are preprocessed.
- The aiding systems can significantly improve the overall accuracy of INS when they are applied under convenient conditions: for example the ACC-based corrections need to be applied under static or low-dynamic conditions; the magnetometer corrections can be applied only if the Earth magnetic field is not disturbed, and so on. To determine the convenient conditions for usage of aiding sources, the development of algorithms for detection of dynamics and validation of data are nowadays challenge in field of navigation systems.

## References

- [1] D. Jurman, M. Jankovec, R. Kamnik and M. Topic, "Calibration and data fusion solution for the miniature attitude and heading reference system," *Sensors and Actuators A: Physical*, vol. 138, no. 2, pp. 411-420, 2007.
- [2] N. Barbour and G. Schmidt, "Inertial sensor technology trends," *IEEE Sensors Journal*, p. 332–339, vol. 1, no. 4, Dec 2001.
- [3] M. Sipos, P. Paces, J. Rohac and P. Novacek, "Analyses of Triaxial Accelerometer Calibration Algorithms," *IEEE Sensors Journal*, vol. 12, no. 5, pp. 1157-1165, 2012.
- [4] M. Tarhan and E. Altug, "EKF based attitude estimation and stabilization of a quadrotor UAV using vanishing points in catadioptric images," *Journal of Intelligent & Robotic Systems*, pp. 587-607, vol. 62, no. 3-4, 2011.
- [5] S. Leutenegger and R. Siegwart, "A low-cost and fail-safe Inertial Navigation System for airplanes," *IEEE International Conference on Robotics and Automation*, 2012.
- [6] A. Bry, A. Bachrach and N. Roy, "State estimation for aggressive flight in GPS-denied environments using onboard sensing," *Proceedings of IEEE Intelligent Robotics and Automation Conference*, 2012.
- [7] Q. Tang, X. Wang, Q. Yang and C. Liu, "An improved scale factor calibration model of MEMS gyroscopes," *Proceedings, 2014 IEEE International Instrumentation and Measurement Technology Conference (I2MTC), Montevideo*, pp. 752-755 , 12-15 May 2014.
- [8] M. Kok, J. D. Hol, T. B. G. F. Schön and H. Luinge, "Calibration of a magnetometer in combination with inertial sensors," *2012 15th International Conference on Information Fusion (FUSION)*, pp. 787 - 793, 9-12 July 2012.
- [9] Z. Syed, P. Aggarwal, C. Goodall, X. Niu and N. El-Sheimy, "A new multi-position calibration method for MEMS inertial navigation systems," *Measurement Science and Technology*, vol. 18, no. 7, p. 1897, 2007.
- [10] A. Kim and M. F. Golnaraghi, "Initial calibration of an inertial measurement unit using optical position tracking system," *Proceedings of PLANS 2004: Position Location and Navigation Symposium*, p. 96–101, 2007.
- [11] R. Zhang, F. Höflinger and L. M. Reindl, "Calibration of an IMU Using 3-D Rotation Platform," *IEEE Sensors Journal*, pp. 1778-1787, vol. 14, No. 6', June 2014.
- [12] D. H. Titterton and J. L. Weston, *Strapdown Inertial Navigation Technology*, London, U.K.: Peter Peregrinis, 1997.
- [13] H. Pang, D. Chen, M. Pan, S. Luo, Q. Zhang, J. Li and F. Luo, "A New Calibration Method of Three Axis Magnetometer With Nonlinearity Suppresion," *IEEE Transactions on Magnetics*, pp. 5011-5015, vol. 49, No. 9, Sep 2013.
- [14] Z. Li and F. Duan, "Low Cost and Automatic Calibration for MEMS Gyroscope," *2012 Spring Congress on Engineering and Technology (S-CET), Xian*, pp. 1-4, 27-30 May 2012.
- [15] M. Glueck, D. Oshinubi and Y. Manoli, "Automatic realtime offset calibration of gyroscopes," *2013 IEEE Sensors Applications Symposium (SAS), Galveston, TX*, pp. 214 - 218 , 19-21 Feb. 2013.
- [16] S. Y. Cho and C. G. Park, "A calibration Technique for a Redundant IMU Containing Low-grade Inertial Sensors," *ETRI Journal*, pp. 418-426, 2005.
- [17] S. P. Won and F. Golnaraghi, "A triaxial accelerometer calibration method using a mathematical model," *IEEE Transaction on Instrumentation and Measurement*, p. 2144–2153, vol. 59, no. 8, Aug 2010.

- [18] V. Petrucha, P. Kaspar, P. Ripka and J. M. G. Merayo, "Automated system for the calibration of magnetometers," *Journal of Applied Physics*, pp. 07E704 - 07E704-3 , Vol. 105 , Issue 7, Apr 2009.
- [19] I. Skog and P. Handel, "Calibration of a MEMS inertial measurement unit," in *XVII IMEKO World Congress*, 2006.
- [20] T. Pylvanainen, "Automatic and adaptive calibration of 3D field sensors," *Applied Mathematical Modelling*, p. 575-587, vol. 32, no. 4, Apr 2008.
- [21] S. Bonnet, C. Bassompierre, C. Godin, S. Lesecq and A. Barraud, "Calibration methods for inertial and magnetic sensors," *Sensors and Actuators A: Physical*, p. 302–311, vol. 156, no. 2, Dec. 2009.
- [22] S. Luo, H. Pang, J. Li, Q. Zhang, D. Chen, M. Pan and F. Luo, "Calibration strategy and generality test of three-axis magnetometers," *Measurement*, p. 3918–3923, vol. 46, issue 10, Dec 2013.
- [23] K. Mohamadabadi and M. Hillion, "An Automated Indoor Scalar Calibration Method for Three-Axis Vector Magnetometers," *IEEE Sensors Journal*, pp. 3076 - 3083, vol. 14, issue 9, Sept. 2014.
- [24] S. Feng, L. Fengli and F. Xirui, "A new method of zero calibration of the strapdown inertial navigation system," In *Proceedings of the International Conference on Mechatronics and Automation (ICMA), Chengdu, China*, p. 1586–1590, 5–8 Aug 2012.
- [25] A. Olivares, G. Olivares, J. M. Gorri and J. Ramirez, "High-Efficiency Low-cost Accelerometer-Aided Gyroscope Calibration," *ICTM '09. International Conference on Test and Measurement*, pp. 354-360, 5-6 Dec. 2009.
- [26] M.-S. Kim, S.-B. Yu and K.-S. Lee, "Development of a High-Precision Calibration Method for Inertial Measurement Unit," *International Journal of Precision Engineering and Manufacturing*, pp. 567-575, vol. 15, 2014.
- [27] M. Sipos, J. Rohac and P. Novacek, "Improvement of Electronic Compass Accuracy Based on Magnetometer and Accelerometer Calibration," *Acta Physica Polonica A*, pp. 945-949, no. 4, vol. 121, 2012.
- [28] M. Sipos and J. Rohac, "Calibration of Tri-axial Angular Rate Sensors," *Proceedings of 10th International Conference Measurement, Diagnostics, Dependability of Aircraft Systems*, 20-21 Oct 2010.
- [29] R. Dai, R. Stein, B. Andrews, K. James and M. Wieler, "Application of tilt sensors in functional electrical stimulation," *Rehabilitation Engineering, IEEE Transactions on*, pp. 63-72, vol.4, no.2, Jun 1996.
- [30] F. B.V., "MEMS (Micro-Electro-Mechanical Systems)," FRABA B.V., 2014. [Online]. Available: [https://www.posital.com/en/products/inclinometers/mems/mems\\_1.php](https://www.posital.com/en/products/inclinometers/mems/mems_1.php). [Accessed 27 Jan 2015].
- [31] D. Pheifer, "Position/Presence/Proximity, The Electrolytic Tilt Sensor," True North Technologies LLC, 1 May 2000. [Online]. Available: <http://www.sensorsmag.com/sensors/position-presence-proximity/the-electrolytic-tilt-sensor-1063>. [Accessed 27 Jan 2015].
- [32] "Electrolytic Tilt Sensor Selection & Operation," The Fredericks Company, 2008. [Online]. Available: [http://www.frederickscom.com/sens\\_tech\\_select.tpl](http://www.frederickscom.com/sens_tech_select.tpl). [Accessed 27 Jan 2015].
- [33] "The Electrolytic Tilt Sensor," True North Technologies, 2014. [Online]. Available: <http://www.tntc.com/Products/WhitePapers/The%20Electrolytic%20Tilt%20Sensor.pdf>. [Accessed 27 Jan 2015].
- [34] Honeywell, "Digital Compass Solution HMR3000," Sept. 2006. [Online]. Available: <http://www.farnell.com/datasheets/703070.pdf>. [Accessed 05 Jan 2015].
- [35] S. E. BesTech, "Electrolytic Tilt Sensors," [Online]. Available: <http://www.bestech.com.au/electrolytic-tilt/>. [Accessed 05 Jan 2015].

- [36] E. Marianovsky, "DX-008 / DX-045 Dual Axis Tilt Sensors," Advanced Orientation Systems, Inc., 2014. [Online]. Available: <http://www.aositilt.com/se/dx-polymer-sensors/>. [Accessed 05 Jan 2015].
- [37] S. G. a. E. Incorporated, "Electrolytic Tilt Sensors," Spectron Glass and Electronics Incorporated, 2014. [Online]. Available: <http://www.spectronsensors.com/tilt-sensors.php>. [Accessed 05 Jan 2015].
- [38] J. C. Choi, Y. C. Choi, J. K. Lee and S. H. Kong, "Miniaturized Dual-Axis Electrolytic Tilt Sensor," *Japanese Journal of Applied Physics*, pp. 06FL13-1-06FL13-5, 2012.
- [39] A. Ruether, "Designing Products that Require Angle Measurement: Have you Considered Electrolytic Tilt Sensors?," The Fredericks Company, 2008. [Online]. Available: <http://www.frederickscom.com/news1.tpl>. [Accessed 27 Jan 2015].
- [40] P. D. Groves, GNSS, Inertial, and Multisensors Integrated Navigation, USA: Paul. D Groves, 2013.
- [41] D. M. Bevly and S. Cobb, GNSS for Vehicle Control, Norwood: Artech House, 2010.
- [42] L. Ojeda, G. Reina, D. Cruz and J. Borenstein, "The FLEXnav Precision Dead-reckoning System," *International Journal of Vehicle Autonomous Systems (IJVAS)*, pp. 173-195, Vol 4., No. 2-4 2006.
- [43] J. H. Doty, "Synthesized attitude and heading inertial reference". USA Patent US 5841537 A, 24 Nov 1997.
- [44] Advancement of Assistive Technology, Amsterdam: IOS Press, 1997.
- [45] A.-J. Baerveldt and R. Klang, "A Low-cost and Low-weight Attitude Estimation System for an Autonomous Helicopter," *Proceedings., 1997 IEEE International Conference on Intelligent Engineering Systems, 1997. INES '97*, pp. 391-395 , 15-17 Sep 1997.
- [46] H. Jung, C. J. Kim and K. S. Ho, "An optimized MEMS-based electrolytic tilt sensor," *Sensors and Actuators A: Physical*, p. 23-30, 27 Sep 2006.
- [47] M. Sipos and J. Rohac, "Comparison of Electrolytic Tilt Modules for Attitude Correction," *Proceedings of 12th International Conference Measurement, Diagnostics, Dependability of Aircraft Systems*, pp. 1-11, 2012.
- [48] M. Sipos, J. Rohac and P. Novacek, "Analyses of Electronic Inclinometer Data for Tri-axial Accelerometer's Initial Alignment," *Przeglad Elektrotechniczny*, NR 1a, r. 88, 2012.
- [49] M. Sipos, J. Simanek and J. Rohac, "Practical Approaches to Attitude Estimation in Aerial Applications," *International Journal of Aerospace Engineering*, submitted fot publication 2014.
- [50] R. Munguía and A. Grau, "A Practical Method for Implementing an Attitude and Heading Reference System," *International Journal of Advanced Robotic Systems*, 11:62 2014.
- [51] M. Wang, Y. Yang, R. R. Hatch and Y. Zhang, "Adaptive filter for a miniature MEMS based attitude and heading reference system," *Position Location and Navigation Symposium, 2004. PLANS 2004*, pp. 193 - 200 , 26-29 April 2004.
- [52] R. Mahony, T. Hamel and J.-M. Pflimlin, "Nonlinear Complementary Filters on the Special Orthogonal Group," *IEEE Transactions on Automatic Control*, pp. 1203-1218 , June 2008.
- [53] H. G. d. Marina, F. J. Pereda, J. M. Giron-Sierra and F. Espinosa, "UAV Attitude Estimation Using Unscented Kalman Filter and TRIAD," *IEEE Transactions on Industrial Electronics*, pp. 4465-4474 , Aug. 2011.
- [54] J. Diebel, "Representing Attitude: Euler Angles, Unit Quaternions, and Rotation Vectors," 26 Oct 2006. [Online]. Available: [http://www.astro.rug.nl/software/kapteyn/\\_downloads/attitude.pdf](http://www.astro.rug.nl/software/kapteyn/_downloads/attitude.pdf). [Accessed 05 Jan 2015].

- [55] J. K. Lee, E. J. Park and S. N. Robinovitch, "Estimation of Attitude and External Acceleration Using Inertial Sensor Measurement During Various Dynamic Conditions," *IEEE Transactions on Instrumentation and Measurement*, pp. 2262-2273, 20 March 2012.
- [56] D. Gebre-Egziabher, R. Hayward and J. Powell, "Design of multi-sensor attitude determination," *IEEE Transactions on Aerospace and Electronic Systems*, pp. 627- 649, vol. 40, no. 2, 2004.
- [57] J. F. G. Castellanos, S. Lesecq, N. Marchand and J. Delamare, "A low-cost air data attitude heading reference system for the tourism airplane applications," *IEEE Sensors 2005*, Oct. 30 2005-Nov. 3 2005 2005.
- [58] D. Gebre-Egziabher, R. C. Hayward and J. D. Powell, "A low-cost GPS/inertial attitude heading reference system (AHRS) for general aviation applications," *Position Location and Navigation Symposium, IEEE 1998*, pp. 518-525 , 20-23 Apr 1998.
- [59] M. Euston, P. Coote, R. Mahony and J. Kim, "A complementary filter for attitude estimation of a fixed-wing UAV," *IROS 2008. IEEE/RSJ International Conference on Intelligent Robots and Systems*, pp. 340-345, 22-26 Sept. 2008.
- [60] J. Calusdian, X. Yun and E. Bachmann, "Adaptive-gain complementary filter of inertial and magnetic data for orientation estimation," *2011 IEEE International Conference on Robotics and Automation (ICRA)*, pp. 1916-1922, 9-13 May 2011.
- [61] A. Bachrach, S. Prentice, R. He and N. Roy, "RANGE - Robust autonomous navigation in GPS-denied environments," *Journal of Field Robotics*, pp. 644-666, vol. 28, no. 5, 2011.
- [62] J. L. Crassidis, F. L. Markley and Y. Cheng, "Survey of nonlinear attitude estimation methods," *Journal of Guidance Control and Dynamics*, 12-28 vol. 30, no. 1, 2007.
- [63] S. S. Young, "Orientation Estimation Using a Quaternion-Based Indirect Kalman Filter With Adaptive Estimation of External Acceleration," *IEEE Transactions on Instrumentation and Measurement*, pp. 3296-3305, 10 May 2010.
- [64] D.-J. Jwo and T.-S. Cho, "Critical remarks on the linearised and extended Kalman filters with geodetic navigation examples," *Measurement*, p. 1077–1089, vol. 43, issue 9, Nov 2010.
- [65] Y. Pan, P. Song, K. Li and Y. Zhou, "Attitude Estimation of Miniature Unmanned Helicopter using Unscented Kalman Filter," *2011 International Conference on Transportation, Mechanical, and Electrical Engineering (TMEE)*, pp. 1548-1551 , 16-18 Dec. 2011.
- [66] M. Cordoba, "Attitude and heading reference system I-AHRS for the EFIGENIA autonomous unmanned aerial vehicles UAV based on MEMS sensor and a neural network strategy for attitude estimation," *MED '07. Mediterranean Conference on Control & Automation*, pp. 1-8, 27-29 June 2007.
- [67] M. Sotak, M. Sopata and F. Kmec, "Navigation systems using Monte Carlo method," in *Guidance, Navigation and Control Systems*, 2006.
- [68] J. L. Marins, X. Yun, E. R. Bachmann, R. B. McGhee and M. J. Zyda, "An Extended Kalman Filter for Quaternion-Based Orientation Estimation Using MARG Sensors," *Proceedings of the 2001 IEEE/RSJ International Conference on Intelligent Robots and Systems*, pp. 2003-2011, Oct. 29 - Nov. 03, 2001 2001.
- [69] L. Fei, L. Jie, W. Haifu and L. Chang, "An improved quaternion Gauss–Newton algorithm for attitude determination using magnetometer and accelerometer," *Chinese Journal of Aeronautics*, p. 986–993, 27(4), 2014.
- [70] S. O. Madgwick, A. J. Harrison and R. Vaidyanathan, "Estimation of IMU and MARG orientation using a gradient descent algorithm," *011 IEEE International Conference on Rehabilitation Robotics, ETH Zurich Science City, Switzerland*, pp. 1-7, June 29 - July 1 2011.

- [71] X. Yun, C. Aparicio, E. R. Bachmann and R. B. McGhee, "Implementation and Experimental Results of a Quaternion-Based Kalman Filter for Human Body Motion Tracking," *Proceedings of the 2005 IEEE International Conference on Robotics and Automation Barcelona, Spain*, April 2005.
- [72] X. Yun and E. R. Bachmann, "Design, Implementation, and Experimental Results of a Quaternion-Based Kalman Filter for Human Body Motion Tracking," *IEEE TRANSACTIONS ON ROBOTICS, VOL. 22, NO. 6*, pp. 1216 - 1227, 2006.
- [73] R. Jategaonkar, "Bounded-variable Gauss–Newton algorithm for aircraft parameter estimation," *Journal of aircrafts*, pp. 742-744, 37(4), 2000.
- [74] J. Rohac, M. Sipos, J. Simanek and O. Teren, "Inertial Reference Unit in a Directional Gyro Mode of Operation," *IEEE SENSORS 2012 - Proceedings*, pp. 1356-1359, 28-31 Oct. 2012.
- [75] M. Alam, M. Sipos, J. Rohac and J. Simanek, "Calibration of a Multi-sensor Inertial Measurement Unit with Modified Sensor Frame," *Proceedings of International Conference on Industrial Technology ICIT 2015*, p. Accepted for publication, 17-19 Mar. 2015.
- [76] J. Rohac, M. Sipos and J. Simanek, "Calibration of the Low-cost Triaxial Inertial Sensors," *Instrumentation & Measurement Magazine*, Submitted for publication in 2014.
- [77] M. Sipos, J. Rohac and M. Stach, "System for Vibration Testing," *Proceedings of 11th International Conference Measurement, Diagnostics, Dependability of Aircraft Systems*, pp. 213-225, 2011.
- [78] J. Rohac and M. Sipos, "Sensors and Data Processing Methods Used in Navigation Systems," *Proceedings of the International Scientific Conference Modern Safety Technologies in Transportation*, pp. 342-348, 2011.

## Appendix A: Author's Publications and Grants

### A.1. Publications Related to the Thesis

#### A.1.1. Publications in Journals with Impact Factor

- [J1] Šipoš, M.; Pačes, P.; Roháč, J.; Nováček, P.: "Analyses of Triaxial Accelerometer Calibration Algorithms", IEEE Sensors Journal, 2012, vol. 12, no. 5, p. 1157-1165, ISSN 1530-437X, co-authorship: 65%.
- [J2] Šipoš, M.; Roháč, J.; Nováček, P.: "Improvement of Electronic Compass Accuracy Based on Magnetometer and Accelerometer Calibration", Acta Physica Polonica A, 2012, vol. 121, no. 4, p. 1111-1115, ISSN 0587-4246, co-authorship: 70%.

#### A.1.2. Publications in Peer-reviewed Journals

- [R1] Šipoš, M.; Roháč, J.; Nováček, P.: "Analyses of Electronic Inclinometer Data for Tri-axial Accelerometer's Initial Alignment", Przeglad Elektrotechniczny, 2012, 88, 01a, p. 286-290. ISSN 0033-2097, co-authorship: 60%.
- [R2] Sipos, M.; Simanek, J.; Rohac, J.: "Practical Approaches to Attitude Estimation in Aerial Applications", International Journal of Aerospace Engineering, ISSN 1687-5974, (submitted for publication in 2014), co-authorship: 50%.
- [R3] Reinštein, M.; Šipoš, M.; Roháč, J.: "Error Analyses of Attitude and Heading Reference Systems", Przeglad Elektrotechniczny, 2009, vol. 85, no. 8, p. 114-118, ISSN 0033-2097, co-authorship: 20%.
- [R4] Reinštein, M.; Roháč, J.; Šipoš, M.: "Algorithms for Heading Determination using Inertial Sensors", Przeglad Elektrotechniczny, 2010, vol. 86, no. 9, p. 243-246, ISSN 0033-2097, co-authorship: 5%.
- [R5] Reinštein, M.; Roháč, J.; Šipoš, M.: "Improving Performance of a Low-cost AHRS", Acta Avionica, 2008, vol. X, no. 16, p. 132-137, ISSN 1335-9479, co-authorship: 10%.

#### A.1.3. Conference Proceedings (WoS)

- [W1] Šipoš, M.; Pačes, P.; Reinštein, M.; Roháč, J.: "Flight Attitude Track Reconstruction Using Two AHRS Units under Laboratory Conditions", In IEEE SENSORS 2009 - The Eighth IEEE Conference on Sensors, Christchurch: IEEE Sensors Council, 2009, p. 675-678, ISSN 1930-0395, ISBN 978-1-4244-5335-1, co-authorship: 40%.
- [W2] Roháč, J.; Šipoš, M.; Šimánek, J.; Tereň, O.: "Inertial Reference Unit in a Directional Gyro Mode of Operation", In IEEE SENSORS 2012 – Proceedings, Piscataway: IEEE Service Center, 2012, p. 1356-1359, ISBN 978-1-4577-1765-9, co-authorship: 30%.

#### A.1.4. Conference Proceedings

- [C1] Šipoš, M.; Roháč, J.: "Comparison of Electrolytic Tilt Modules for Attitude Correction", In MDS 2012 - Measurement, Diagnostics, Dependability of Aircraft Systems, Brno: University of Defence, Faculty of Military Technology, p. 1-14. ISBN 978-80-7231-894-0, co-authorship: 80%.
- [C2] Šipoš, M.; Šimánek, J.; Nováček, P.; Popelka, J.; Roháč, J.: "Modular Navigation System for Unmanned Aerial Vehicles", In ICMT'13 - Proceedings of the International Conference on Military Technologies. Brno: University of Defence, 2013, p. 1-10, ISBN 978-80-7231-917-6, co-authorship: 20%.
- [C3] Šipoš, M.; Roháč, J.: "Usage of Electrolytic Tilt Sensor for Initial Alignment of Tri-axial Accelerometer", In ICMT'11 International Conference on Military Technologies 2011, Brno: University of Defence, 2011, p. 685-691, ISBN 978-80-7231-788-2, co-authorship: 60%.

- [C4] Šipoš, M.; Roháč, J.: "Calibration of Tri-axial Angular Rate Sensors", In MDS - Measurement, Diagnostics, Dependability of Aircraft Systems, Brno: University of Defence, Faculty of Military Technology, 2010, p. 148-152, ISBN 978-80-7231-741-7, co-authorship: 80%.
- [C5] Šipoš, M.; Roháč, J.: "Integration of Low-cost Inertial Navigation Unit with Secondary Navigation Systems", In Workshop 2010, Prague: Czech Technical University in Prague, 2010, p. 146-147, ISBN 978-80-01-04513-8, co-authorship: 95%.
- [C6] Šipoš, M.; Roháč, J.; Reinštein, M.: "Measurement with Electrolytic Tilt Sensor". In 2008 PEGASUS-AIAA Student Conference, Prague: Czech Technical University in Prague, 2008, co-authorship: 65%.
- [C7] Šipoš, M.; Reinštein, M.; Roháč, J.: "System for Measuring Tilt-Angle", In New Development Trends in Aeronautics, Košice: Technical University of Košice, 2008, p. 120-121, ISBN 978-80-553-0067-2, co-authorship: 80%.
- [C8] Šipoš, M.; Reinštein, M.; Roháč, J.: "Levenberg-Marquardt Algorithm for Accelerometers Calibration", In MDS 2008 - Measurement, Diagnostics, Dependability of Aircraft Systems, Brno: University of Defence, Faculty of Military Technology, 2008, p. 39-45, ISBN 978-80-7231-555-0, co-authorship: 90%.
- [C9] Šipoš, M.; Roháč, J.: "Improvement of Electronic Compass Accuracy Based on Magnetometer and Accelerometer Calibration", In SPM 2011 - X Symposium of Magnetic Measurements. Częstochowa Branch: Polish Society of Theoretical and Applied Electrical Engineering, 2011, p. 33, co-authorship: 60%.
- [C10] Roháč, J.; Šipoš, M.: "Practical Usage of Allan Variance in Inertial Sensor Parameters Estimation and Modeling", In New Trends in Civil Aviation 2011, Prague: Czech Technical University in Prague and OSL ČR, 2011, p. 107-112, ISBN 978-80-01-04893-1, co-authorship: 5%.
- [C11] Roháč, J.; Šipoš, M.; Nováček, P.: "Azimuth Determination Based on Magnetometer Measurements". In MDS 2011 - Measurement, Diagnostics, Dependability of Aircraft Systems, Brno: University of Defence, Faculty of Military Technology 2011, p. 11-17. ISBN 978-80-7231-828-5, co-authorship: 10%.
- [C12] Roháč, J.; Šipoš, M.: "Sensors and Data Processing Methods Used in Navigation Systems", In Proceedings of the International Scientific Conference Modern Safety Technologies in Transportation. Košice: SUPREMA Ltd., 2011, p. 342-348, ISSN 1338-5232, ISBN 978-80-970772-0-4, co-authorship: 5%.
- [C13] Nováček, P.; Šipoš, M.; Pačes, P.: "Modular System for Attitude and Position Determination". In POSTER 2011 - 15th International Student Conference on Electrical Engineering, Prague: CTU in Prague, Faculty of Electrical Engineering, 2011, p. 1-5, ISBN 978-80-01-04806-1, co-authorship: 30%.
- [C14] Roháč, J.; Šipoš, M.; Nováček, P.; Pačes, P.; Reinštein, M.: "Modular System for Attitude and Position Estimation", Workshop 2011, Prague: Czech Technical University in Prague, 2011, p. 1-4, co-authorship: 20%.
- [C15] Reinštein, M.; Roháč, J.; Šipoš, M.: "Turbulence Modelling for Attitude Evaluation Purposes", In MDS 2008 - Measurement, Diagnostics, Dependability of Aircraft Systems, Brno: University of Defence, Faculty of Military Technology, 2008, p. 46-54, ISBN 978-80-7231-555-0, co-authorship: 5%.
- [C16] Reinštein, M.; Pačes, P.; Roháč, J.; Šipoš, M.: "Advanced Implementations Techniques in Kalman Filtering", In 2008 PEGASUS-AIAA Student Conference, Prague: Czech Technical University, 2008, co-authorship: 5%.
- [C17] Reinštein, M.; Šipoš, M.: "Improving Performance of a Low-cost AHRS", In New Development Trends in Aeronautics. Technical University of Košice, 2008, p. 109-110. ISBN 978-80-553-0067-2, co-authorship: 5%.

### A.1.5. Invited Presentations

- [C18] Šipoš, M.; Roháč, J.: "Comparison of Electrolytic Tilt Modules for Attitude Correction", In MDS 2012 - Measurement, Diagnostics, Dependability of Aircraft Systems, Brno: University of Defence, Faculty of Military Technology, 2012, p. 3-13. ISBN 978-80-7231-894-0, co-authorship: 80%.

[C19] Roháč, J.; Šipoš, M.; Nováček, P.: "Azimuth Determination Based on Magnetometer Measurements", In MDS 2011 - Measurement, Diagnostics, Dependability of Aircraft Systems, Brno: University of Defence, Faculty of Military Technology, 2011, p. 11-17, ISBN 978-80-7231-828-5, co-authorship: 10%.

[C20] Roháč, J.; Šipoš, M.: "Sensors and Data Processing Methods Used in Navigation Systems", In Proceedings of the International Scientific Conference Modern Safety Technologies in Transportation, Košice: SUPREMA Ltd., 2011, p. 342-348, ISSN 1338-5232, ISBN 978-80-970772-0-4, co-authorship: 5%.

## A.2. Publications Not Related to the Thesis

### A.2.1. Publications in Journals with Impact Factor

### A.2.2. Publications in Peer-reviewed Journals

### A.2.3. Conference Proceedings (WoS)

[W3] Pačes, P.; Šipoš, M.; Reinštein, M.; Roháč, J.: "Sensors of Air Data Computers - Usability and Environmental Effects", In ICMT'09 - Proceedings of the International Conference on Military Technologies. Brno: University of Defence, 2009, p. 401-409. ISBN 978-80-7231-649-6, co-authorship: 20%.

### A.2.4. Conference Proceedings

[C21] Šipoš, M.; Bílý, M.; Koudelka, L.; Šimánek, J.; Alam, M. et al.: "Development of Inertial Navigation Systems", In Proceedings of 2014 PEGASUS-AIAA Student Conference, Prague: CTU, 2014, ISBN 978-80-01-05459-8, co-authorship: 20%.

[C22] Šipoš, M.; Roháč, J.; Stach, M.: "System for Vibration Testing", In MDS 2011 - Measurement, Diagnostics, Dependability of Aircraft Systems, Brno: University of Defence, Faculty of Military Technology, 2012, 2011, p. 213-225, ISBN 978-80-7231-828-5, co-authorship: 80%.

[C23] Šipoš, M.; Nováček, P.; Pačes, P.: "Development of Platform for Measurement and Signal Processing of Navigation and Aerometric Data". In POSTER 2011 - 15th International Student Conference on Electrical Engineering. Prague: CTU, Faculty of Electrical Engineering, 2011, p. 1-5. ISBN 978-80-01-04806-1, co-authorship: 50%.

[C24] Nováček, P.; Šipoš, M.; Popelka, J.; Šimánek, J.; Roháč, J.: "Modular Navigation System for Unmanned Aerial Vehicles - Flight Data Monitoring and Recording", In MDS 2012 - Measurement, Diagnostics, Dependability of Aircraft Systems, Brno: University of Defence, Faculty of Military Technology, 2012, p. 157-163. ISBN 978-80-7231-894-0, co-authorship: 20%.

[C25] Pačes, P.; Šipoš, M.; Vesely, M.: "Verification of IEEE1588 Time Synchronization in NASA Agate Data Bus Standard", In IEEE 2009 9th Conference on Electronic Measurement & Instruments. Beijing: IEEE, 2009, ISBN 978-1-4244-3862-4, co-authorship: 15%.

[C26] Pačes, P.; Šipoš, M.: "Introducing Students to Aerospace Board Information Systems Using an Embedded Graphics System Simulator", In ICALT 2010 - Proceedings of 10th IEEE International Conference on Advanced Learning Technologies, Los Alamitos: IEEE Computer Society, 2010, p. 397-399, ISBN 978-0-7695-4055-9, co-authorship: 15%.

[C26] Pačes, P.; Šipoš, M.; Draxler, K.: "Temperature Effects and Non-linearity Corrections of Pressure Sensors", In ICMT'11 International Conference on Military Technologies 2011, Brno: University of Defence, 2011, p. 651-656. ISBN 978-80-7231-788-2, co-authorship: 25%.

[C27] Pačes, P.; Šipoš, M.; Laifr, J.; Batěk, M.: "Small Satellite Systems Control for University Curriculum", In 62nd International Astronautical Congress, Cape Town: South African National Space Agency (SANSA), 2011, p. E1.2.5.1-E1.2.5.9, ISSN 1995-6258, co-authorship: 30%.

- [C28] Pačes, P.; Nováček, P.; Šipoš, M.: "Laboratory System for a Spacecraft Stabilization Principle Demonstration", In MDS - 2011 - Measurement, Diagnostics, Dependability of Aircraft Systems, Brno: University of Defence, Faculty of Military Technology, 2011, s. 145-164. ISBN 978-80-7231-828-5, co-authorship: 25%.

#### A.2.5. Utility Models

- [U1] Roháč, J.; Nováček, P.; Šimánek, J.; Šipoš, M.: "Autonomous System for Attitude Measurement", Utility Model, Industrial Property Office, 26785, 2014-04-14, co-authorship: 25%.
- [U2] Roháč, J.; Šipoš, M.: "Measurement Unit of an Artificial Horizon", Utility Model, Industrial Property Office, 23268, 2012-01-16, co-authorship: 10%.

#### A.2.6. Functional Prototypes

- [F1] Šipoš, M.; Nováček, P.; Bílý, M.; Šimánek, J.; Roháč, J.: "Miniature Inertial Navigation System", Functional Prototype, 2014, co-authorship: 20%.
- [F2] Šipoš, M.; Roháč, J.; Popelka, J.; Pačes, P.; Papaj, J.: "Module with an Electronic Inclinometer for Non-magnetic Calibration Platform Tilt Measurements", Functional Prototype, 2011, co-authorship: 50%.
- [F3] Koudelka, L.; Roháč, J.; Šipoš, M.: "SD Logger of Data from CAN and RS232 Bus", Functional Prototype, 2014, co-authorship: 10%.
- [F4] Nováček, P.; Šipoš, M.; Levora, T.; Roháč, J.; Papaj, J.: "Flight Data Recorder - SD logger", Functional Prototype, 2011, co-authorship: 28%.
- [F5] Pačes, P.; Hospodář, P.; Levora, T.; Popelka, J.; Šipoš, M.: "An Air-speed, Angle-of-Attack and Angle-of-sideslip Measurement Module", Functional Prototype, co-authorship: 10%.
- [F6] Pačes, P.; Popelka, J.; Levora, T.; Šipoš, M.: "Development Platform Illustrating Principles of Sensor Parameters Characterization and Spacecraft Systems Control", Functional Prototype, 2012, co-authorship: 10%.
- [F7] Roháč, J.; Šipoš, M.; Šimánek, J.; Papaj, J.; Bílý, M.: "Navigation Unit", Functional Prototype, 2012, co-authorship: 20%.

#### A.3. Grants and Projects Related to the Thesis

- [G1] Šipoš, M.: "Integration of Low-cost Inertial Navigation Unit with Secondary Navigation Systems (GPS, Magnetometer)", 2009, Czech Technical University in Prague, Czech Republic, CTU0909913.
- [G2] Roháč, J.: "Modern Methods in Development of Inertial Navigation Systems", 2013-2014, Czech Technical University in Prague, Czech Republic, SGS13/144/OHK3/2T/13, member of team.
- [G3] Roháč, J.: "Modular Navigation System for Attitude and Position Estimation", 2010-2012, Czech Technical University in Prague, Czech Republic, SGS13/144/OHK3/2T/13, member of team.
- [G4] Ripka, P.: "Sensors and Intelligent Sensors Systems", 2009-2012, Grant Agency of Czech Republic, GD102/09/H082.
- Šipoš, M.: „Inertial Navigation System based on inertial sensors, magnetometer and GPS“.

#### A.4. Response to Author's Publications

- [J1] Šipoš, M.; Pačes, P.; Roháč, J.; Nováček, P.: "Analyses of Triaxial Accelerometer Calibration Algorithms", IEEE Sensors Journal, 2012, vol. 12, no. 5, p. 1157-1165, ISSN 1530-437X.
1. Luczak, S.: "Dual-Axis Test Rig for MemS Tilt Sensors", Metrology and Measurement Systems, vol. 21, issue: 2, p. 351-362, ISSN 0860-8229, DOI: 10.2478/mms-2014-0030, May 2014.
  2. Nilsson, J.-O.; Skog, I.; Handel, P.: "Aligning the Forces—Eliminating the Misalignments in IMU Arrays", IEEE Transactions on Instrumentation and Measurement, vol. 63, no. 10, p. 2498-2500, Oct 2014, DOI: 10.1109/TIM.2014.2344332.
  3. Blasch, E.: "Enhanced air operations using JView for an air-ground fused situation awareness udop", 2013 IEEE/AIAA 32<sup>nd</sup> Digital Avionics Systems Conference (DASC), p. 5A5-1 - 5A5-11, Oct 2013, DOI: 10.1109/DASC.2013.6712597.
  4. Hsu, Y-L; Chu, Ch.-L.; Tsai, Y.-J.; Wang, J-S: "An Inertial Pen With Dynamic Time Warping Recognizer for Handwriting and Gesture Recognition", Sensors Journal, IEEE, vol. 15, no. 1, p. 154-163, Jan 2015, DOI: 10.1109/JSEN.2014.2339843.
  5. Gao, Y.; Guan, L.; Wang, T.; Cong, X.: "Research on the calibration of FOG based on AFSA," 2013 IEEE International Conference on Mechatronics and Automation (ICMA), p. 412-417, Aug 2013, DOI: 10.1109/ICMA.2013.6617954.
  6. Draganová, K.; Laššák, M.; Praslička, D.; Kán, V.: "Attitude-independent 3-axis Accelerometer Calibration Based on Adaptive Neural network", Procedia Engineering, vol. 87, 2014, p. 1255-1258, ISSN 1877-7058, <http://dx.doi.org/10.1016/j.proeng.2014.11.412>.
  7. Luczak, S.: "Experimental Studies of Hysteresis in MEMS Accelerometers: a Commentary", IEEE Sensors Journal, p. 1-1 DOI: 10.1109/JSEN.2015.2390778.
  8. Li, X.; Li, Z.: "Vector-Aided In-Field Calibration Method for Low-End MEMS Gyros in Attitude and Heading Reference Systems", IEEE Transactions on Instrumentation and Measurement, vol. 63, no. 11, p. 2675-2681, Nov 2014, DOI: 10.1109/TIM.2014.2313434.
  9. Montorsi, F.; Pancaldi, F.; Vitetta, G.M.: "Design and implementation of an inertial navigation system for pedestrians based on a low-cost MEMS IMU", 2013 IEEE International Conference on Communications Workshops (ICC), pp. 57-61, June 2013, DOI: 10.1109/ICCW.2013.6649201.
  10. Łuczak, S.: "Effects of Misalignments of MEMS Accelerometers in Tilt Measurements", Mechatronics, Springer International Publishing, 2013, p. 393-400, ISBN 978-3-319-02293-2, DOI: 10.1007/978-3-319-02294-9\_50.
  11. Song, N.; Cai, Q.; Yang, G.; Yin, H.: "Analysis and calibration of the mounting errors between inertial measurement unit and turntable in dual-axis rotational inertial navigation system", Measurement Science and Technology, 24, 115002, ISSN: 2234-7593, DOI:10.1088/0957-0233/24/11/115002.
  12. Łuczak, S.: "Guidelines for tilt measurements realized by MEMS Accelerometers", International Journal of Precision Engineering and Manufacturing, March 2014, vol. 15, issue 3, p. 489-496, ISSN: 2234-7593, DOI: <http://dx.doi.org/10.1007/s12541-014-0558-8>.
- [J2] Šipoš, M.; Roháč, J.; Nováček, P.: "Improvement of Electronic Compass Accuracy Based on Magnetometer and Accelerometer Calibration", Acta Physica Polonica A, 2012, vol. 121, no. 4, p. 945-949, ISSN 0587-4246, co-authorship: 70%.
1. Matandirotya, E.; Van Zyl, R. R.: "Evaluation of a Commercial-Off-the-Shelf Fluxgate Magnetometer for CubeSat Space Magnetometry", Journal of Small Satellites, vol. 2, no. 1, p. 133-146, 2013.

- [R1] Šipoš, M.; Roháč, J.; Nováček, P.: "Analyses of Electronic Inclinometer Data for Tri-axial Accelerometer's Initial Alignment", *Przeglad Elektrotechniczny*, 2012, vol. 88, no. 01a, p. 286-290. ISSN 0033-2097, co-authorship: 60%.
1. Paces, P.; Popelka, J.: "IMU aiding using two AHRS units", 2012 IEEE/AIAA 31st Digital Avionics Systems Conference (DASC), p. 5B1-1,5 - B1-13, Oct 2012, DOI: 10.1109/DASC.2012.6382359.
- [R3] Reinštein, M.; Šipoš, M.; Roháč, J.: "Error Analyses of Attitude and Heading Reference Systems", *Przeglad Elektrotechniczny*, 2009, vol. 85, no. 8, p. 114-118, ISSN 0033-2097, co-authorship: 20%.
1. Sotak, M.: "Coarse alignment algorithm for ADIS16405", *Przegląd Elektrotechniczny*, ISSN 0033-2097, r. 86, nr. 9/2010, p. 247-251.
  2. Adamčík, F.: "Error Analysis of the Inertial Measurement Unit", Aviation, Taylor & Francis, Apr 2011, vol. 15, issue 1, 2011, p. 5-10, ISSN 1648-7788, DOI: 10.3846/16487788.2011.566311.
- [R4] Reinštein, M.; Roháč, J.; Šipoš, M.: "Algorithms for Heading Determination using Inertial Sensors", *Przeglad Elektrotechniczny*, 2010, vol. 86, no. 9, p. 243-246, ISSN 0033-2097, co-authorship: 5%.
1. Sotak, M.: "Sequential Monte Carlo methods for navigation systems", *Przegląd Elektrotechniczny*, ISSN 0033-2097, r. 87 nr. 6/2011, p. 249-252.
- [W1] Šipoš, M.; Pačes, P.; Reinštein, M.; Roháč, J.: "Flight Attitude Track Reconstruction Using Two AHRS Units under Laboratory Conditions", In *IEEE SENSORS 2009 - The Eighth IEEE Conference on Sensors*, Christchurch: IEEE Sensors Council, 2009, p. 675-678, ISSN 1930-0395, ISBN 978-1-4244-5335-1, co-authorship: 40%.
1. Qiang, Y.; Bin, X.; Yao, Z.; Yanping, Y.; Haotao, L.; Wei, Z.: "Visual simulation system for quadrotor unmanned aerial vehicles", 2011 30th Chinese Control Conference (CCC), p. 454-459, July 2011.
- [C25] Pačes, P.; Šipoš, M.; Veselý, M.: "Verification of IEEE1588 Time Synchronization in NASA Agate Data Bus Standard", In *IEEE 2009 9th Conference on Electronic Measurement & Instruments*. Beijing: IEEE, 2009, ISBN 978-1-4244-3862-4, co-authorship: 15%.
1. Río, J.; Toma, D.; Shariat-Panahi, S.; Mànuel, A.; Ramos H.G.: "Precision timing in ocean sensor systems", *Measurement Science and Technology*, 23, no. 2, 025801, ISSN: 1361-6501, DOI:10.1088/0957-0233/23/2/025801.